# NANOSCALE STUDIES ON CANCER THERAPY BY TARGETED DRUG DELIVERY SYSTEM

**Ph.D THESIS**

*by*

**HARMEET SINGH**

**DEPARTMENT OF BIOTECHNOLOGY**
**INDIAN INSTITUTE OF TECHNOLOGY ROORKEE**
**ROORKEE-247667 (INDIA)**
**JUNE, 2018**

# NANOSCALE STUDIES ON CANCER THERAPY BY TARGETED DRUG DELIVERY SYSTEM

**A THESIS**

***Submitted in partial fulfilment of the requirements for the award of the degree***

*of*

**DOCTOR OF PHILOSOPHY**

*in*

**BIOTECHNOLOGY**

*by*

**HARMEET SINGH**

**DEPARTMENT OF BIOTECHNOLOGY**
**INDIAN INSTITUTE OF TECHNOLOGY ROORKEE**
**ROORKEE-247667 (INDIA)**
**JUNE, 2018**

# INDIAN INSTITUTE OF TECHNOLOGY ROORKEE
# ROORKEE

## CANDIDATE'S DECLARATION

I hereby certify that the work which is being presented in the thesis entitled "**NANAOSCALE STUDIES ON CANCER THERAPY BY TARGETED DRUG DELIVERY SYSTEM**", in partial fulfilment of the requirements for the award of the degree of Doctor of Philosophy and submitted in the Department of Biotechnology of the Indian Institute of Technology Roorkee, Roorkee is an authentic record of my own work carried out during a period from July, 2012 to June, 2018 under the supervision of Dr. Vikas Pruthi, Professor, Department of Biotechnolgy, Indian Institute of Technology Roorkee, Roorkee.

The matter presented in the thesis has not been submitted by me for the award of any other degree of this or any other institute.

(**HARMEET SINGH**)

This is to certify that the above statement made by the candidate is correct to the best of my knowledge.

(VIKAS PRUTHI)
Supervisor

The Ph. D. Viva-Voce examination of **Mr. Harmeet Singh**, Research Scholar has been held on ……..

**Chairman, SRC** **Signature of External Examiner**

This is to certify that student has made all the corrections in the thesis.

**Signature of Supervisor** **Head of the Department**

**Dated: _____**

# *ACKNOWLEDGMENTS*

*Foremost, I thank God for endowing me with health, patience, and knowledge to complete this work.*

*First, I would like to express my sincere gratitude and appreciation to my supervisor, Professor Vikas Pruthi, Department of Biotechnology, IIT Roorkee for his continuous guidance, support and motivation. It was his cordial behaviour, constructive criticism and valuable support due to which I could complete this challenging work. It has been a great honour to work with him.*

*I would like to convey my gratitude towards Dr. Gopinath Pakirisami, Center of Nanotechnology, IITR Roorkee for providing research facilities to complete this work.*

*My heartfelt appreciations are extended to Dr. Parul A. Pruthi, my SRC committee members: Professor Sanjoy Ghosh, Dr. Naveen K. Navani, Dr. Mala Nath; DRC Chairman: Professor R. Prasad; Head of the Department: Professor A.K. Sharma, all faculty members for their constant support.*

*I am also thankful to all my lovely friends and helping lab mates (Dr. Priya Vashisth, Dr. Alok Patel, Dr. Richa Panwar, Dr. Sonal, Navdeep Raghuvanshi , Neha Arora, Sonam Gupta, Amit Kumar Srivastava, Tara Chand Yadav, Ekta, Shweta Tripathi and Pursottam Mishra). During this journey, I have created a bond with them that I will never forget. I am very thankful to each one of them for the jovial company in making this journey of IITR so wonderful. I will always cherish the times we spent in lab as well as in nescafe, hospital canteen and play ground. It would not have been possible without you people. My appreciation is due for all the research scholars of Biotechnology department who helped me any way during the course of my research work.*

*I appreciate the financial support from the All India Council for Technical Education (AICTE), New Delhi, India throughout my study.*

*Furthermore, I would like to thank all the people working as administration and technical staff at Institute Instrumentation centre (IIC, IITR), Quality Improvement Centre and academics section of IITR, for making my work easier.*

*I would like to extend my gratitude to Dr. Pankaj Sharma (Director) and colleagues (especially Ms. Shami Chaddha and Mr. Vijay Arora) of Smt. Tarawati Institute of Biomedical and Allied*

*Sciences, Roorkee (Uttarakhand), India, without the help of all those people, the work presented in this thesis could not have been possible. Therefore, I would like to take this opportunity to express my deep sense of appreciation towards them.*

*I bow to my adorable parents for their support and encouragement. Everything I have achieved here is because of them. They are the most selfless people who have provided me strength and motivation during the course of my work. Thank you so much Papa to have faith and pride in me. I acknowledge your sacrifices and love showered on me.*

*Finally, I am extremely grateful to my wife "Shweta" for her great patience, support, encouragement, and dedication, for being the person who shared with me all the moments, and for being a wonderful mother of our son "Gurnimit".*

# *ABSTRACT*

Breast cancer is a heterogenous disease and differs greatly among different patients and even within each individual. This change in heterogeneity significantly changes the efficacy of cancer therapy and therefore, requires the designing of a novel formulation that can deliver therapeutics more efficiently to the cancer cells and can be directed even after the administration of the formulation. Over the last couple of decades, cancer diagnosis and treatment has improved drastically through the expansion of development in novel technologies used in diagnostic, surgical, and therapeutic treatments. However, due to the complexity and diversity of cancers, it is still a challenge to cure cancer using conventional therapies. The development of treatment strategy in cancer is one of the most difficult part because of cancer heterogeneity and challenges in selectively targeting cancer cells without affecting any healthy tissue. The conventional chemotherapy suffers from the limitations of imparting higher degree of toxicity to the body and losing its efficacy because of drug resistance. To circumvent these problems development of nanofromulation and nanomedicine has become one of the important area of research for strategizing cancer therapy.

In present study, different nanoformulations of 5-Fluorouracil were prepared with the aim of improving therapeutic potential of the drug for breast cancer. The thesis comprises of five chapters (1-5), dealing with the synthesis of nanoformulations of 5-Fluorouracil which targets the drug to the desired site by use of a magnetic nanocarrier system.

**Chapter 1 (Introduction and Literature Review),** this chapter reveals both the conventional as well as the novel technologies now being used for the treatment of cancer. It highlights the development of different treatment strategies and their mechanism of action in cancer treatment. The chapter also highlights the profile of 5-Fluorouracil (5FU) and various excipients used in the study. Beside this it includes the different commercially available nanoparticulate products for cancer treatment and their mechanism of action has also been summarized

**Chapter 2 deals with synthesis and characterization of magnetic nanoparticles,** the work presented elaborates the synthesis and characterization of magnetic nanoparticles which are the carrier species used for targeting the drug on to the tumor cells. Superparamagnetic nanoparticles were synthesized with the help of a co-precipitation method using a 2:1 molar ratio of ferric nitrite and ferrous sulphate with liquid ammonia. The prepared nanoparticle was in the size range of 15-25

nm when analyzed using field emission scanning electron microscopy (FESEM) and possess superparamagnetic behavior which was reflected in the vibrating sample magnetometer (VSM) analysis.

**Chapter 3 focuses on the synthesis and characterization of HTCC-5FU-Magnetic nanoparticles,** this chapter elaborates the formulation of HTCC-5FU magnetic nanoparticles using the bottom up approach. In this approach nanoparticles were prepared using encapsulation of 5FU along with magnetic nanoparticles to form N-(2-hydroxy) propyl-3-trimethyl ammonium chitosan chloride nanoparticles (HTCC-5FU magnetic nanoparticles). The optimization study was conducted on the developed HTCC-5FU magnetic nanoparticles for the selection of a suitable polymer concentration used for encapsulation of 5FU which provides the best encapsulation efficiency and stability to the system. The detailed physiochemical characterization of optimized formulations was also conducted using different biophysical techniques. Differential scanning calorimetry revealed that there were no physical and chemical incompatibilities between the drug and excipients. The size of nanoformulation was measured using transmission electron microscopy (TEM) and FESEM and found to be 180 nm. Infrared spectroscopy of the formulation was also performed to investigate the ionic gelation taking place between HTCC and sodium tripolyphosphate (STP) during the formulation of nanoparticles. The magnetic behaviour of the formulation was accessed using VSM analysis. Further the *in vitro* release kinetics of drug from the formulations were also conducted which indicated a diffusion release form the formulation showing the best fit in Korsmeyer-Peppa's ($R^2$ = 0.9798, n = 0.239).

**Chapter 4 describes the synthesis and characterization of 5FU gold magnetic nanoparticles,** This chapter defines the approach used for formulation of 5FU gold magnetic nanoparticles. The formulation of a 5FU gold magnetic nanoparticles was achieved in two steps (i) the direct coating of gold on the synthesised magnetic nanoparticles to form a gold nanoparticles encapsulating magnetic particles and (ii) Conjugating 5FU with the gold magnetic nanoparticles. The formulation was characterized using the UV-spectrophotometric study revealing a consistent peak at 550 nm indicating a stable gold nanoparticles being formed. Further the characterization by TEM and zeta potential were carried out to ensure the size and stability of nanoformulations. IR spectrophotometric study of the formulations was also conducted to evaluate the mechanism of formation of 5FU on

gold nanoparticles. It was noticed that there was a decrease in the magnetic property of gold 5FU magnetic nanoparticles as compared the bare magnetic nanoparticles.

**Chapter 5 deals with the cytotoxicity and *in vivo* anticancer activity,** The chapter investigates the cytotoxicity of HTCC-5FU magnetic nanoparticles and gold 5FU magnetic nanoparticles on MCF-7 cell lines using MTT assay and *in vivo* anticancer activity for measuring the targeting efficacy of magnetic nanoformulation (HTCC-5FU-Magnetic nanoparticles and 5FU gold magnetic nanoparticles ) in treating breast cancer. Allograft model was used to evaluate the anticancer activity of developed magnetic nanoparticles. Healthy Female Balb/c mice of 5-6 weeks of age were used for study. Tumors were generated by an orthotopic injection of 4T1 breast cancer cell lines and tumor generated mice were treated with the different formulations. Further, a constant monitoring of animal body weight and tumor volume during the course of treatment reflected a significant effect of formulations in controlling the tumor volume. Histopathological examination was performed to confirm the accumulation of magnetic nanoparticle in tumors and the therapeutic efficacy of magnetic nanoparticles was also evaluated.

# *TABLE OF CONTENTS*

# *LIST OF TABLES*

# *LIST OF FIGURES*

# *ABBREVATIONS AND ACRONYMS*

| | |
|---|---|
| 5FU | 5-Fluorouracil |
| ACS | American Cancer Society |
| CPCSEA | Committee for the Purpose of Control And Supervision of Experiments on Animals |
| CS | Chitosan |
| DLS | Dynamic Light Scattering |
| DMEM | Dulbecco's Modified Eagle's Medium |
| DMSO | Dimethyl Sulfoxide |
| DNA | Deoxy ribose nucleic acid |
| DOX | Doxorubicin |
| °C | Degree Celsius |
| DSC | Differential scanning calorimetry |
| emu/g | Electromagnetic unit per gram |
| EPR | Enhanced Permeation and Retention |
| EPTAC | 2,3-Epoxypropyl)trimethylammonium chloride |
| FBS | Fetal Bovine Serum |
| FdUMP | Fluordeoxyuridine monophosphate |
| FE-SEM | Field Emission Scanning Electron Microscopy |
| FTIR | Fourier-Transform Infrared spectroscopy |
| FUTP | Fluorouridine triphosphate |
| g | Grams |
| GI50 | 50% Growth Inhibition |
| GTMAC | Glycidyltrimethylammonium chloride |
| H | Magnetic strength |

| | |
|---|---|
| h | Hour |
| HAuCl4 | Chloroauric Acid |
| HCPT | 10-hydroxycamptothecin |
| HTCC | N-(2-hydroxyl) propyl-3-trimethyl ammonium chitosan chloride |
| IEAC | Institutional Animal Ethics Committee |
| IV | Intravenous |
| kOe | Kilooersted |
| M | Magnetization |
| MCF-7 | Michigan Cancer Foundation-7 |
| MIC | Minimum Inhibitory Concentration |
| min | Minute |
| ml | MilliLiter |
| mM | Millimolar |
| MNPs | Magnetic Nanoparticles |
| MRI | Magnetic Resonance Imaging |
| MTT | [3-(4,5-dimethylthiazol-2-yl)-2,5-diphenyltetrazolium bromide] |
| MTX | Methotrexate |
| $NaBH_4$ | Sodium Borohydride |
| NCI | National Cancer Institute |
| NF | Nanoformulation |
| nm | Nanometer |
| NPs | Nanoparticles |
| OD | Optical Density |
| PBS | Phosphate Buffer Saline |
| Pdl | Polydispersity Index |

| | |
|---|---|
| RES | Reticulo Endothelial System |
| RNA | Ribose nucleic acid |
| rpm | Rotation per minute |
| SAED | Selected Area Diffraction |
| SPR | Surface Plasmon Resonance |
| STP | Sodium tripoly phosphate |
| TEM | Transmission Electron Microscopy |
| TNF-α | Tumor Necrosis Factor Alpha |
| TPP | Sodium tripoly phosphate |
| TS | Thymidylate synthetase |
| UV-vis | Ultra violet Spectroscopy |
| V | Volume |
| VSM | Vibrating Sample Mgnetometer |
| XRD | X-Ray Diffraction |
| λmax | Absorption maxima |
| μg | Microgram |
| μL | Microliter |

# *LIST OF PUBLICATIONS*

1. Singh, H., & Pruthi, V. (2018). Synthesis, characterization and antitumor potential of HTCC-5FU Magnetic Nanoparticles. Pharmaceutical Nanotechnology. (communicated)

2. Raghuwanshi, N., Pathak, A., Patel, A., Vashisth, P., Singh, H., Srivastava, A. K., & Pruthi, V. (2017). Novel biogenic synthesis of silver nanoparticles and their therapeutic potential. *Frontiers in Bioscience*, *9*, 33–43. https://doi.org/http://dx.doi.org/10.2741/783

3. Vashisth, P., Raghuwanshi, N., Srivastava, A. K., Singh, H., Nagar, H., & Pruthi, V. (2017). Ofloxacin loaded gellan/PVA nanofibers - Synthesis, characterization and evaluation of their gastroretentive/mucoadhesive drug delivery potential. *Materials Science and Engineering C*, *71*, 611–619. https://doi.org/10.1016/j.msec.2016.10.051

4. Vashisth, P., Sharma, M., Nikhil, K., Singh, H., Panwar, R., Pruthi, P. A., & Pruthi, V. (2015). Antiproliferative activity of ferulic acid-encapsulated electrospun PLGA/PEO nanofibers against MCF-7 human breast carcinoma cells. *3 Biotech*, *5*(3), 303–315. https://doi.org/10.1007/s13205-014-0229-6

**Book Chapter**

Vashisth, P., Singh, H., Pruthi, P. A., & Pruthi, V. (2015). Gellan as Novel Pharmaceutical Excipient. In *Handbook of Polymers for Pharmaceutical Technologies* (Vol. 1, pp. 1–21). https://doi.org/10.1002/9781119041375.ch1

# *PAPER PRESENTED IN CONFERENCE & AWARDS*

1. Singh, H., Vashisth, P., Mallick, V., & Pruthi, V. Magnetic Nanocarriers: An Upcoming Targeted Drug Delivery Approach for Cancer Treatment in 1st **International Conference on Emerging Trends of Nanotechnology in Drug Discovery** May 26-27, 2014, Delhi.

2. Singh, H., Vashisth, P., Mallick, V., Panwar, R., Puthi, P., & Pruthi, V. Polymeric approach to synthesise magnetic nanocarrier for targeted drug delivery" in **International Conference on Pharmaceutical Sciences, on the theme " Present trends and future prospects in pharmaceutical sciences "** February 14-15, 2014, Dehradun.

3. Vashisth, P., Singh, H., Pruthi, P., Singh, R.P., & Pruthi, V. Evaluation of gellan based electrospun nanofibers for wound healing. **6th International Conference on Nanomaterials - Research & Application (NANOCON-2014),** November 5-7, 2014, Brno, Czech Republic, Europe.

## AWARDS

1. **Best Oral Presentation Award** Singh, H., Vashisth, P., Mallick, V., Panwar, R., Puthi, P., & Pruthi, V. Polymeric approach to synthesize magnetic nanocarrier for targeted drug delivery" in **International Conference on Pharmaceutical Sciences, on the theme " Present trends and future prospects in pharmaceutical sciences "** February 14-15, 2014, Dehradun.

# CHAPTER 1

## 1. INTRODUCTION

### 1.1 Breast Cancer

Breast cancer is among the highest ranked cancer found among the Indian females with a rate as high as 25.8 in every 100,000 women and a mortality rate of 12.7 in every 100,000 women. There is a big difference in the cancer cases reported and breast cancer-specific mortality, when considered globally. In United states the survival rate of cancer continues to increase attributing to the advances in early detection and treatment. Further, the American Cancer Society (ACS) and the National Cancer Institute (NCI) have collaboratively initiated different programs to impart the knowledge with regard to the disease and its management to help the patients for a better life. According to the latest epidemiological data there were almost 15.5 million cancer patients who managed to survive because of this collaborative initiation as on January 2016, and this figure is expected to reach approximately 20 million by January 2026 [1].

Generally, a greater incidence rate of breast cancer is reported in the developed nations where as higher mortality rate for breast cancer is seen in the developing nations. The similar pattern is observed within India where the incidence of mortality in comparison to incidence of occurrence was found to be 66 % in rural areas whereas as this value was merely 8 % in urban areas [2]. This is attributed to a complex combination of factors including factors related to lifestyle, limitations of data and dissimilarity in the methods of breast cancer diagnosis and treatment [3].

In India, incidence rate of breast cancer was found to be highest for Delhi with 41 per 100,000 women reported with the disease, followed by Chennai, Bangalore and Thiruvananthapuram districts where the incidence rate reported are of 37.9 %, 34.4 %, and 33.7 % respectively. Projected figures for patients suffering from breast cancer in India by 2020 indicates an alarming high of 1797900 patients [2]. A better awareness, screening programmes, and treatment facilities would favour a positive clinical picture in the country.

### 1.2 Development of Novel Strategies to Cure Cancer

Over the last couple of decades, cancer diagnosis and treatment have improved drastically through the expansion of development in novel drug delivery technologies used in diagnostic, surgical, and therapeutic treatments. However, due to the complexity and diversity of cancers, it is still a challenge to cure cancer [4,5]. The development of treatment strategies in cancer is one

of the most difficult parts because of cancer heterogeneity and challenges in selectively targeting cancer cells without affecting healthy tissue. The limitations of conventional cancer drug therapy include higher degree of associated toxicity and drug resistance. To circumvent these problems, use of nanofromulation (NF) and nanomedicine has become one of the choice for development of cancer therapy. In recent years, nanoformulations has proved as a rapidly evolving field with aims of improving therapeutic potential of already existing drugs in cancer treatments by the virtue of properties like high surface to mass ratio, better drug absorption and high drug payload. Nanoformulation is referred to the formulation which is designed using nanoscale materials with an aim to increase their uptake by the targeted cells along with their reduced systemic toxicity [6].

### 1.3 Desirable Characteristics Required by Nanoformulation

One of the advantage of nanoformulation is the ability to 'protect' the drug from either rapid degradation or clearance. The shielded drug in the nanoformulation has an altered pharmacokinetic pattern i.e., a changed absorption, distribution, metabolism, and excretion profile and similarly a different pharmacodynamic profile i.e., effects of drug on the body compared to free drug. Nanoparticles can have a significantly prolonged circulation time for therapeutic agents encapsulated in them leading to increased extravasation into tumors [7]. These properties of nanoformulation gives further advantage of less frequent doses, a lower toxicity, and improved patient compliance [8]. The parameters that critically influence drug delivery through nanoformulation are targeting, particle size and shape, surface charge, lipophilicity of the nanoparticle. These physical properties can be easily manipulated as per the choice of route of administration and targeting site to optimize their use in diagnostic and therapeutic.

### 1.4 Different Approaches for Drug Targeting in Cancer Cells

Nanoformulations are systems which are designed and structured with dimensions in nanometer (nm) size. Nanoparticles can usually have a dimension that is designed based on their intended clinical use. One of the purpose of these constructed nanoformulations (NFs) is to accumulate inside the cancerous tissue. A naoparticle as compared to a bulk product of higher dimension carries an advantage of passing through the leaky junction of cancer endothelium to reach the cancer cells which causes a preferential accumulation of the NFs at tumor sites. These tumor cells have a deficient lymphatic system, resulting in enhanced permeation and retention effect (EPR) of the drug. Nanoparticle targeting to tumors can be achieved passively thorough the enhanced permeability and retention (EPR) effect. The pores in the tumor vasculature ranges

from some 100 to 600 nm in size, which allows nanoformulation with a maximum size of ~400 nm to extravasate into the tumor tissue [9,10]. This mechanism of drug targeting has also been explored for drug delivery in cancer by cancer nanotubes [11].

### 1.4.1 Dendrimers

Dendrimers are class of nanoparticles which forms a branched macromolecular three dimensional structure (Figure 1.1). They can be prepared using either a divergent or a convergent technique. They have a well-defined structure with branches coming out of the central core resulting from polymerization in the central core [12]. Resulting branches may vary in length due to steric limitations and dendrimer attains a spherical shape [13]. Drug moieties may be incorporated with help of bonding of drug with the chemical groups present on the surface of dendrimer or encapsulation of drug inside the dendrimer [14,15]. These dendrimers are found suitable in carrying different nature of carrier molecules, both lipophilic and hydrophilic in nature, and may act as a potential system for drug and gene delivery. These nanoparticles are reported to have a potential targeting against tumor cells where h-foliate receptor have been designed using dendrimers.

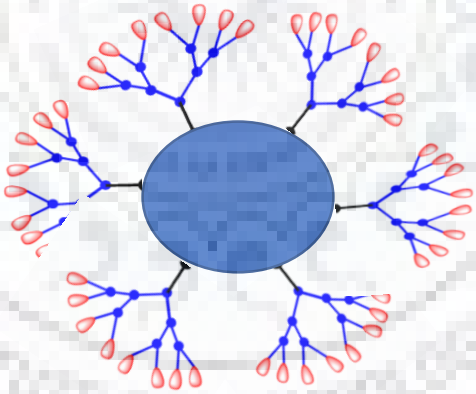

**Figure 1.1 Diagrammatic Representation of a Dendrimers**

### 1.4.2 Micelles

Micelles are self-assembled, nano-sized (5–100 nm), bilayer spherical structure, that consist of amphiphilic polymers, which form spontaneously in an aqueous environment (Figure 1.2) [12]. The mechanism of formation involves the clumping of hydrophobic end of the molecules to form

the central core of the sphere and the hydrophilic ends are then aligned with the surrounding aqueous medium and form the outer shell. Inner core is used as reservoir of drugs which is responsible for protection of the drug till the time it is delivered at the desired site whereas the outer shell defines the properties like stability and hydrophilicity of the micellar structure. Moreover, outer shells can also be structurally modified for providing the specificity to the interaction of micelles with the biocomponents [14,16]. These systems are therefore a potential carrier for delivery of drugs such as paclitaxel [17], Doxorubicin [18], Epirubicin [19].

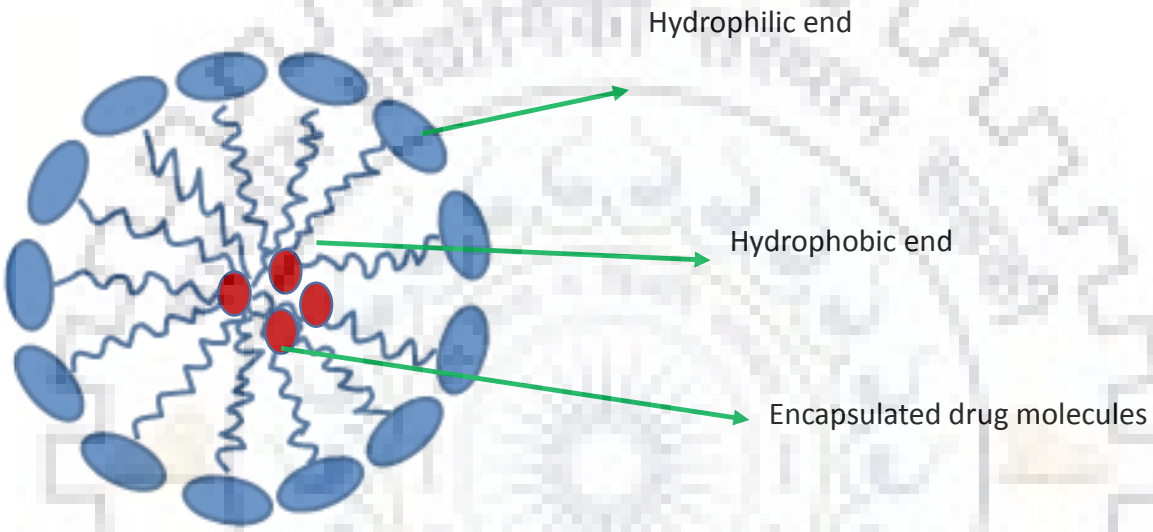


**Figure 1.2 Diagrammatic Representation of a Micelle**

### 1.4.3 Nanospheres

Nanospheres are more often a matrix system and forms a spherical structure in which drug may be either entrapped, attached, or encapsulated (Figure 1.3). They can be used in targeted drug delivery by functionalizing the surface and attaching the relevant polymers or biological materials such as ligands or antibodies on their surface. A hollow mesoporous silica nanoparticles is one such example which have been utilized for controlled and targeted drug delivery of doxorubicin [20,21], antibiotics [22] and analgesics [23].

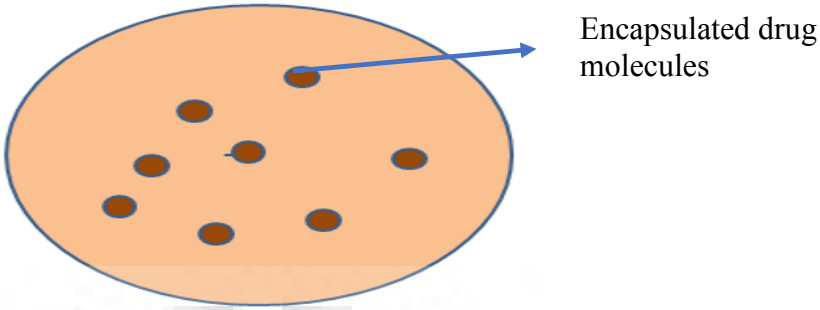


**Figure 1.3 Diagrammatic Representation of a Nanosphere**

### 1.4.4 Nanocapsules

These are vesicular systems with a central core in which the drug is encapsulated or entrapped and a polymeric membrane surrounding the core to which targeting ligands such as an antibodies or protein may be attached (Figure 1.4). Nanocapsule can encapsulate a core product which may be either liquid or a solid. Nanocapsules are found suitable for various applications related to drug delivery. They have potential application in the field of oral delivery of drugs, as vehicle for oral administration of acid labile products like proteins and peptide, such as poly (isobutylcyanoacrylate) nanocapsules [24,25] or in targeted therapy for cancer such as nanocapsules encapsulating siRNAs [26], cisplatin [27] and doxorubicin [28].

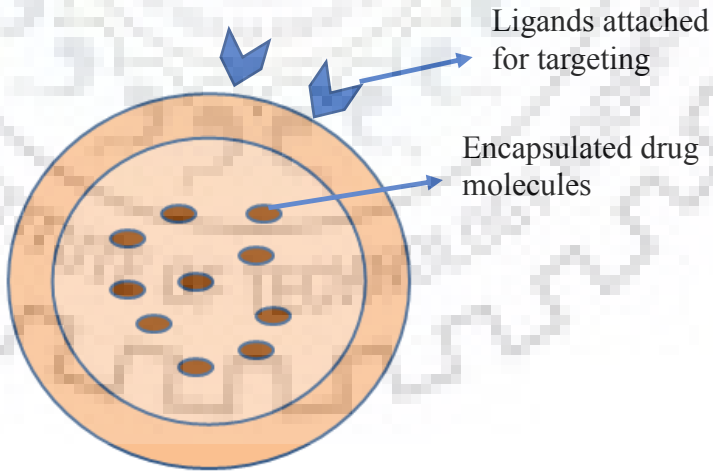


**Figure 1.4 Diagrammatic Representation of a Nanocapsule**

### 1.4.5 Liposomes

Liposomes are carriers which can encapsulate both hydrophilic and hydrophobic drug within its core [29]. They are vesicular in nature and are composed of lipid layers (Figure 1.5) [12]. They

are defined according to the number of lipid bilayer. Unilamellar liposome is a system having a single lamellar structure with an aqueous core and hence are more suitable for entrapment of hydrophilic drugs; in contrary to multilamellar liposomes which entraps lipophilic drugs. Although there are many novel drug delivery systems for treatment of cancer in clinical trials or approved, liposomes is one of the most extensively researched vehicle for drug delivery [30,31]

Doxil, is the first liposomal formulation approved by the Food & Drug Administration (FDA) for the treatment of Kaposi's sarcoma [32,33]. DaunoXome, is another liposomal formulation of daunorubicin which is approved for the treatment of Acquired Immune Deficiency Syndrome (AIDS) related Kaposi's sarcoma [34,35]. Marqibo, is another liposomal formulation of vincristine made for the treatment of acute lymphoblastic leukemia [36,37].

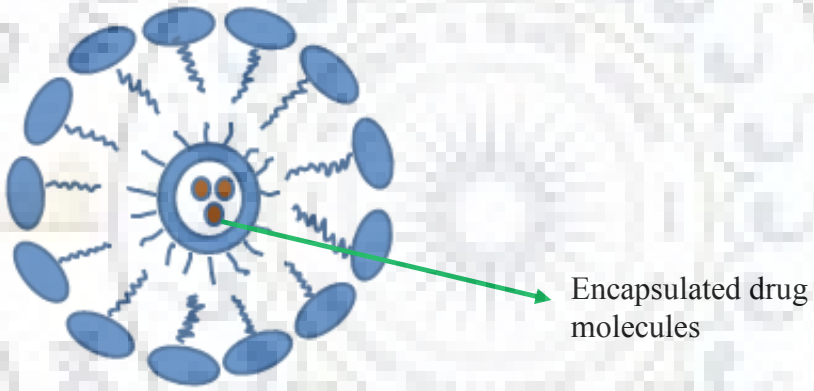


**Figure 1.5 Diagrammatic Representation of a Liposome**

## 1.5 Drug and Excipients Related Literature Survey

### 1.5.1 5-Fluorouracil (5FU)

Fluorouracil (5FU) is chemically an analogue of pyrimidine which clinically lies in the category of anticancer drug (Figure 1.6). It is among the few first line drug recommended for the treatment of multiple solid tumors including colon, rectal and breast. It is also a part of conjugate therapy in case of gastric, pancreatic, ovarian, bladder and liver cancer.

**Chemical Structure:**

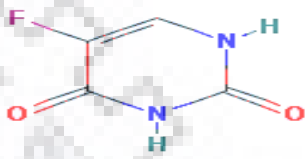


**Figure 1.6: Chemical structure of 5 Fluorouracil**

IUPAC Name: 5-fluoro-1H-pyrimidine-2,4-dione

Molecular formula: $C_4H_3FN_2O_2$

Molecular weight: 130.078 g/mol

Half-life: 10-20 min

Physical state: 5FU is a solid white to nearly white crystalline powder; practically odorless.

pKa: 8.02

Log P: -0.89

Log S: -1.07

Log Kow: -0.89

Melting point: 282-283°C

Solubility: Solubility varies based on type of solvent, it is found to be sparingly soluble in water (< 1mg/ml at 77°F) and slightly soluble in alcohol.

Protein binding: 8-12%

Routes of administration: Parentral (IV), topical , oral

Brand available: Adrucil, Adria; Fluorouracil Injection, Goldline, Lyphomed

Dosage form and dosage: Parenteral Injection, for iv use, 50 mg/mL, Topical Cream, 1% (w/w)

**Toxicity:**

Hepatotoxicity is reported as the major effect of 5FU affecting more than 70 % of patients under chemotherapy because of 5FU. It seems that 5FUcause an elevation in serum aminotransferase level in treated patients. Other reported toxicity are mucositis and myelosuppression [38].

**Mechanism:**

5 Fluorouracil is an analogue of uracil, a pyriminde base and structurally differs by having a fluorine atom at carbon-5 instead of a hydrogen atom present in uracil. Being an analogue of uracil its uptake is quite rapid and in the similar manner as of uracil. Inside the cell, it gets metabolized to various active metabolites such as fluorodeoxyuridine monophosphate (FdUMP), fluorodeoxyuridine triphosphate (FdUTP) and fluorouridine triphosphate (FUTP). These metabolites are responsible for inhibiting the synthesis of deoxy ribonucleic acid (DNA) and ribose nucleic acid (RNA) by covalently binding with thymidylate synthetase (TS) and thus causing cell death [39].

**Table 1.1 Some 5FU Loaded Nanoparticulate Carrier Based Drug Delivery System**

| SNo | Formulation type | Inference | Reference(s) |
|---|---|---|---|
| 1 | Solid lipid nanoparticles | Enhanced anticancer effect was observed using 5FU loaded SLN as compared to pure 5FU. | [40] |
| 2 | Chitosan-based nanoparticles | Chitosan-loaded 5FU nanoformulation provided with improved localization of drug at colon region, a sustained release action for 24h and decreased drug induced toxicity. | [41] |
| 3 | Chitosan-based nanoparticles | Nanoparticles formed using chitosan were found to have a pH-responsive drug delivery for cancer treatments. | [42] |
| 4 | PLGA nanoparticles | The prepared 5FU nanoparticles of PLGA were investigated on HT-29 cell | [43] |

| | | | |
|---|---|---|---|
| | | lines using MTT assay method and the results revealed that the nanoformulation prominently exhibited an effect on the cancer cells. | |
| 5 | Folic acid and PLGA conjugates | 5FU loaded PLGA nanoparticles were found to possess significant cytotoxicity which was found proportional to the folic acid conjugated with the nanoparticles. | [44] |
| 6 | 5FU encapsulated pectin based nanoparticles | 5FUloaded in pectin based magnetic nanocarriers were synthesized and on were found to be effective against cell lines for colon cancer, liver cancer, and pancreatic cancer. | [45] |
| 7 | Silica nanoparticles | Conjugation of 5FU loaded hyaluronic acid (HA) was done with silica nanoparticles (SiNPs) and the result revealed that HA-conjugated NP was more effective in inducing apoptosis in cancer cells than non-targeted NP | [46] |

### 1.5.2 Polymers

Polymers are formed by a chemical reaction involving a sequential joining of number of monomer units to form a large polymeric unit. These polymers have become an integral part of the advancement in drug delivery technology. They provide a sustained as well as controlled release when used in the delivery of therapeutic agents both of hydrophilic and hydrophobic nature [47].

Smart polymers are the now a days a choice of excipient to be used in pharmaceuticals. These polymers show a stimuli responsive change in their properties in response to the change in biological conditions. These stimuli may be generated by changes in temperature, pH, pressure, magnetic field, electric field, light or a change in concentration, ionic strength, and redox potential etc. [48].

### 1.5.2.1 N-(2-hydroxyl) propyl-3-trimethyl ammonium chitosan chloride (HTCC)

**Chemical Structure:**

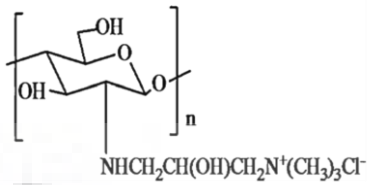


**Figure 1.7: Chemical structure for N-(2-hydroxyl) propyl-3-trimethyl ammonium chitosan chloride (HTCC)**

N-(2-hydroxyl) propyl-3-trimethyl ammonium chitosan chloride (HTCC) (Figure 1.7) is a novel polymer that is biocompatible, biodegradable and economical in production. It can be prepared by a single pot and easy chemical reaction of Chitosan and epoxy propyl trimethyl ammonium chloride (EPTAC). Moreover in comparison to chitosan the parent polymeric system, HTCC has a methyl group instead of amino group making it as a polymer with an excellent water solubility not only in acidic but basic pH also. HTCC therefore, dissolves in neutral and alkaline conditions also as compared to chitosan [49]. Besides, HTCC also has a great potential to be used as an agent to enhance absorption across epithelial due to its mucoadhesive and permeability enhancing property [50,51]. HTCC has become a choice for making nanoparticles based on ionic gelation process of HTCC and sodium tripolyphosphate (TPP).

**Table 1.2 Some HTCC encapsulated nanoparticulate system**

| S.No. | Drug | Inference | Reference |
|---|---|---|---|
| 1. | Ribavirin | The results revealed that HTCC is a promising CS derivative for the encapsulation of hydrophilic drugs with sustained action. | [52] |
| 2. | Parathyroid Hormone | The study showed that HTCC/PTHrP1–34 nanoparticles were successfully formulated using ionic gelation technique and is useful for the treatment of osteoporosis, because of sustained action. | [53] |
| 3. | Bovine Serum Albumin (BSA) | The study concluded with the fact that HTCC by means of ionic gelation technique is a suitable polymer to form nanoparticulate system with a sustained drug delivery. | [54] |

| | | | |
|---|---|---|---|
| 4. | Methotrexate (MTX) | The formulated nanoparticle were found to be suitable for delivery of anticancer drug MTX to the targeted cells. | [55] |
| 5. | pGL3 luciferase plasmid | The results revealed that HTCC may work as a means of carrying a non-viral vector for safe and efficient DNA delivery. | [56] |

### 1.6 Nanoparticles in Pharmaceuticals

The purpose of any drug formulation is to deliver its payload i.e., drug to the site of action without any loss in the stability and efficacy of drug. The most common approach for treatment of cancer includes surgery, radiotherapy, chemotherapy, and hormonal therapy. But all of these approaches carries a major disadvantage of being non-specific in delivery of drug towards cancer cells making them non-effective in number of patients. Moreover, non-specific targeting of drug leads to a higher doses of drug required to reach the tumor region. Therefore, the prerequisite in designing of any novel drug delivery system for cancer are firstly, targeting of drug delivery to cancer cells only and secondly, minimum distribution of drug in healthy cells. Nanoformulations (NFs) or nanoparticles (NPs) are one of the promising new tools which can assist in drug delivery directly into the tumor cells with a minimum drug distribution in the healthy cells. [57]. Different US-FDA approved nanoparticulate system is shown in Figure 1.8 [58]

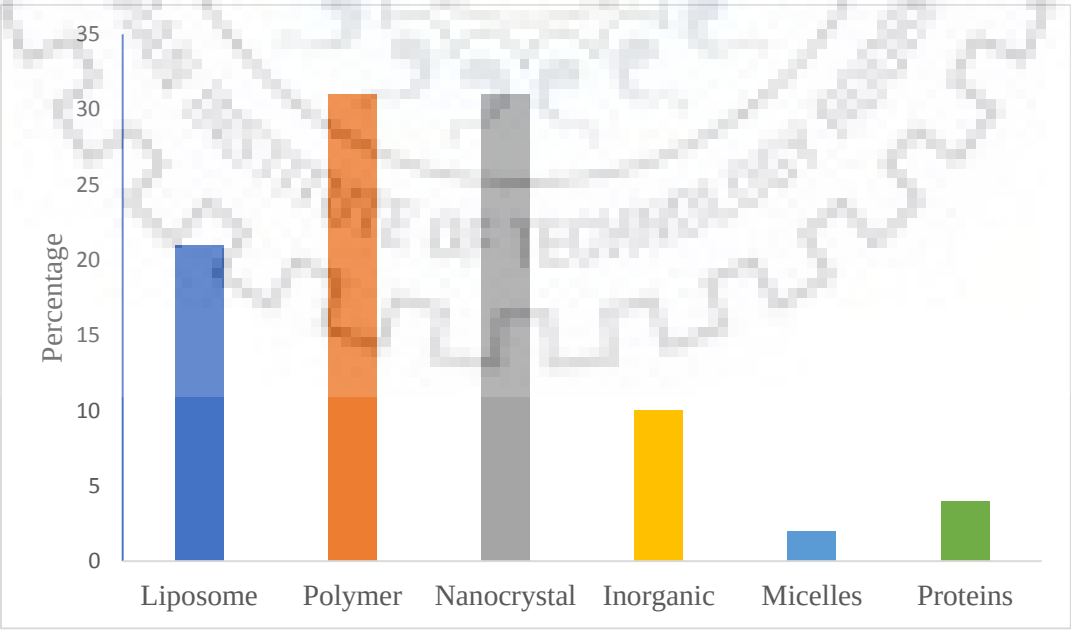


**Figure 1.8 : Types of US-FDA approved nanoparticles available for clinical use**

**Table 1.3 Commercially Approved Nanodrugs Available for Clinical applications**

| SNo | Brand Name | Generic Name | Indication | Category |
|---|---|---|---|---|
| 1. | Abelcet | Liposomal amphotericin B lipid complex | Fungal infections | Liposome |
| 2. | Abraxane | Albumin-bound paclitaxel | Breast cancer, pancreatic cancer | Albumin nanoparticle/Protein NPs |
| 3. | Adagen | Pegademase bovine | Immunodefficiency | Polymeric Nanoparticles |
| 4. | Adynovate | Recombinant Antihemophilic factor, pegylated | Hemophilia | Polymeric Nanoparticles |
| 5. | AmBIsome | Liposomal amphotericin B | Fungal infections | Liposome |
| 6. | Avinza | Morphine sulfate | Psychostimulant | Nanocrystal |
| 7. | Cimzia | Certolizumab pegol | Rheumatoid arthritis, psoriatic arthritis | Polymeric Nanoparticles |
| 8. | Copaxone | Glatimer acetate | Multiple sclerosis | Polymeric Nanoparticles |
| 9. | Curosurf | Poractant alfa | Respiratory disease | Liposome |
| 10. | DepoCyt | Liposomal cytarabine | Meningitis | Liposome |
| 11. | DepoDur | Liposomal morphine sulphate | Postoperative analgesia | Liposome |
| 12. | Dexferrum | Iron dextran | Iron deficiency | Inorganic NPs |
| 13. | Doxil | Doxorubicin HCl liposome injection | Cancer | Liposome |
| 14. | Eligard | Leuprolide acetate and polymer | Cancer | Polymeric Nanoparticles |
| 15. | Emend | Aprepitant | Antiemetic | Nanocrystal |
| 16. | EquivaBone | Hydroxyapatite | Bone substitute | Nanocrystal |

| | | | | |
|---|---|---|---|---|
| 17. | Estrasorb | Micellar estradiol | Vasomotor symptoms in menopause | Micelles |
| 18. | Feraheme | Ferumoxytol | Iron deficiency | Inorganic NPs |
| 19. | Ferrlecit | Sodiumferric gluconate | Irondeficiency | Inorganic NPs |
| 20. | Focalin | Dexamethylphenidate HCl | Psychostimulant | Nanocrystal |
| 21. | Infed | Iron dextran | Iron deficiency | Inorganic NPs |
| 22. | Invega Sustenna | Paliperidone palmitate | Schizophrenia, schizoaffective disorder | Nanocrystal |
| 23. | Krystexxa | Pegloticase | Chronic gout | Polymeric Nanoparticles |
| 24. | Macugen | Pegaptinib | Neovascular AMD | Polymeric Nanoparticles |
| 25. | Marqibo | Liposomal vincristine | Cancer | Liposome |
| 26. | Megace ES | Megestrol acetate | Antianorexic | Nanocrystal |
| 27. | Mircera | Beta form of methoxy polyethylene glycol-epoetin | Anemia | Polymer Nanoparticles |
| 28. | NanOss | Hydroxyapatite | Bone substitute | Nanocrystal |
| 29. | Neulasta | Pegfilgrastim | Chemotherapy-induced neutropenia | Polymeric Nanoparticles |
| 30. | Oncaspar | Pegaspargase | Cancer | Polymeric Nanoparticles |
| 31. | Onivyde | Liposomal irinotecan | Cancer | Liposome |
| 32. | Ontak | Denileukin diftitox | Cancer | Targeted T-cell specificity, lysosomal escape |
| 33. | OsSatura | Hydroxyapatite | Bone substitute | Nanocrystal |
| 34. | Ostim | Hydroxyapatite | Bone substitute | Nanocrystal |
| 35. | Pegasys | Pegylated form of IFN alpha-2a | Hepatitis B,& C | Polymeric Nanoparticles |

| | | | | |
|---|---|---|---|---|
| 36. | PegIntron | Pegylated form of IFN alpha-2b | Hepatitis C only | Polymeric Nanoparticles |
| 37. | Plegridy | Pegylated IFN beta-1a | Multiple sclerosis | Polymeric Nanoparticles |
| 38. | Rapamune | Sirolimus | Immunosuppressant | Nanocrystal |
| 39. | Rebinyn | Coagulation factor IX (recombinant), glycopegylated | Hemophilia B | Polymeric Nanoparticles |
| 40. | Renvela and Renagel | Sevelamer carbonate; and Sevelamer HCl | kidney disease | Polymeric Nanoparticles |
| 41. | Ritalin LA | Methylphenidate HCl | Psychostimulant | Nanocrystal |
| 42. | Ryanodex | Dantrolene sodium | Malignant hypothermia | Nanocrystal |
| 43. | Somavert | Pegvisomant | Acromegaly | Polymeric Nanoparticles |
| 44. | Tricor | Fenofibrate | Hyperlipidemia | Nanocrystal |
| 45. | Venofer | Iron sucrose | Iron deficiency | Inorganic NPs |
| 46. | Visudyne | Liposomal verteporfin | Ocular histoplasmosis, myopia | Liposome |
| 47. | Vitoss | Calcium phosphate | Bone substitute | Nanocrystal |
| 48. | Vyxeos | Liposomal daunorubicin and cytarabine | Cancer | Liposome |
| 49. | Zanaflex | Tizanidine HCl | Muscle relaxant | Nanocrystal |
| 50. | Zilretta | Triamcinolone acetonide ER injectable suspension | Osteoarthritis knee pain | Polymeric Nanoparticles |

# CHAPTER 2

# PREFORMULATION STUDIES OF 5 FLUOROURACIL AND SYNTHESIS OF MAGNETIC NANOPARTICLES

## 2.1 Introduction

Every drug has certain chemical and physical properties which needs to be evaluated before development of a pharmaceutical formulation. The preformulation study is the first step in the rational development of a dosage form, which involves a series of studies that entirely focus on the physicochemical properties of the drug [59]. The properties such as solubility, partition coefficient, melting point, organoleptic properties and spectroscopic studies could affect the drug performance in the physiological system. The prefromulation study therefore provide with some important information regarding the design and development of the formulation and support the need for any changes required during the development of the new formulation. These physiochemical properties provides the framework for drugs combination with pharmaceutical excipients in the fabrication of dosage form. Objective of preformulation study is to develop the elegant, stable, efficacious and safe dosage form by establishing drug's physiochemical characteristics, and compatibility with the other formulation additives. Preformulation studies includes (i) identification of the physiochemical parameters for new and existing drug substances and (ii) investigation of compatibility of the drug with the formulation additives.

Magnetic nanoparticles have physical and chemical properties that are unique and are characteristic of neither the atom nor the bulk counterparts [60]. The large surface area and quantum effect of magnetic nanoparticles drastically change their magnetic properties and exhibit superparamagnetic phenomena, as each nanoparticle can be considered as a single magnetic domain [61]. Due to their unique properties, superparamagnetic nanoparticles have been widely used in the fields of biotechnology and ferrofluid technology.

These magnetic nanoparticle can be easily directed towards the target tissue by the application of an external magnetic field. Superparamagnetic nanoparticles are considered as safe and effective as a targeting as well as a contrasting agent in magnetic resonance imaging. The magnetic nanoparticles are derived from different inorganic core of iron oxide, such as magnetite ($Fe_3O_4$), maghemite ($\gamma$-$Fe_2O$), or other insoluble ferrites [62]. These are used for various applications by means of coating with polymers such as dextran, chitosan, polyethylene glycols

(PEGs), or pectin [63]. In recent years, magnetite an important type of superparamagnetic material has gained an increasing attention for its wide application in catalyst development, and biomedical applications, such as contrast agent in magnetic resonance imaging, bio separation by manipulation of magnitude of magnetic field, magnetic drug targeting, and in therapeutics as hyperthermia [64,65]. Magnetic nanoparticles of iron oxide have been extensively studied for their biomedical applications, not only in the controlled magnetic transportation for the delivery of anticancer drugs but also in the generation of hyperthermia at a localized area [66,67].

## 2.2 Materials and Methods

### 2.2.1 Materials

5-Fluorouracil (5FU), ferric nitrite ($Fe(NO_3)_3$. $9H_2O$), ferrous sulphate ($FeSO_4$. $7H_2O$), liquid ammonia, and all other reagents used were of analytical grade and were purchased from Sigma Aldrich. Millipore water was used in all the experiments.

### 2.2.2 Preformulation Studies of 5FU

#### 2.2.2.1 Physical Properties

The morphological characterization of 5FU is required firstly, for identification of drug and secondly, for comparing the initially received drug with that of the formulated drug in different batches. The physical properties of 5FU like colour, odour, and physical appearance were analysed.

#### 2.2.2.2 Identification of 5FU by UV-Visible spectroscopy

UV spectrophotometric studies using 0.001%w/v 5FU were carried out in acetate buffer (pH 4.7) in a scanning range of 200-400 nm and values obtained were compared with those reported in Indian pharmacopeia (Indian Pharmacopoeia, 1996).

#### 2.2.2.3 Fourier transform infrared (FTIR) analysis

5 FU was mixed with IR grade potassium bromide in a proportion of 1:50 and converted to pellets. The FTIR (Perkin Elmer Spectrophotometer) spectrum of pellets was recorded in the range of 400 to 4000 $cm^{-1}$. The peaks of 5FU were compared with the standard IR spectrum reported in Indian pharmacopoeia for evaluation of its purity [68].

#### 2.2.2.4 Preparation of Standard Plot

5FU (10mg) was dissolved in 100 ml of millipore water to get a stock solution of 100 µg/ml. Further, using this stock solution different concentrations of dilutions in the range of 2-12 µg/ml were prepared and analyzed at 263 nm to get the calibration curve. The data recorded was subjected to linear regression analysis [69].

##### 2.2.2.4.1 Preparation of Phosphate Buffer (PBS) pH 7.4

The preparation of PBS pH 7.4 was carried out by dissolving 2.83 g of dihydrogen phosphate and 0.19 g of potassium dihydrogen phosphate in millipore water and then 8.0 g of sodium chloride was added to the above solution. The volume of buffer solution was then adjusted to 1000 ml with millipore water (Indian Pharmacopoeia, 1996).

##### 2.2.2.4.2 Preparation of Stock solution of 5FU

To prepare 5FU stock solution, 5FU (10 mg) was weighed and transferred to 100 ml volumetric flask. 5FU was then dissolved in 10 ml of PBS (pH 7.4) and volume was later made up to the 100 ml mark using PBS, with a final strength of stock solution as 100 µg/ml. Stock solution was than diluted with millipore water to obtain working solutions in the concentration range of 2-12 µg/ml.

#### 2.2.2.5 Equilibrium solubility determination

To determine the equilibrium solubility known amount of 5FU was suspended in distilled water (10 ml) and phosphate buffer pH 4.8, pH 6.8, pH 7.4, pH 7.8 and pH 8.2 at a temperature maintained at 37°C ± 0.5°C. The flasks were then shaken for a minimum of 24 h in water bath shaker. The suspension was then filtered, analyzed spectrophotometrically at 263 nm and further the equilibrium solubility was determined [70].

### 2.2.3 Synthesis of magnetic nanoparticles (MNPs)

For the synthesis of MNPs, a mixture of ferric nitrite and ferrous sulphate (molar ratio of 2:1) was prepared to which liquid ammonia solution was rapidly added, until pH 10 of the solution is attained. The mixture was then stirred vigorously for 45 min. Nanoparticles were maintained in a uniformly dispersed form by addition of surfactant (Tween 80). The excess surfactant was removed using magnetic decantation and resulted MNPs were washed with Millipore water [71].

Synthesised magnetic nanoparticles were then lyophilized before subjecting them to any further application.

### 2.2.4 Characterization of Magnetics Nanoparticles

The magnetic properties of MNPs were recorded by analysing the sample of synthesised magnetic nanoparticles using vibrating sample magnetometer (VSM). The measurements such as analysis of saturated magnetization level and identification of superparamagnetic behaviour were recorded using VSM, from the hysteresis loop of M–H curve in the range ±10 kOe at room temperature [72].

## 2.3 Results and Discussion

### 2.3.1 Physical Observations

The first part of preformulation study is identification of the drug and asserting its purity. Physical properties like colour, odour, and physical appearance can be used as the first clue of drug's purity. They may not provide with a detailed information of level of impurity or the reason(s) of contamination but still are an important property for investigation of drug's physiochemical behaviour. The following parameters were analysed as a part of physical observation of drug for its identification:

**Table 2.1 Physical properties observed in the sample of 5FU**

| | |
|---|---|
| Colour | White |
| Odour | Odourless |
| Physical appearance | White crystalline powder |

All these characteristics were in compliance with the standard of 5FU as reported in Indian Pharmacopoeia.

### 2.3.2 UV spectrophotometric study

Every drug investigated under UV spectrophotometer provides a specific wavelength at which the drug absorbs the maximum energy, which is also referred as absorption maxima ($\lambda_{max}$ ) of that drug. This absorption maxima ($\lambda_{max}$ ) is an intrinsic property of every molecule and can be used to establish the purity of the drug. UV spectrophotometric study of 5FU was carried out in an acetate buffer (pH 4.7) in a scanning range of 200-400 nm. The $\lambda_{max}$ obtained were recorded in and compared with literature value authenticated the study. (Table 2.2, Figure 2.1)

**Table 2.2 Comparative λmax of 5 Fluorouracil in acetate buffer pH 4.7 with literature as well as experimental λmax**

| Solvent | λmax | |
|---|---|---|
| | Experimental | As per Indian Pharmacopoeia |
| Acetate Buffer (pH 4.7) | 266 | 266 |

The experimental value and the literature value of 5FU were found to be same indicating a high level of purity in the procured drug sample.

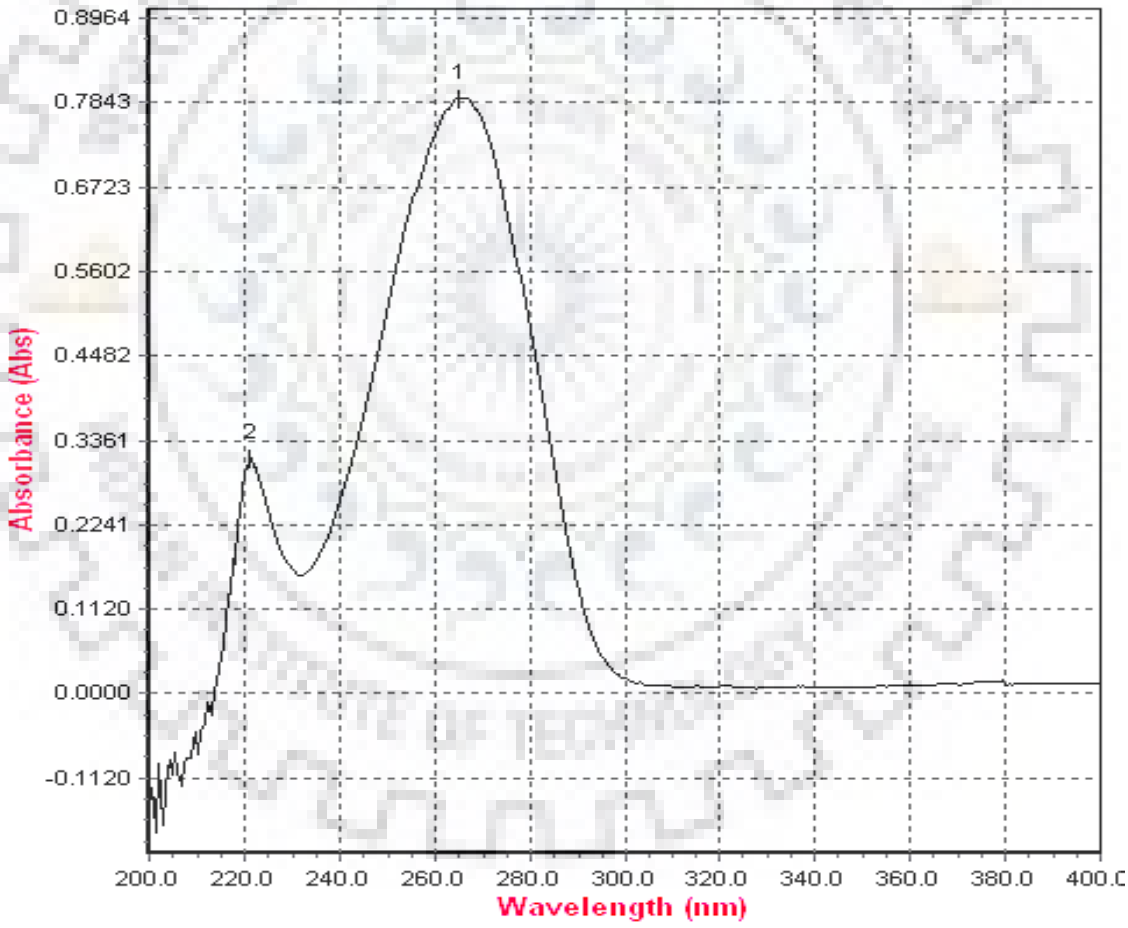


**Figure 2.1 UV Spectra of 5FU solution (0.001% w/v) in acetate buffer (pH-4.7)**

### 2.3.3 Equilibrium Solubility of 5FU

The solubility of 5FU was measured in different medium phosphate buffer (pH 4.8, pH 6.8, pH 7.4, pH 7.8 and pH 8.2). The results clearly depicts that the solubility of 5FU increases with an

increase in the pH of medium (Figure 2.2). These results can be attributed to the fact that 5FU is an acidic drug and its ionisation is promoted in a basic medium thereby increasing the solubility of the drug [73,74]. Solubility of 5FU is investigated during the preformulation studies to predict the amount of drug which can be dissolved in a specific pH of solvent during the development of formulation.

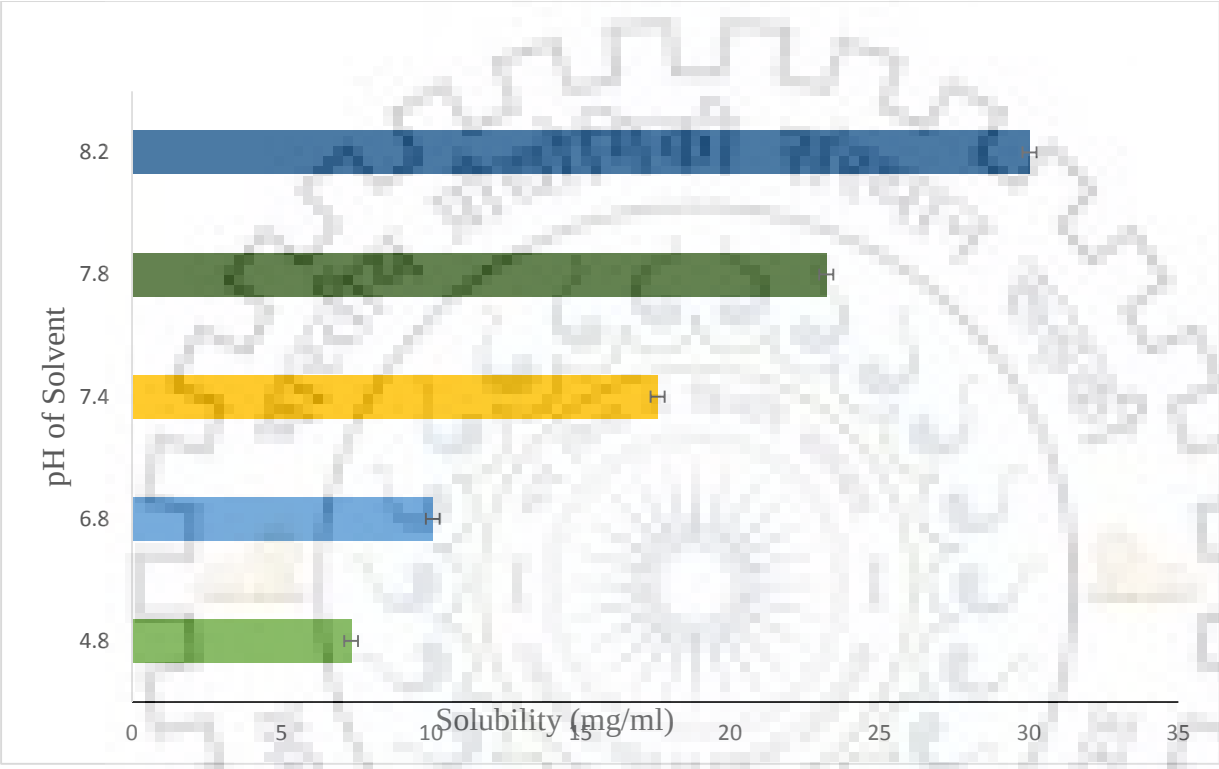


**Figure 2.2 Effect of pH of medium on solubility of 5FU**

### 2.3.4 Fourier Transform Infrared (FTIR) Analysis

The IR absorption spectrum of 5FU was found to be concordant when compared with the reference spectrum of 5FU (Figure 2.3). The typical peaks of the analyzed drug sample were also interpreted (Table 2.3). The peak of C-F bond was observed at 1181 $cm^{-1}$, presence of aromatic ring produced a peak between 500-600 $cm^{-1}$ and also between 2500-3000 $cm^{-1}$. There were C=C stretching peak at 1346 $cm^{-1}$ and 1554 $cm^{-1}$. The spectra did not reveal any shift or any new peak thus confirming the purity of the sample [75].

**Table 2.3 IR spectral peaks with their respective stretching**

| Wave number ($cm^{-1}$) | Vibration mode |
|---|---|
| 993.6 | C-F bond |
| 500-600 and 2500-3000 | Aromatic ring region |
| 1300-1550 | C=C and C≡N stretching |
| 2868 | N-H stretching |
| 1181 | C-N and C-O vibration |

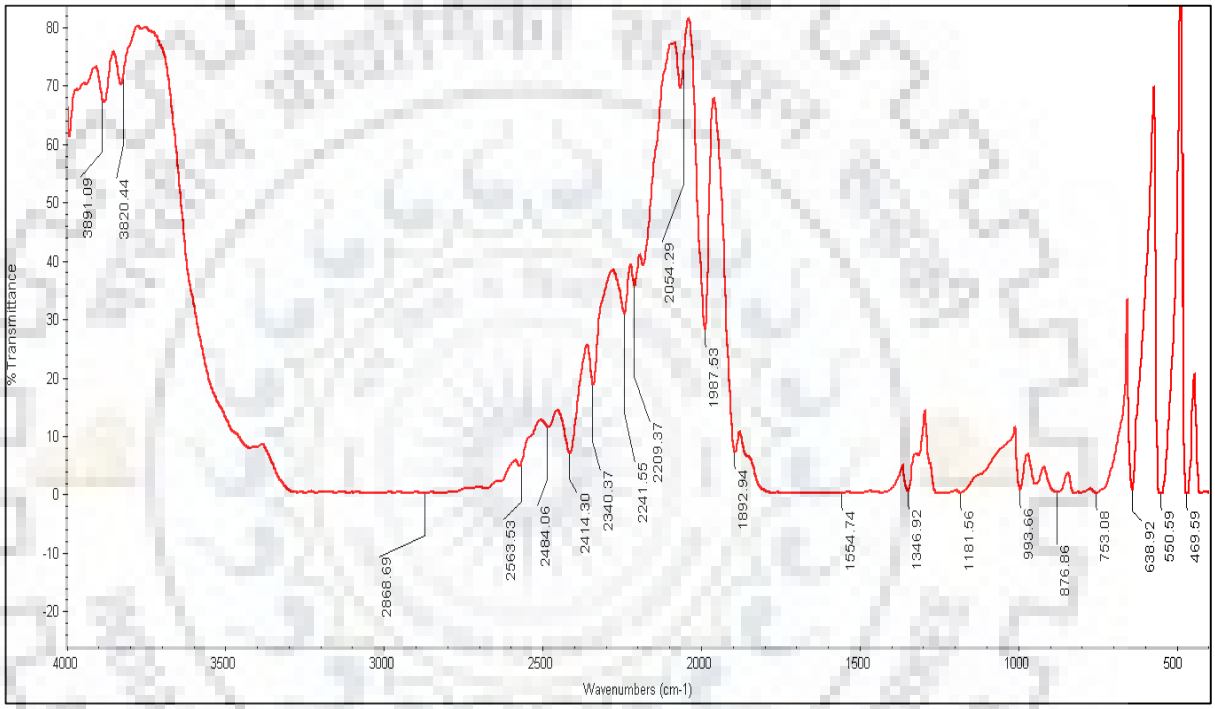


**Figure 2.3 FTIR spectra of 5FU showing different characteristic peaks**

### 2.3.5 Preparation of calibration curve

The quantitative estimation of amount of drug present in any formulation requires the accurate estimation of its calibration curve. The absorbance of standard concentrations of 5FU (2-12 µg/ml) were plotted (Figure 2.4) and linearity was observed with an $r^2$=0.9995 and $r^2$ =0.9997 in millipore water and phosphate buffer pH 7.4 respectively (Table 2.3). Solutions of 5FU in 2-12 µg/ml range also exhibited linearity with regression equations y=0.0621x + 0.0054 and y= 0.089x + 0.0063 in phosphate buffer pH 7.4 and distilled water when analyzed at $\lambda_{max}$ of 263 nm [45].

These regression value obtained in water and buffer suggest that 5FU can be accurately quantified in the range of 2-12 µg/ml.

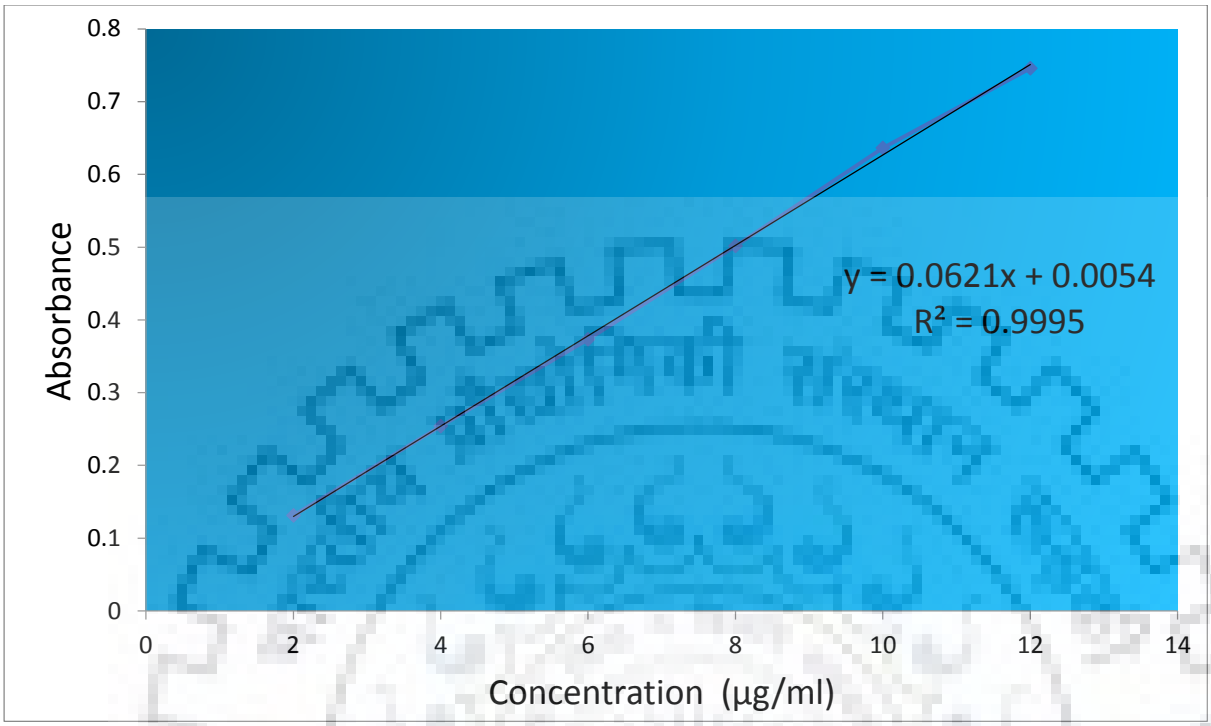


**Figure 2.4 (A)**

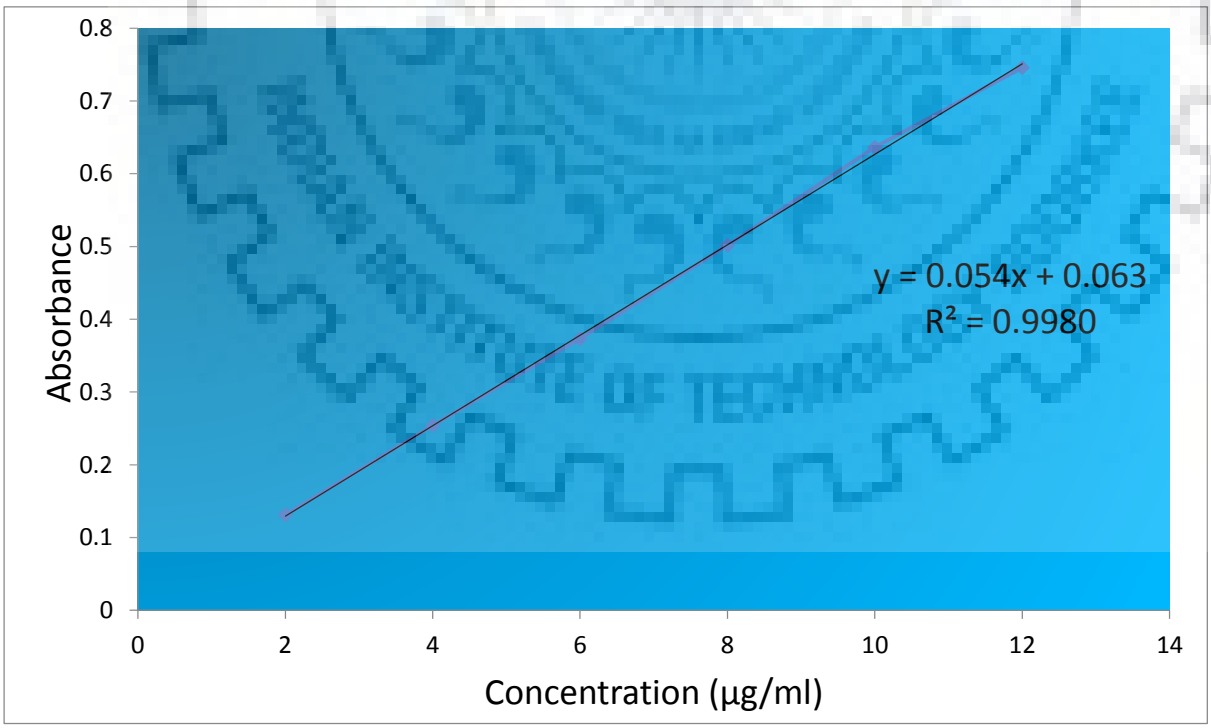


**Figure 2.4 (B)**

**Figure 2.4 Standard plot of (A) 5FU in (PBS) pH-7.4 and (B) distilled water**

### 2.3.6 Characterization of magnetic nanoparticle

Fourier transform infrared spectroscopy (FTIR) of the as-synthesised magnetite nanoparticle was performed and spectra revealed the peaks at around 648 $cm^{-1}$ which is the characteristic peak of magnetite, related to Fe-O bond [76]. Another peak observed in spectra at 3405 $cm^{-1}$ relates to the -OH group (Figure 2.5).

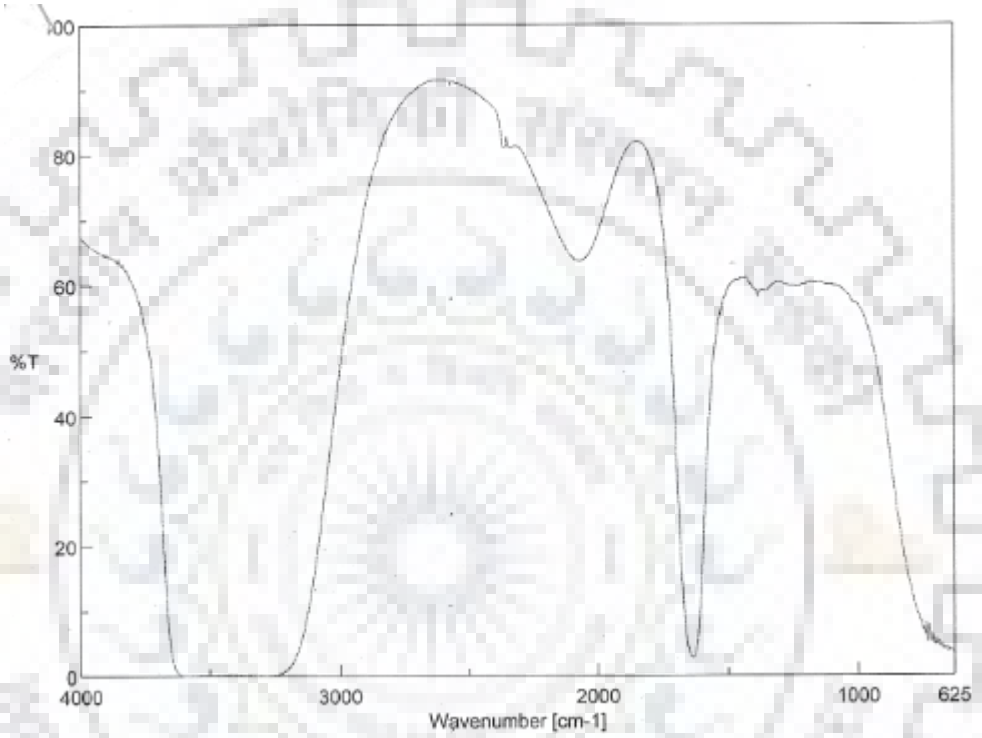


**Figure 2.5 Fourier transform infrared (FTIR) spectra of synthesized magnetite nanoparticles**

Further synthesized MNPs were characterized for particle size analysis using FE-SEM. Magnetic nanoparticles showed discrete, homogenous and spherical particles in the size range of 15-25 nm (Figure 2.6). The particle size of synthesized magnetic nanoparticles was optimal as it can easily be used for further application in designing of a targeted therapy for cancer. Also, the surface morphology of the magnetic nanoparticle was visualized under 100KX magnification and was found to be spherical in shape with a smooth surface. A smooth, spherical structure accounts for a high surface area which is essentially required for coating of these particles further for their use in designing of new nanoformulation.

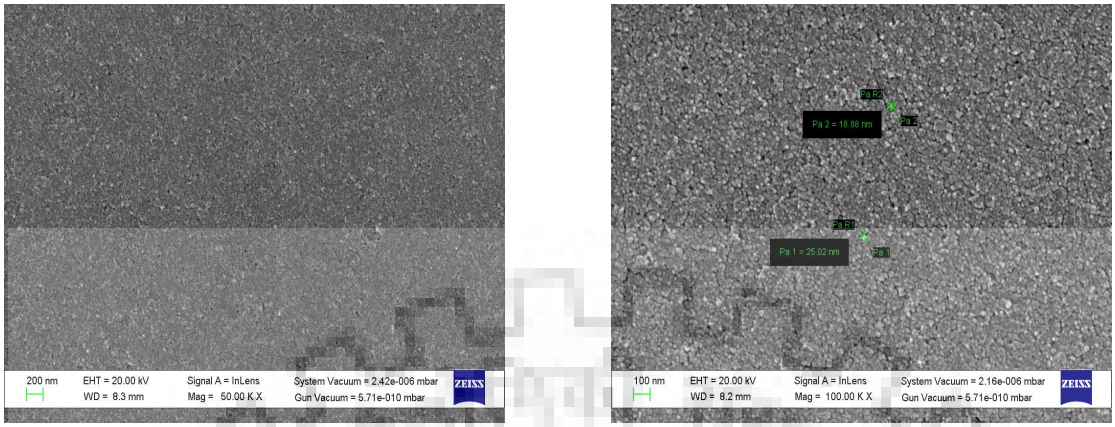


**(A)** **(B)**

**Figure 2.6 FE-SEM of magnetics nanoparticles at 50 KX(A) and 100 KX(B)**

After the analysis of the structure and shape of the system, magnetic property of nanoparticles was also investigated. For this, the visual examination using an external magnetic source was done, which clearly illustrated that the synthesized magnetite nanoparticle holds the magnetic property and can be directed to any particular area by means of application of external magnetic field (Figure 2.7).

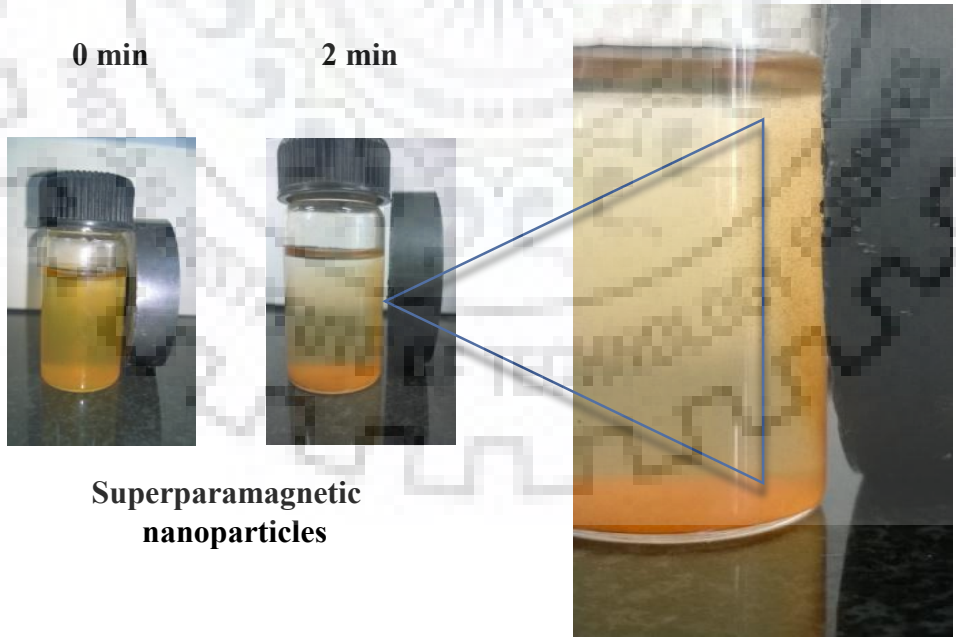


**Figure 2.7 Deviation of magnetic nanoparticles under the influence of external magnetic field**

These magnetic nanoparticles were further analyzed for quantifying its magnetic strength using vibrating sample magnetometer (VSM). The saturation magnetization of the magnetic nanoparticles was found to be 43 emu/g, which suggest that magnetic nanoparticles holds a strong magnetic property that can be utilized for directing it in *in vivo* conditions also (Figure 2.8). According to VSM results the sample also possess a superparamagnetic character which is quite evident by the nature of hysteresis loop obtained [77].

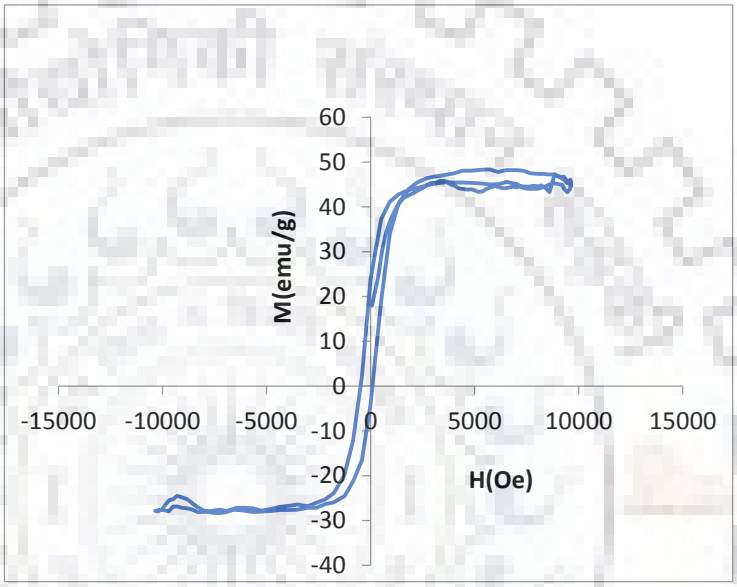


**Figure 2.8 Magnetization plot of synthesized magnetic nanoparticles**

# CHAPTER 3

# SYNTHESIS AND CHARACTERIZATION OF HTCC 5FU MAGNETIC NANOPARTICLES

## 3.1 Introduction

Development of pharmaceutical therapeutics often involves different categories of polymers for their application in improvement of shelf life of drugs, bioavailability and imparting physical and chemical stability [78]. In recent years, the polymers of biological origin are widely explored because of their unique properties such as better biocompatibility and easy to design [79]. One of the most promising application of biopolymer is in the development of nanoparticulate drug delivery system which is not only used for imparting protection to drugs by preventing degradation but also has a role in controlled release properties to encapsulated drug [80].

Chitosan and its derivative N-(2-hydroxy) propyl-3-trimethyl ammonium chitosan chloride (HTCC) are among the most extensively explored carbohydrate biopolymers. These polymers possess favourable properties like biodegradability, biocompatibility and non-toxicity [81]. Although Chitosan is a well-established polymer with a wide range of applications e.g., as carriers for therapeutic molecules and as non-viral gene carrying vector, but it still have certain limitations when it comes to application in different pH values. Chitosan is poorly soluble above pH-6.5 which makes it unsuitable candidate for drug delivery in parts of body which have neutral to alkaline pH. The replacement of the amino group by methyl group in chitosan which is done using the reaction between and epoxy propyl trimethyl ammonium chloride (EPTAC) results in formation of N-(2-hydroxy) propyl-3-trimethyl ammonium chitosan chloride (HTCC), which possess an excellent solubility over a wide pH range. Besides this, HTCC also holds the property of working as absorption and permeation enhancer. It also has been used in controlling the release of bovine serum albumin (BSA) and parathyroid hormone by forming an encapsulated nanoparticulate system [51].

Different tumour-targeted nanotherapies have been developed and investigated over the years, and a substantial improvement in the therapeutic index of anticancer agents was observed by the use of chitosan [42]. Different studies are reported where novel hyaluronidase enzyme core-5-fluorouracil-loaded chitosan-polyethylene glycol-gelatin polymer nanocomposites have been successfully evaluated for their role in targeted and controlled drug delivery [82]. Targeting

nanoparticles based on magnetic effect were also investigated in 5-Fluorouracil encapsulated pectin nanoformulation [45].

5FU has been extensively used for the treatment of solid tumors of colon, rectum and breast. However, like other chemotherapeutic agents used for cancer therapy, it also affects the growth of normal healthy cells and often precipitates side effects such as diarrhea, nausea, vomiting, hair loss, fatigue, birth defects and liver disease [42]. Thus, it has been suggested that HTCC nanoparticles might help in localizing 5FU only in the cancerous tissues by means of EPR effect and prevent the side effects induced by 5FU. Moreover, magnetically targeted system provides with an additional benefit of targeting the drug to the site of action in addition to the passive targeting (Enhanced Permeability and retention effect). In the present study, we prepared 5FU encapsulated HTCC magnetic nanoparticles and investigated the conditions optimal for production of tumor-localized drug delivery applications. The release of 5FU from chitosan nanoparticles were evaluated by further mathematical models and the effectiveness of magnetically targeted system was evaluated.

### 3.2 Materials and Methods

#### 3.2.1 Materials

Chitosan (CS) and 5-Fluorouracil (5FU), glycidyl-trimethyl-ammonium chloride (GTMAC), and sodium tripolyphosphate (TPP) were purchased from Sigma Aldrich U.S.A. Ferric nitrite, ferrous sulphate, and liquid ammonia, were procured from Rankem. All the chemicals used in the study were of analytical of grade.

#### 3.2.2 Synthesis of Chitosan Based Magnetic Nanocarriers

Coprecipitation of 2:1 molar ratio of ferric nitrite (2.9 g) and ferrous sulphate (1 g) with liquid ammonia was used for preparation of superparamagnetic nanoparticles. Briefly, Liquid ammonia was added to a mixture of ferric nitrite and ferrous sulphate (molar ratio 2:1) until the pH of the solution reaches 10 ± 0.1. Mixture was continuously stirred for another 45 min. Magnetic nanoparticles (MNPs) thus formed were magnetically separated and washed with Millipore water and lyophilized for further use [71].

### 3.2.3 Deacetylation of chitosan

HTCC synthesis was carried out by dispersing chitosan (1g) in a basic medium (pH-8-9), 10mL of 10% (w/w) sodium hydroxide (NaOH) solution containing (sodium borohydride) $NaBH_4$ (1 g) as an antioxidant [83]. After 5 h of continuous stirring at a temperature of 110 ˚C, the mixture obtained was filtered over a glass filter and washed repeatedly with distilled water until pH turned neutral. The chitosan was then washed using methanol and acetone and dried overnight at 70 ˚C under vacuum.

### 3.2.4 Synthesis of HTCC

The HTCC was prepared by a method of Lim & Hudson, 2004. The deacetylated chitosan (1 g) was dispersed in distilled water (10 ml) at 85 ˚C. Glycidyl-trimethyl-ammonium chloride GTMAC (3.45 ml) was added to the deacetylated chitosan in three equal portions of 1.15 ml each, at 2 h intervals. After the reaction time of 10 h, the solution was poured into cold acetone (30 ml) while continuous stirring and kept at a temperature between 2-8 ˚C overnight. Acetone was then decanted, and the left over product was dissolved in methanol (20 ml). The solution was precipitated in 4:1 acetone–ethanol (40 ml). The final product was dried at 70 ˚C overnight [52]. .

### 3.2.5 Preparation of HTCC 5FU Magnetic Nanoparticles

HTCC solution of varied concentration (0.5-3.0 mg/ml) were prepared in distilled water and 5FU (1mg/ml) was dissolved in it with constant stirring at room temperature. Magnetic nanoparticles (0.2 g ) were than dispersed in this solution. Further, TPP aqueous solution (0.6 ml) with various concentrations (0.6, 0.8, 1.0, and 1.2 mg/ml) was then added to 1 ml of HTCC mixture. Three different type of formations in the form of solution, aggregates and opalescent suspension were observed. The compositions producing opalescent suspension were chosen for further examination [84].

### 3.2.6 Physicochemical Characterization of HTCC 5FU Magnetic Nanoparticles

The size and structure of the prepared HTCC 5FU magnetic nanoparticles were performed by TEM-100CXII. Briefly, TEM(FEI Tecnai G2 operated at 200 kV) analysis was done using samples prepared by transferring a drop of nanoparticles on carbon-coated copper grid and air dried before analysis. Particle size distribution of 20 particles (HTCC 5FU magnetic nanoparticles) were calculated using ‘Image J 1.49’ software (NIH, USA). Further, the magnetic

properties of MNPs were recorded by analysing the sample of synthesised magnetic nanoparticles using vibrating sample magnetometer (VSM). The measurements such as analysis of saturated magnetization level and identification of superparamagnetic behaviour were recorded using VSM, from the hysteresis loop of M–H curve in the range ±10 kOe at room temperature.

### 3.2.7 Optimization Study of Nanoparticles

The size and zeta potential of the nanoparticles are important parameters which dictate the conditions for selection of the optimized formulation. The study design was based on the nanoparticle prepared by mixing HTCC solution of various concentrations (0.5, 1.0, 1.5, 2.0, 2.5 and 3.0 mg/ml), with TPP aqueous solution of concentrations (0.6, 0.8, 1.0, and 1.2 mg/ml) [51].

### 3.2.8 Infrared Spectroscopy

Potassium bromide pellet method was utilized for identification of modified functionality in the parent structure of chitosan while the conversion into HTCC took place. The sample under study was mixed with IR grade potassium bromide in the proportion of 1:50 and converted to pellets by application of ten metric ton of pressure. The formed pellets were then scanned over the range of 400 to 4000 $cm^{-1}$. The peaks obtained in the spectra were used for structure elucidation of the formed polymer [85].

### 3.2.9 Determination of Surface Potential

Measurement of surface charge is important for predicting the interaction capability of nanoformulation with the biological system and also for analyzing the colloidal property and physical stability of the formulation during storage. For the stability of any disperse system the value of zeta potential must lie either above +30 mv or below -30 mv.

The surface potential of HTCC 5FU magnetic nanoparticles was measured using zeta sizer (Malvern Zeta Sizer ZS90). Briefly, a uniformly dispersed nanoformulation of 5FU was placed in the capillary cell of in the instrument and loaded into the sample holder of zeta potential analyser [68,86].

### 3.2.10 Determination of Entrapment Efficiency

Any drug when incorporated into a polymeric coat has a tendency of getting attached either on the surface of polymeric system or may be entrapped within the polymeric coat. In both the cases

the drug is bonded with the formulation and the amount of drug bonded needs to be calculated. This property is known as drug entrapment efficiency and is an important aspect of polymeric formulation which is required to be calculated for further calculation of drug release or during the *invitro* and *in vivo* studies [87].

The entrapment efficiency is expressed as:

$$\% EE = \frac{Total\ Drug\ used\ for\ formulation - free\ drug\ in\ Supernatant\ layer}{Total\ Drug\ used\ for\ formulation}\ X\ 100$$

Briefly, a known amount of nanoformulation was added in to phosphate buffer solution and centrifuged at 15,000 X g for 30 min, the amount of free 5FU was determined in the clear supernatant liquid using UV spectrophotometer at 263 nm. Encapsulation efficiency was then calculated using the above formula [88,89].

### 3.2.11 Drug-Excipient Compatibility Study

Differential scanning calorimetric (DSC) is widely used to technique to investigate and predict any physiochemical interaction between drug and excipients [90]. Differential scanning calorimetric (DSC) curves were measures using a scanning calorimeter (Pyris Diamond, Perkin Elmer, USA). A small amount of HTCC 5FU magnetic nanoparticles and sample of pure 5FU was placed in the aluminium pan and heated from 0°C to 700°C at a heat flow rate of 10 °C/min under nitrogen spurge [91].

### 3.2.12 Evaluation of *In Vitro* Drug Release

In vitro drug release of 5FU from HTCC 5FU magnetic nanoparticles was measured by dialysis bag diffusion technique. Briefly, nanoparticles carrying 5 mg equivalent of 5FU was weighed and dispersed in 5 ml PBS 7.4 and transferred in a dialysis bag (molecular cut-off between 12-14KDa). The dialysis bag was then suspended in a receptor compartment containing 95 ml PBS 7.4 with continuous stirring at 100 rpm. For the estimation of drug release, at specific time intervals sample (equivalent to 1.5 ml) were withdrawn from the receptor compartment and replaced with the same amount of fresh PBS 7.4. The samples were centrifuged at 15,000 rpm for 15 min to separate the free 5FU and was analysed using LI 2800 (lasnay international) UV visible spectrophotometer against appropriate blank [45,92- 93].

### 3.2.13 Stability Studies

The stability of pharmaceutical product is an essential requirement which need to be attained by all the products before they can be accepted for scaleup. Stability study ensures that the product quality is retained in the formulation for a desire period of time [94]. Briefly, the freshly prepared nanoformulation were packed in glass vials and placed at 40 ± 2°C, 75 ± 5% relative humidity (RH) as per ICH guidelines for a period of 6 months. Nanoformultion was re-dispersed in PBS pH-7.4 and analysed for its percentage entrapment during the course of study.

## 3.3 Results and Discussion

### 3.3.1 Synthesis of HTCC from chitosan

One of the important step before the formulation of HTCC 5FU magnetic nanoparticle could actually take place is the conversion of chitosan to HTCC. The derivatisation of chitosan to HTCC is carried out by the replacing the amino group of chitosan by a methyl group. This makes the polymer ionizable even at pH value that is towards the basic value, thus making it a suitable candidate for nanoparticle formation even with those system which involves basic medium (Figure 3.1). After the synthesis of HTCC from chitosan it was evaluated for its conversion. Initially, it is predicted by checking its solubility in water and in phosphate buffer pH 7.4, but for confirmation of the same it was investigated using infrared (IR) spectroscopy. The analysis of IR spectra of HTCC was compared to that of parent polymer that is chitosan and it was found that the peak of $-NH_2$ disappeared which is normally at around 1600 $cm^{-1}$ because of N-H bending, in HTCC while it was present in chitosan. This amino group is replaced by methyl group there is an additional peak around 1416 $cm^{-1}$ observed in Figure 3.2.

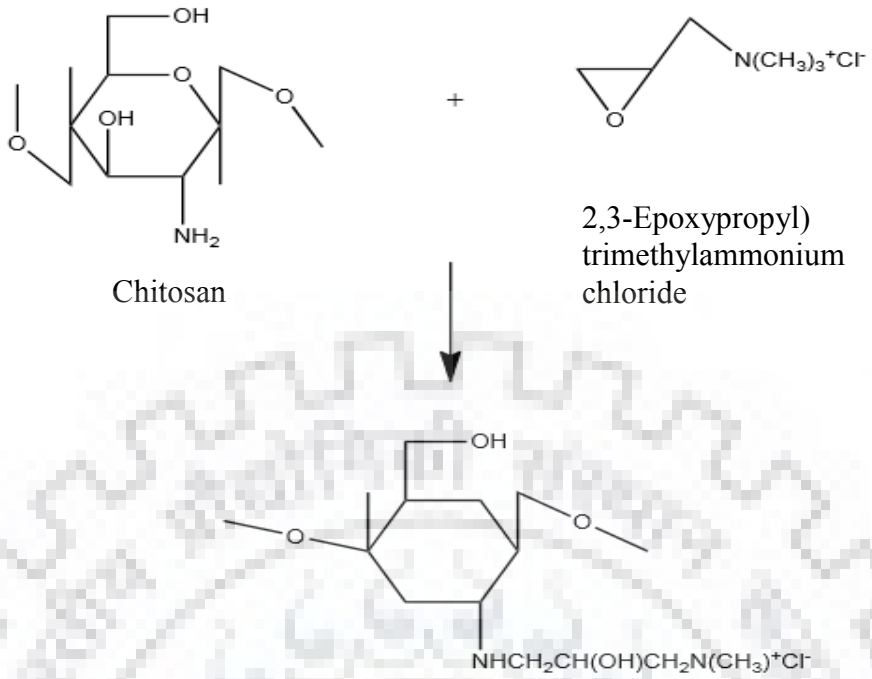


N-(2-hydroxyl) propyl-3-trimethyl ammonium chitosan chloride

**Figure 3.1 Synthesis of HTCC from chitosan**

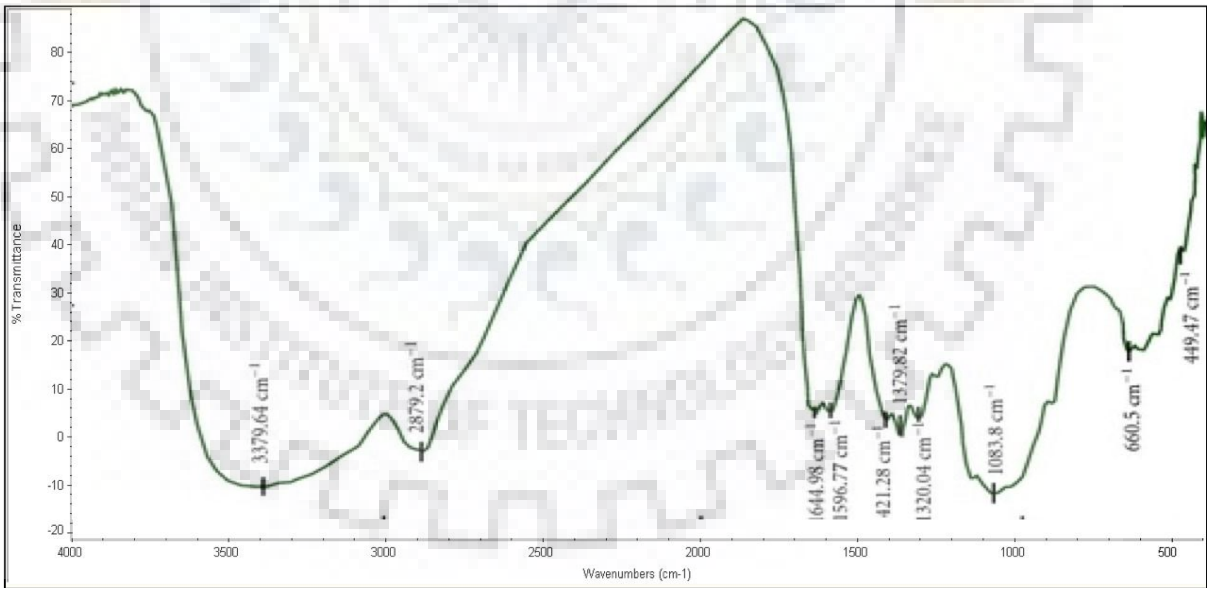


**(A)**

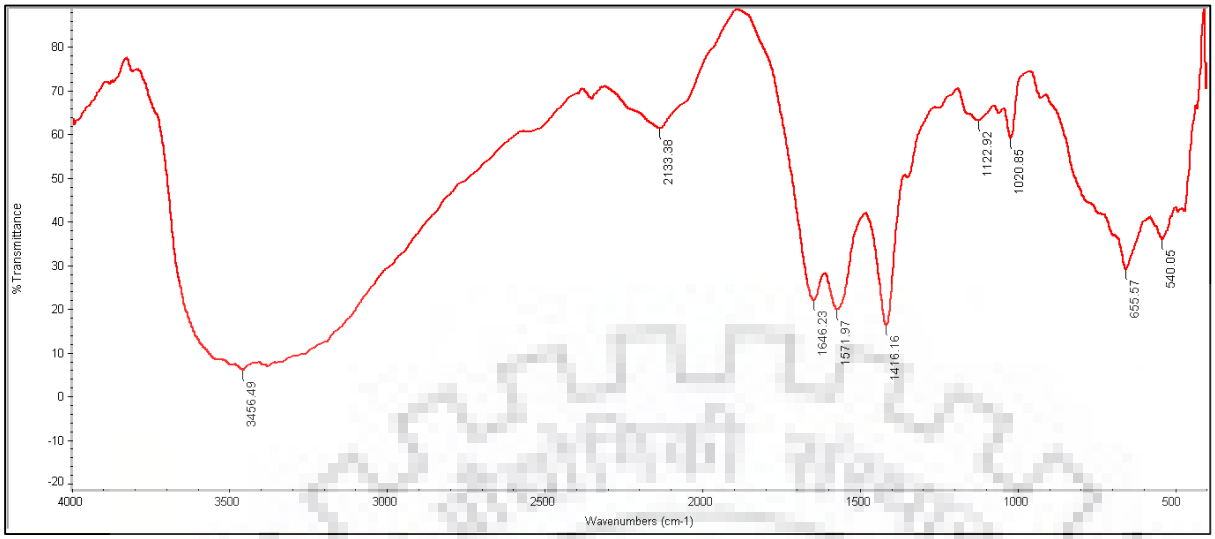


**(B)**

**Figure 3.2 IR spectra of (A) chitosan and (B) N-(2-hydroxyl) propyl-3-trimethyl ammonium chitosan chloride (HTCC)**

### 3.3.2 Physiochemical characterization of nanoparticles

5FU encapsulated nanoparticles were formulated using ionic gelation techniques at room temperature, which involves the interaction between the positively charged HTCC and negatively charged STP resulting in the spontaneous formation of nanoparticles. Particle size measurement may reveal some information about the entrapment of drug, their clearance from body and even the targeting mechanism.

Generally, a larger particle may have a large centric core and will allow for more efficient drug entrapment and a slow diffusion of drug from them. Further, a nanoparticle of size less than 10 nm may be rapidly cleared by kidney whereas more than 100 nm may be phagocytosed by cells of reticuloendothelial system (RES). The size of particle again dictates the mechanism of targeting attained by them, particle size between 100-400 nm are probably a better choice for passive targeting and shows an enhanced permeability and retention (EPR) effect. TEM analysis of the formulated nanoparticles indicate that the nanosystem exhibit a smooth surface and fine morphology, with a mean diameter of ~180 nm (Figure 3.3). TEM analysis of nanoparticles also revealed the encapsulation of magnetic nanoparticles in the nanocarrier system which is evident with the formation of concentric rings due to the presence of polycrystalline magnetite nanoparticles as seen using selected area electron diffraction (SAED) measurement [95]. The

observed zeta potential values were above +37.8 mV (Figure 3.4), confirming the stability of prepared nanocarrier.

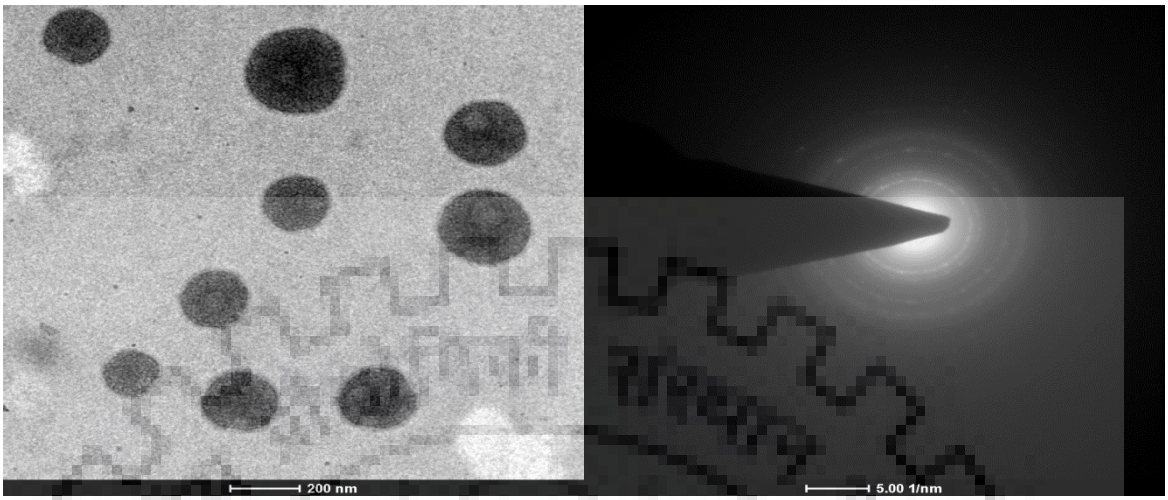


**Figure 3.3 Transmission electron microscopy and SAED images showing encapsulated 5FU and magnetite nanoparticles**

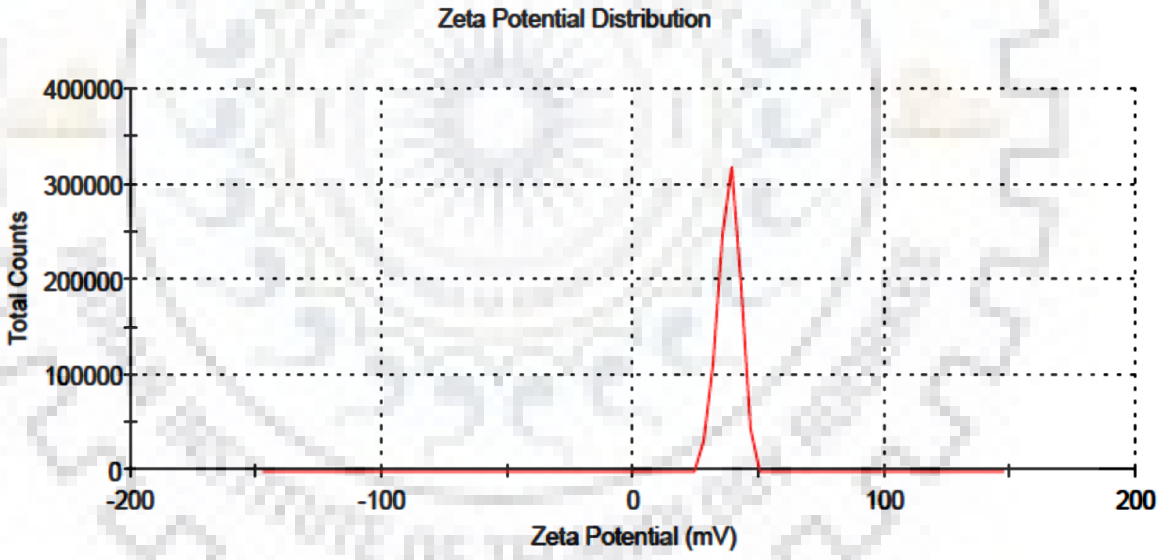


**Figure 3.4 Zeta potential of the samples measured to be +37.8 mV**

### 3.3.3 Optimization of the nanoformulation

Nanoformulation were prepared using a different combination of HTCC concentrations (0.5 -3.0 mg/ml) and STP concentration (0.6 - 1.2 mg/ml) (Table 3.1). These different combination of polymers results in different property of the formulated system. To identify the best possible combination which can further be evaluated for the *invitro* and *in vivo* activity % encapsulation efficiency of each combination was extensively evaluated. It was observed that the best

combination to give the maximum encapsulation efficiency is one with HTCC concentration of 0.5 mg/ml and STP concentration of 0.8 mg/ml which showed a percentage encapsulation of 95.83 (Figure 3.5). It was evident from the data of encapsulation efficiency that an increase in the STP concentration in all the combination of HTCC lead to aggregate formation or sometime very large particle size. To have a particle size in the optimal range and to avoid any chances of aggregation the composition used for nanoparticle played an important role. Again from the Table 3.1 it was concluded that aggregate formation was observed when the concentration of HTCC was comparatively higher than the STP concentration, which may be attributed to crosslinking of multiple chains of HTCC in the presence of high concentration of STP. This best combination of HTCC and STP was therefore, used further for the evaluation of invitro drug release and *in vivo* anticancer activity.

**Table 3.1 Influence of HTCC concentration and STP concentration on encapsulation efficiency of nanoformulation**

| HTCC Concentration (mg/ml) | STP Concentration (mg/ml) | Appearance | Encapsulation Efficiency (%) |
|---|---|---|---|
| 0.5 | 0.6 | Turbid | 89.78 |
| | 0.8 | Turbid | 95.83 |
| | 1.0 | Aggregate | 95.08 |
| | 1.2 | Aggregate | 94.52 |
| 1.0 | 0.6 | Turbid | 94.52 |
| | 0.8 | Turbid | 94.05 |
| | 1.0 | Turbid | 93.95 |
| | 1.2 | Aggregate | 93.36 |
| 1.5 | 0.6 | Turbid | 92.22 |
| | 0.8 | Turbid | 91.35 |
| | 1.0 | Turbid | 91.70 |
| | 1.2 | Turbid | 91.13 |
| 2.0 | 0.6 | Turbid | 91.32 |
| | 0.8 | Turbid | 90.40 |
| | 1.0 | Turbid | 90.80 |
| | 1.2 | Turbid | 90.68 |
| 2.5 | 0.6 | Clear solution | 89.60 |
| | 0.8 | Clear solution | 90.25 |
| | 1.0 | Turbid | 89.42 |
| | 1.2 | Turbid | 89.69 |
| 3.0 | 0.6 | Clear Solution | 89.83 |
| | 0.8 | Clear solution | 89.91 |
| | 1.0 | Turbid | 89.46 |
| | 1.2 | Turbid | 89.35 |

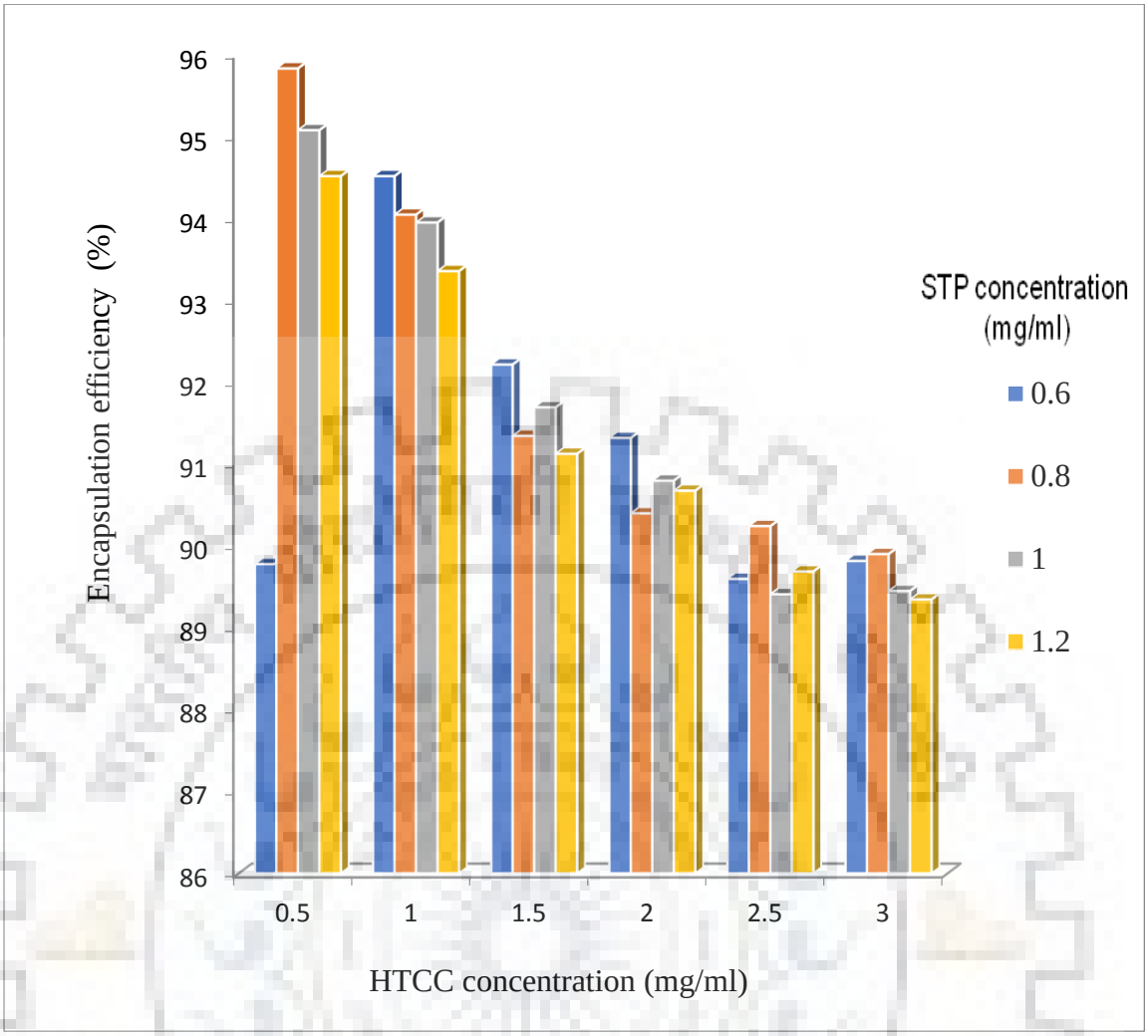


**Figure 3.5 Influence of HTCC concentration and STP concentration on encapsulation efficiency of nanoformulation**

### 3.3.4 Magnetic Properties of Targeting MNPs

Magnetic behaviour of the MNPs was investigated by measuring magnetization (M) against applied magnetic field (H) at room temperature using vibrating sample magnetometer by the alignment of dispersed magnetic particles towards the externally placed magnet (Figure 3.6 (A) and Figure 3.6 (B). The curve obtained indicates a typical superparamagnetic behaviour in both the curves which is attributed to magnetite nanoparticles. In the curve obtained after VSM analysis of naked magnetic nanoparticles and HTCC 5FU magnetic nanoparticles it was observed that the saturation magnetization level in naked magnetic nanoparticles was higher 45 emu/g (blue curve) which reduced to 30 emu/g (red curve) in case of HTCC 5FU magnetic nanoparticles. This decrease in the magnetic behaviour of magnetic nanoparticles may be attributed to the phenomenon of encapsulation.

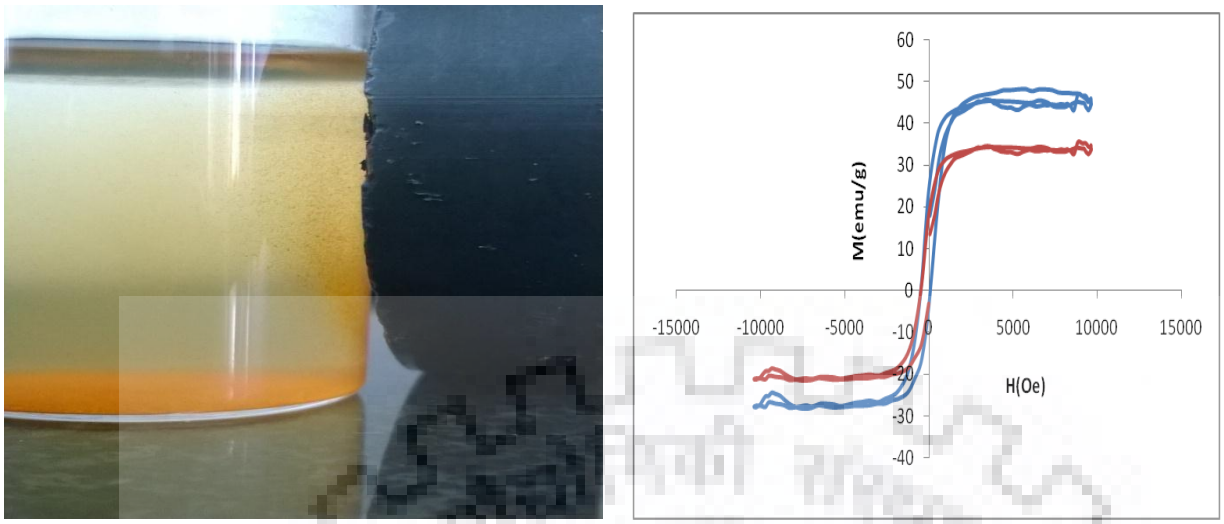


**(A)** **(B)**

**Figure 3.6 (A) Dispersion of the HTCC 5FU magnetic NPs attracted to the externally placed magnetic and (B) Magnetization Vs field (M-H) curve of naked magnetic nanocarrier (blue curve) and HTCC 5FU Magnetic NPs (red curve) measured using VSM**.

### 3.3.5 Drug-Excipient Compatibility Study

Comparing the physiochemical property of drug alone and in the formulation along with excipients is one the means of evaluating the kind and extent of interaction between the drug and excipients. Here in this study the thermal behavior of pure 5FU and in mixture was investigated by heating the respective samples at 10°C/min (Figure 3.7). For the first sample (pure 5FU) an endothermic peak was observed at 284°C. The second sample (HTCC 5FU magnetic nanoparticles) also retained the same endothermic peak. This clearly showed that there was no interaction between the drug and other excipients used in the study. Further, the formulation retained as a white coloured product after the completion of the study which reveals that there was no physical interaction between the drug and the excipients.

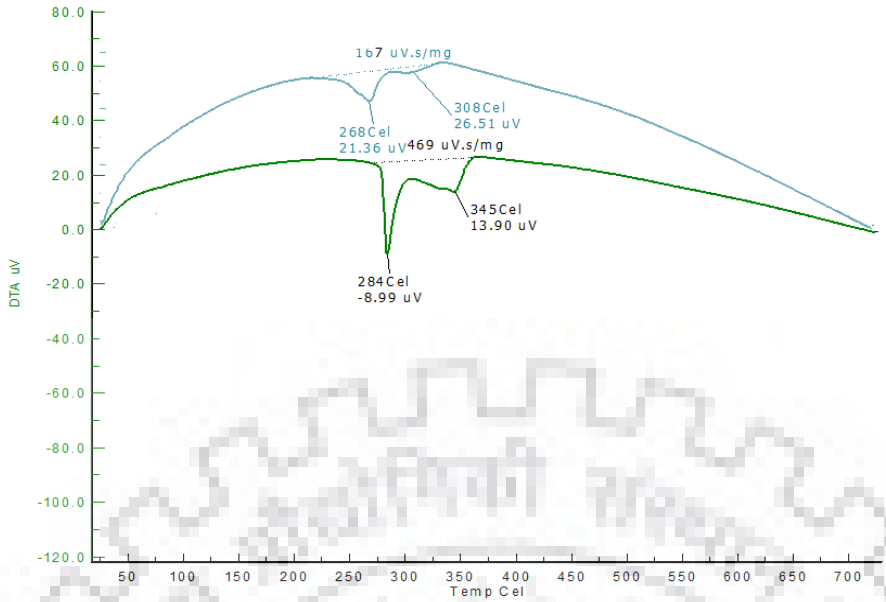


**Figure 3.7 DSC of 5FU (green curve) and Nanoformulation containing 5FU (blue curve)**

### 3.3.6 *In vitro* Drug Release

A first initial burst release of 25.6%, due to the drug desorption from the particles surface was observed as shown in Figure 3.8. Then, a slower sustained release followed for the period of 120 h. A sustained release of the drug for 3 days from the polymer matrix was observed over the period of study. Generally, there might be diffusion of the drug through the polymer matrix or an erosion of the coated polymer for releasing the drug through the nanoformulation into the external environment. The dissolution data was therefore subjected to different mathematical kinetic models to understand the mechanism of drug release from the nanoformulation and it was found that the best fit model for the HTCC 5FU magnetic nanoparticles was Korsmeyer-Peppa's with the $R^2$ value of 0.9798 and n value of 0.239 (Table 3.2) suggesting the release mechanism to be diffusion from the formulation [96].

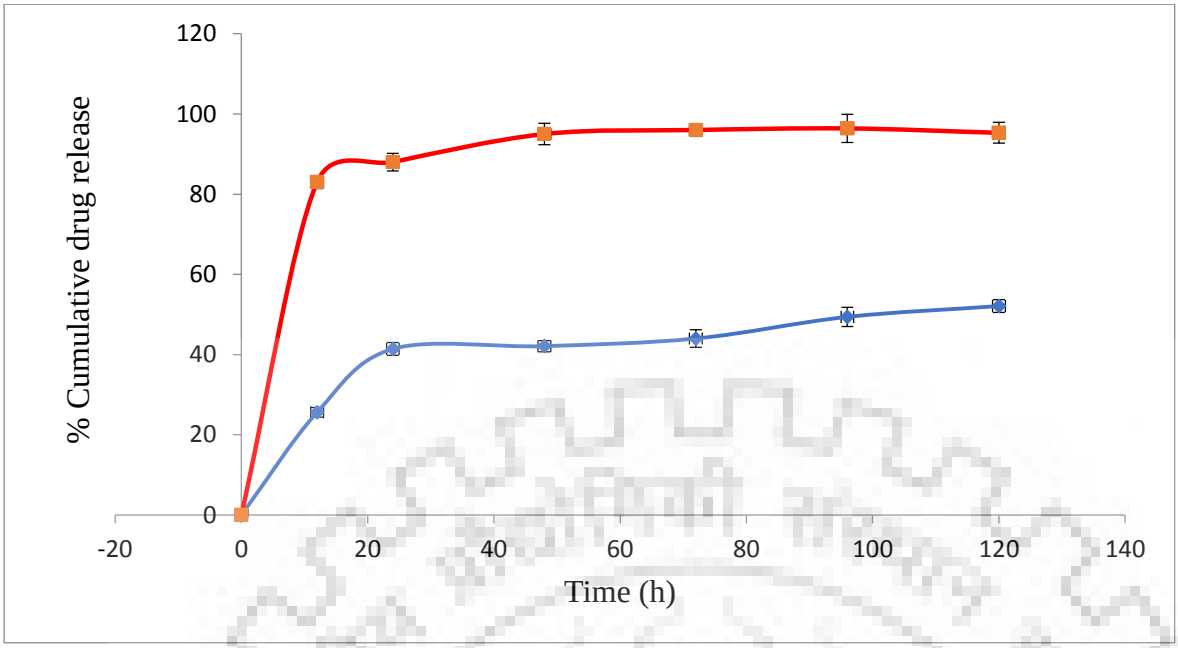


**Figure 3.8 5FU release profile from HTCC 5FU magnetic nanoparticles (HTCC 0.5 mg/ml, TPP 0.8 mg/ml) (blue curve) and 5FU dispersion (red curve)**

**Table 3.2: Determination of $R^2$ value for various mathematical models for the nanoformulation**

| **Zero order** | **First Order** | **Higuchi's** | **Korsmeyer-Peppa's** | |
|---|---|---|---|---|
| $R^2$ | $R^2$ | $R^2$ | $R^2$ | n |
| 0.6575 | 0.7458 | 0.8767 | 0.9798 | 0.239 |

### 3.3.7 Stability Studies

The investigation on the stability of nanoparticles over a period of six months indicated no stability issues with the prepared nanoparticles. In all the samples of nanoparticles which were analysed at the fixed time point (0, 2, 4, and 6 months) the changes in percentage drug entrapment efficiency was found to be statistically insignificant (Table 3.3). Moreover, no signs of physical incompatibility or degradation of the product were observed. This study further comply with the result observed during the drug-excipient compatibility study.

**Table 3.3 Stability study data of the HTCC 5FU magnetic nanoparticles**

| Time (months) | Appearance | Encapsulation efficiency (%) |
|---|---|---|
| 0 | White coloured powder | 94 .6 ± 2.2 |
| 2 | White coloured powder | 93.2 ± 1.6 |
| 4 | White coloured powder | 94.8 ± 1.8 |
| 6 | White coloured powder | 93.6 ± 2.4 |

# CHAPTER 4

## SYNTHESIS AND EVALUATION OF 5FU GOLD MAGNETIC NANOPARTICLES

### 4.1 Introduction

Combinational therapy has always been the better approach than having a single independent drugs acting against cancer [97]. There are different studies which investigated the effect of using multiple drug in a single formulation against cancer. A similar kind of study revealed that a combination of 10-hydroxycamptothecin (HCPT) and doxorubicin (DOX) in a nanoparticulate system not only enhance the retention of the drugs in drug resistant cancer cells but also enhance the efficacy of the drug against tumor cells [97]. A combination of HCPT integrated with methotrexate (MTX)–chitosan conjugate also helped in increasing the cellular uptake and sustained effect of the drug against HeLa cells [98]. The similar study was conducted for improving vaccines by a synergistic effect between biodegradable polymeric nanoparticles and aluminum based adjuvant [99]. An important aspect of designing any formulation for cancer involves the use of a specific targeting approach which in most of the cases is passive targeting (EPR effect) by virtue of the size of the particles in the formulation. However, it suffers from the limitation of missing out the targets in highly perfused area. Moreover, they do not have any ligand for binding with the targets and therefore, can also accumulate into the healthy cells. An active targeting approach therefore is a better choice for targeting the drug to the affected cells [100]. An active targeting approach has been designed by use of ligand targeting the drug to the site, chemical modification of drug itself or otherwise using some physical means of magnetic targeting or pH controlled drug delivery [101]. Chemical modification for targeting of drug may cause changes to the drug's therapeutic potential or even make it toxic, a physical targeting can therefore be a used as preferential approach towards the development of targeted drug delivery system. In the current study, a combinational therapy of 5FU and gold, using magnetic nanoparticles was developed. 5FU has been a well-established first line drug for solid tumors of colon, liver, and breast [102,103]. Gold is also reported to have potential antitumor activity [104,105]. It was expected that using both the agents in combination is not only going to generate a synergistic effect but will also have a reduced toxicity. Magnetite nanoparticles are considered to be very useful in active targeting due to their unique superparamagnetic properties and finds potential application in areas such as magnetically guided drug delivery systems, imaging of cancer cells for diagnostics, and providing treatment of solid tumors by hyperthermia [106].

Magnetic resonance imaging (MRI) is an important diagnostic tools which involves the application of magnetic nanoparticles by functioning as magnetic probes with significant increase of signal-enhancing capabilities. However, a lack of stability is one of the major barrier in the use of these MNPs for clinical applications. Coating MNPs within a polymers shell, or inorganic shell, can eliminate such problems associated with the bare MNPs and enhance its stability and functionality. The coating of MNPs with polymers or silica shell has been studied revealing some promising results [107]. Also, some research investigated the use of gold and silver as coating materials and found them as an ideal material for biomedical applications with low reactivity, high stability, and better biocompatibility properties [108]. Gold coatings promotes surface customization and can have further functionalization for medical applications. MNPs can therefore become stable in biological conditions and their surface can be altered using different attachment after coating with gold [109].

## 4.2 Materials and Methods

### 4.2.1 Materials

Chloroauric acid($HAuCl_4$), trisodium citrate and 5 fluorouracil (5FU) were procured from Sigma-Aldrich, ferric nitrite ($Fe(NO_3)_3$. $9H_2O$), ferrous sulphate ($FeSO_4$. $7H_2O$), liquid ammonia, and all the other reagents used in the study were of analytical grade and purchased from Rankem, India.

### 4.2.2 Synthesis of Magnetic Nanoparticles (MNPs)

For the synthesis of MNPs, a mixture of ferric nitrite and ferrous sulphate (molar ratio of 2:1) was prepared to which liquid ammonia solution was rapidly added, until pH 10 of the solution is attained. The mixture was then stirred vigorously for 45 min. Nanoparticles were maintained in a uniformly dispersed form by addition of surfactant (Tween 80). The excess surfactant was removed using magnetic decantation and resulted MNPs were washed with Millipore water [71] . Synthesised magnetic nanoparticles were then lyophilized before subjecting them to any further application.

### 4.2.3 Synthesis of Gold Coated Magnetic Nanoparticles

The synthesis of gold coated magnetic nanoparticles was carried out using the earlier reported protocol [110]. An aqueous solution of 15 ml chloroauric acid solution (2.0 mg/ml) was added to 105 ml of water and then boiled for 20 min. To this 5 ml of as-synthesised magnetic

nanoparticles solution was added, followed by the addition of 5 ml of 80 mM sodium citrate dihydrate, under stirring condition. The mixture was boiled for 10-20 min with constant stirring at 500 rpm. The gold-coated magnetic nanoparticles were well dispersed in water [111].

### 4.2.4 Preparation of 5FU coated magnetic gold nanoparticles

For the preparation of 5FU coated gold magnetic nanoparticles, 50 $cm^3$ of the as-synthesized gold magnetic nanoparticles were dispersed along with 5FU (5 mM) in water (25 $cm^3$) and stirred effectively for 12 h until the colour change from wine red to blue is observed [112]. The 5FU gold magnetic nanoparticles were then subjected to further studies for its characterization.

### 4.2.5 Characterization of 5FU gold magnetic nanoparticles

#### 4.2.5.1 UV-visible spectroscopic studies of 5FU gold magnetic nanoparticles

The UV-visible spectroscopic study was conducted for analysing the effect of time on the formulation of 5FU gold magnetic nanoparticles. The samples of 5FU gold magnetic nanoparticles were drawn at an interval of 6 h and analysed using uv-visible spectroscopy [113].

#### 4.2.5.2 Infrared spectroscopic studies of 5FU gold magnetic nanoparticles

5FU gold magnetic nanoparticles were mixed with IR grade potassium bromide in a proportion of 1:50 and converted to pellets. The FTIR (Perkin Elmer Spectrophotometer) spectrum of pellets was recorded in the range of 625 to 4000 $cm^{-1}$. The infrared spectra were used for characterization of the formulation.

#### 4.2.5.3 Particle size and surface morphology

TEM (FEI Tecnai G2 operated at 200 kV) analysis was done using samples prepared by transferring a drop of 5FU gold magnetic nanoparticles on carbon-coated copper grid and air dried before analysis. Particle size distribution of 20 particles (5FU gold magnetic nanoparticles) were calculated using 'Image J 1.49' software (NIH, USA).

### 4.2.6 Drug encapsulation efficiency

The 5FU loaded gold magnetic nanoparticles were separated from free 5FU by centrifugation at 14,000 rpm for 1 h at 25 °C. Concentration of 5FU in the supernatant was determined from its UV absorbance at 263 nm. Entrapment efficiency was calculated using the following formula [114]:

$$\% EE = \frac{Total\ Drug\ used\ for\ formulation - free\ drug\ in\ Supernatant\ layer}{Total\ Drug\ used\ for\ formulation}\ X\ 100$$

### 4.2.7 Magnetic Behaviour of 5FU Gold Magnetic Nanoparticles

The magnetic properties of 5FU gold magnetic nanoparticles were compared with bare magnetic nanoparticles recorded by vibrating sample magnetometer (VSM). The magnetization measurements using VSM were recorded from the hysteresis loop of M–H curve in the range ±10 kOe at room temperature [115].

### 4.2.8 Evaluation of *in vitro* Drug Release

*In vitro* release of 5FU was performed to understand the kinetics as well as mechanism of its release from the formulation (5FU gold magnetic nanoparticles). In brief, nanoparticle equivalent to 5 mg was placed in a dialysis bag (molecular cutoff between 12-14KDa). The dialysis bag containing 5FU gold magnetic nanoparticles was then suspended in a phosphate buffer solution at pH 7.4 (receptor compartment) and stirred continuously at 50 rpm. A 1.5 ml sample form receptor compartment was then withdrawn at specific time intervals and was replaced back with equal volume of fresh medium. The samples were further centrifuged at 15,000 rpm for 15 min, and the percentage (%) cumulative release of 5FU from 5FU gold magnetic nanoparticles was determined by analysing the supernatant liquid using LI 2800 (Lasnay International) UV visible spectrophotometer against appropriate blank. The release data was also subjected to mathematical modelling to understand the mechanism of drug release.

## 4.3 Results and Discussion

### 4.3.1 UV spectroscopic studies of 5FU gold magnetic nanoparticles

Gold nanoparticles are characterized using their plasmon band measured using UV-visible spectrum which is generally observed around 520 nm. Similarly the characterization of pure 5FU indicated a absorption maxima at 265 nm. While 5FU is added to gold colloid it was observed that the intensity of 5FU decreased and apart from the peak of gold nanoparticles observed at 520 nm there is an emergence of additional peak at 620 nm observed after 12h of reaction time, which is a result of nanoparticles aggregation (Figure 4.1). This aggregation of nanoparticles may have resulted because of the replacement of citrate molecules present on surface of gold nanoparticles by 5FU molecules. The 5FU molecules is having a greater electrostatic attraction

with gold nanoparticles than the citrate groups, later therefore is replaced easily by 5FU resulting in an additional plasmon band at higher wavelength [116].

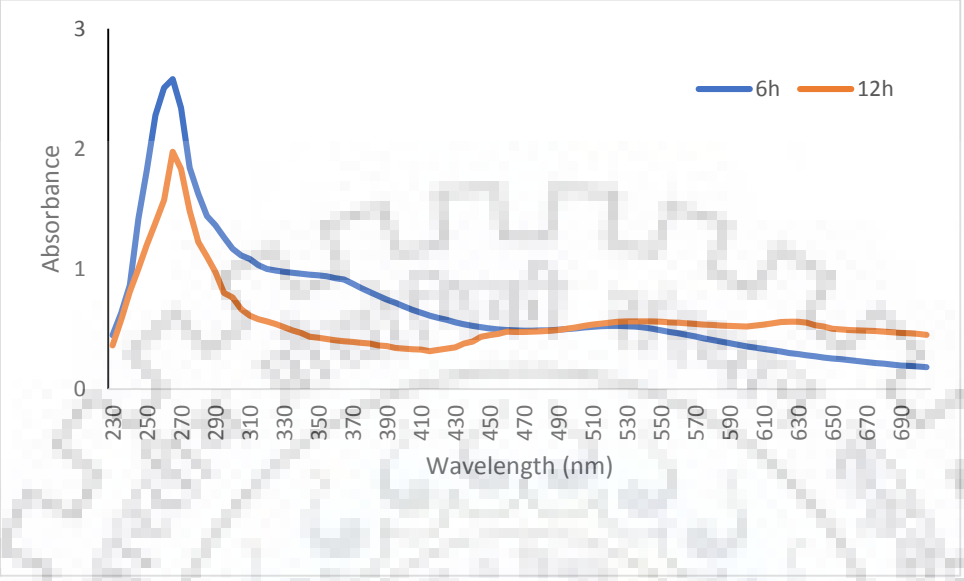


**Figure 4.1 Comparative UV-visible spectra of 5FU gold magnetic nanoparticles at 6 h and 12 h of synthesis**

### 4.3.2 Infrared spectroscopic studies of 5FU gold magnetic nanoparticles

The investigation of interaction of 5FU with gold nanoparticles were evaluated by subjecting the samples to infrared spectroscopy. Infrared spectra of pure 5FU (Figure 4.2 A) was compared with that of 5FU gold magnetic nanoparticles (Figure 4.2 B) and it was observed that the characteristic peak of -NH group present in 5FU at around 2868 $cm^{-1}$ shifted to 3434 $cm^{-1}$ and is broader than compared to the sample of pure drug. This also suggested that there is an interaction between the -NH group of 5FU and gold nanoparticles [117].

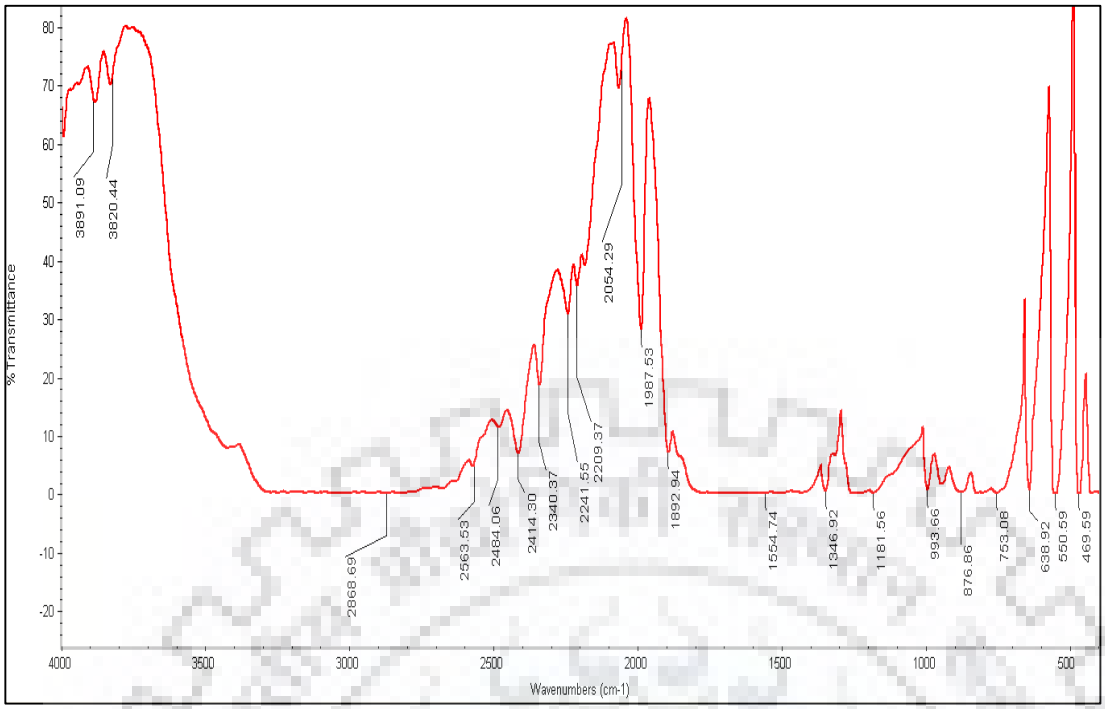


**Figure 4.2 (A)**

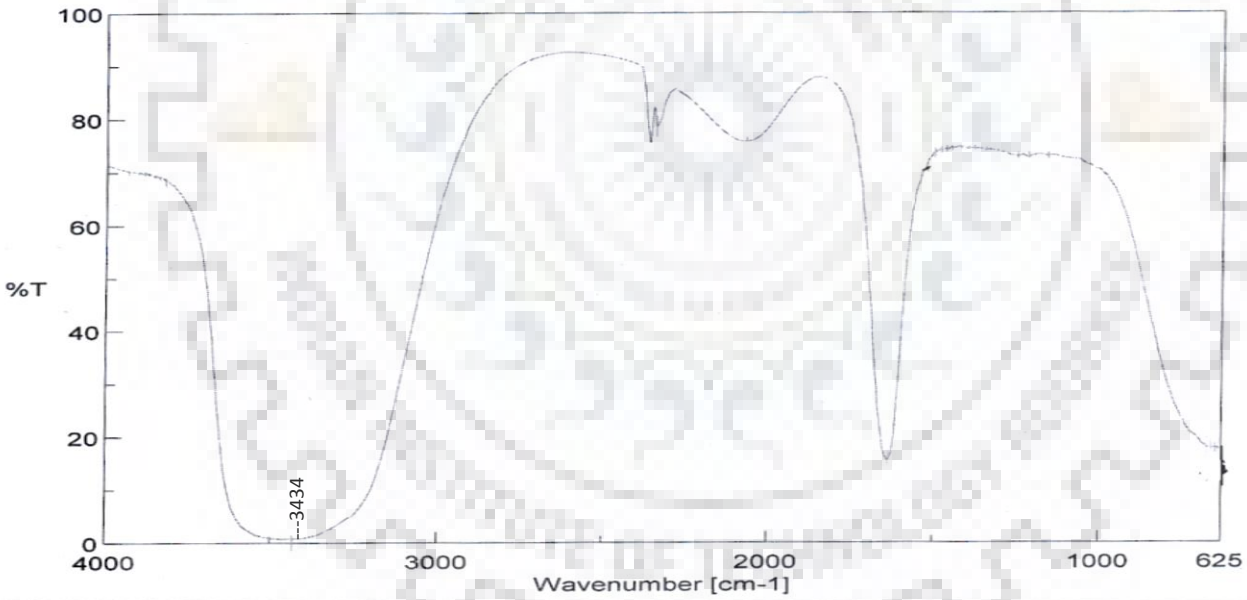


**Figure 4.2 (B)**

**Figure 4.2 (A) Infrared spectra of Sample of 5FU and (B) synthesised 5FU gold magnetic nanoparticle**

### 4.3.3 Magnetic behaviour of 5FU gold magnetic nanoparticles

Magnetic behaviour of the 5FU gold magnetic nanoparticles was studied by measuring the intensity of magnetization (M) of nanoparticles with the corresponding change in applied

magnetic field (H) at room temperature using vibrating sample magnetometer (VSM) and also through the alignment of dispersed magnetic particles towards the externally placed magnet (Figure 4.3). The curve obtained indicates a typical superparamagnetic behaviour in both the curves which is attributed to magnetite nanoparticles. In the curve obtained after VSM analysis of naked magnetic nanoparticles and 5FU gold magnetic nanoparticles it was observed that the saturation magnetization level in naked magnetic nanoparticles was higher 45 emu/g (blue curve) which reduced to 28 emu/g (red curve) in case of 5FU gold magnetic nanoparticles. This decrease in the magnetic behaviour of magnetic nanoparticles may be attributed to the phenomenon of encapsulation.

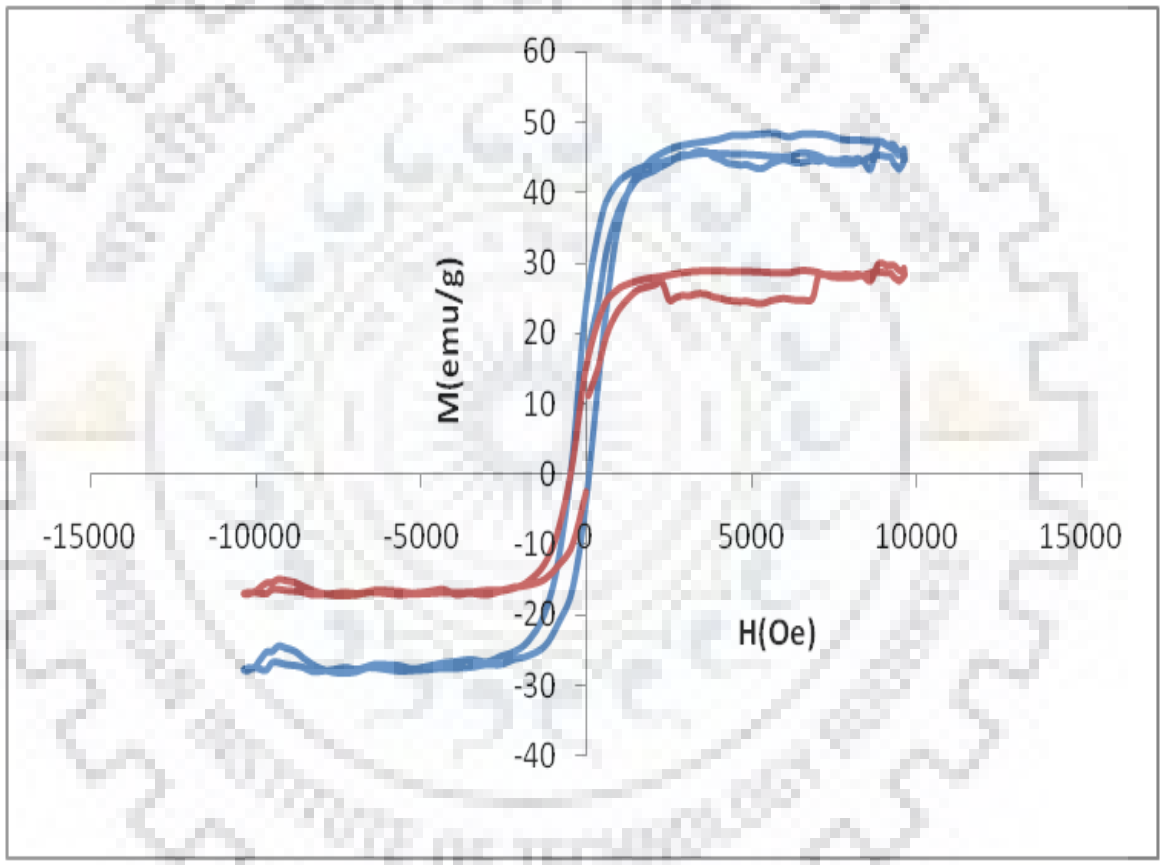


**Figure 4.3 Magnetization Vs field (M-H) curve of naked magnetic nanocarrier (blue curve) and 5FU gold magnetic nanoparticles (red curve) measured using VSM**

### 4.3.4 Particle Size and Drug Entrapment Efficiency (%)

5FU magnetic nanoparticles were found to have spherical structures and have a mean diameter of 42.5 nm as compared to bare magnetic nanoparticles which have a mean size of particles as 18 nm (Figure 4.4). The increase in the particle size of 5FU gold magnetic nanoparticles may be

attributed to the encapsulation of the bare magnetic nanoparticles by gold and then by 5FU which may result in increment in the size.

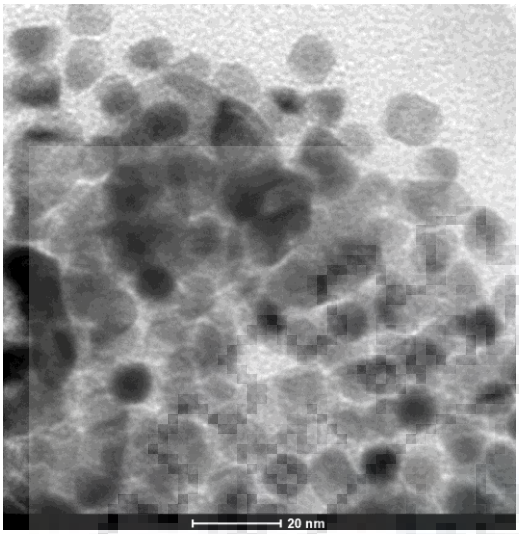


**Figure 4.4 (A)**

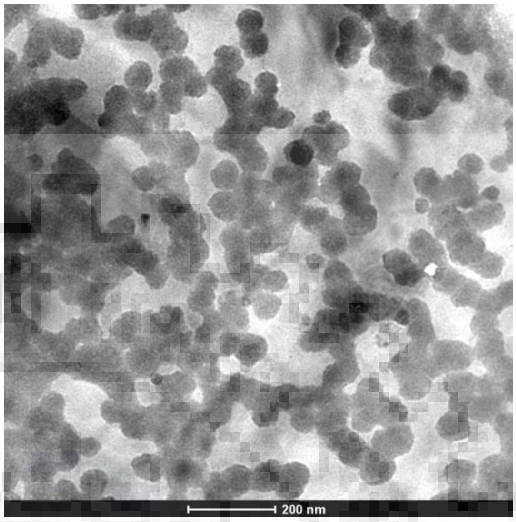


**Figure 4.4 (B)**

**Figure 4.4 TEM images of (A) Magnetic nanoparticles (B) 5FU gold magnetic nanoparticles**

Entrapment efficiency of the formulated 5FU gold magnetic nanoparticles were used for optimizing the time period required for incubation of 5FU with gold coated magnetic nanoparticles. It was observed on increasing the time of incubation the entrapment efficiency of 5FU also increased but this only reached a maximum percentage of 60.2 at 12 h of incubation time beyond which there was no further increase in entrapment of 5FU (Figure 4.5) This may be because 5FU is bound to gold coated magnetic nanoparticles by replacement of citrate group on the surface of gold surface, as more of 5FU gets attached the gold surface becomes saturated and hence, there is no further attachment of 5FU.

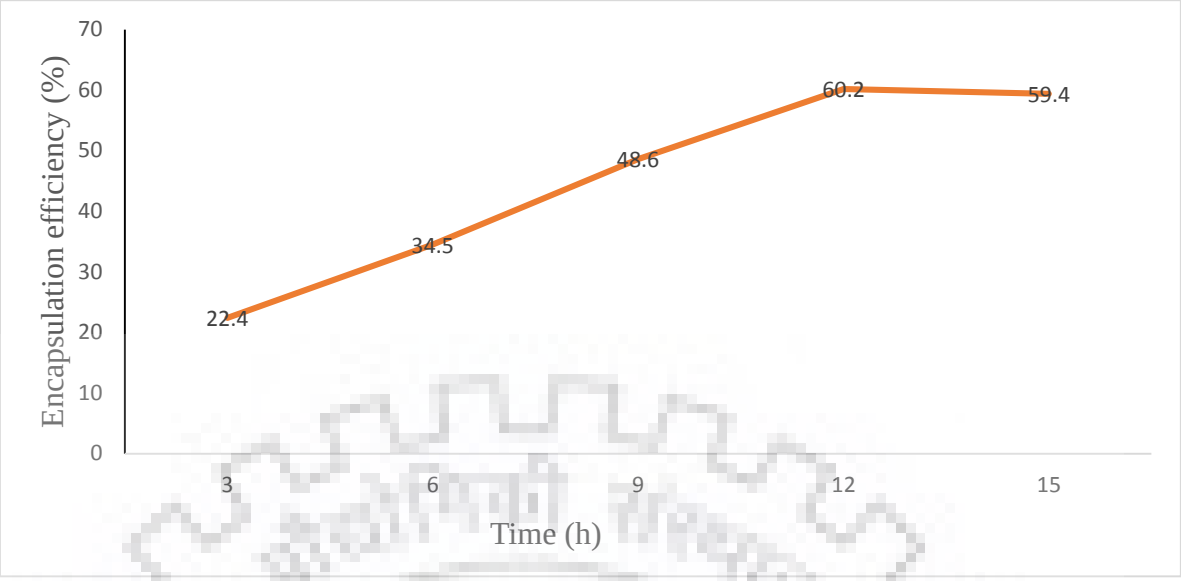


**Figure 4.5 Effect of time on the encapsulation efficiency of 5FU**

### 4.3.5 *Invitro* Drug Release Studies

A burst release of 24 %, due to the drug desorption from the particles surface was observed as shown in Figure 4.6, followed by a slower sustained release for the period of 60 h. A constant sustained release of the 5FU from 5FU gold magnetic nanoparticles was observed over the period of 60 h of dissolution study. Generally, there might be diffusion of the drug through the formulation or an erosion of the drug through the nanoformulation into the external environment. The dissolution data was therefore subjected to different mathematical kinetic models to understand the mechanism of drug release from the nanoformulation and it was found that the best fit model for the 5FU gold magnetic nanoparticles was Korsmeyer-Peppa's with the $R^2$ value of 0.9889 and n value of 0.534 (Table 4.1) suggesting the release mechanism to be non-fickian diffusion from the formulation [118].

**Table 4.1 Determination of $R^2$ value for various mathematical models for the nanoformulation**

| Zero order | First Order | Higuchi's | Korsmeyer-Peppa's | |
|---|---|---|---|---|
| $R^2$ | $R^2$ | $R^2$ | $R^2$ | n |
| 0.7901 | 0.9717 | 0.9873 | 0.9889 | 0.534 |

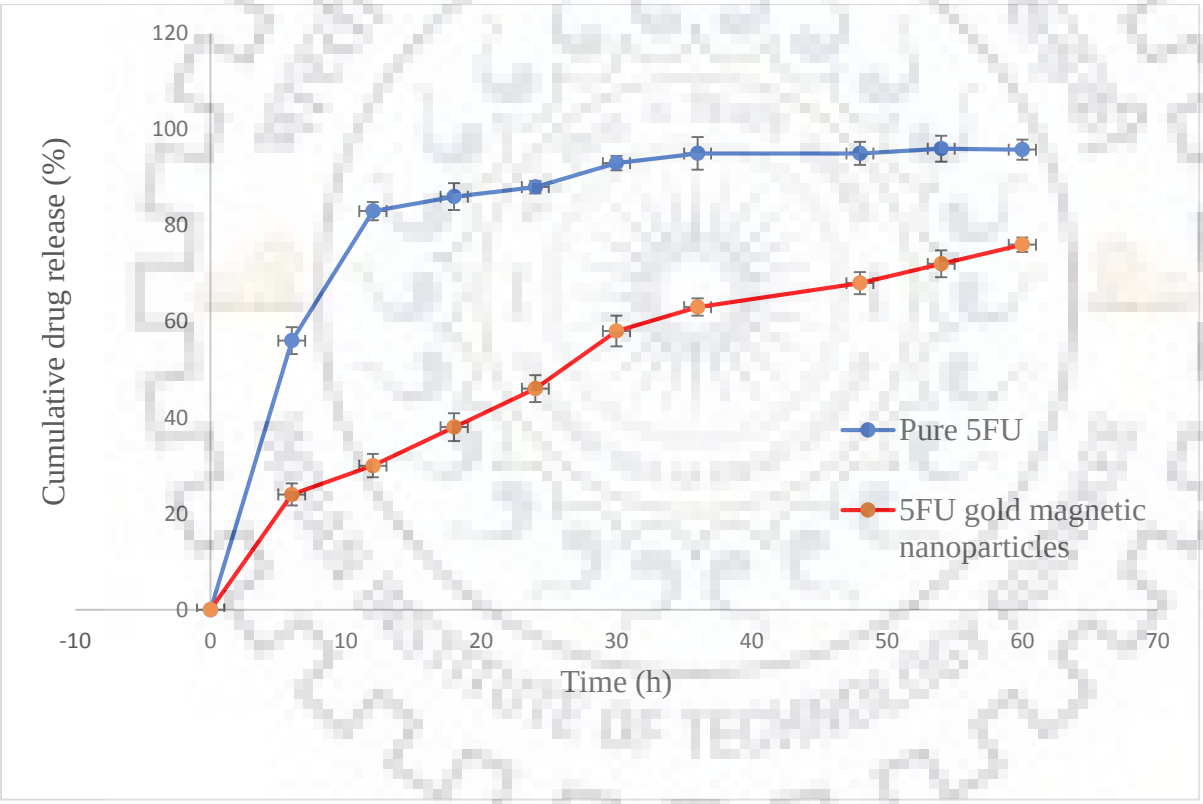


**Figure 4.6 5FU release profile from 5FU gold magnetic nanoparticles (blue curve) and pure 5FU (red curve)**

# CHAPTER 5

## CYTOTOXICITY AND *IN VIVO* ANTICANCER ACTIVITY OF HTCC 5FU MAGNETIC NANOPARTICLES AND 5FU GOLD MAGNETIC NANOPARTICLES

### 5.1 Introduction

Cancer is a disease of unpredictable remission and relapse with multiple aetiologies including genetic, immunological and environmental factors. Being a dreaded disorder effective treatment of cancer is a major challenge for health professionals at the present time. Different treatment strategies such as chemotherapy, immunotherapy, radiation therapy, hormonal therapy, stem cell therapy and surgical interventions are available for the treatment of cancer but their associated and post-treatment side effects are the major challenges which affects the physical and psychosocial life of patient. Although a large group of scientist and health professionals are actively engage in the search of cost effective and safe drug for the treatment of cancer, drug discovery for the cancer is still a challenge [119].

In recent years, significant efforts in the development of novel targeted and therapeutic strategies have been made for the treatment of chronic cancer but they failed to prove their commercial applications due to the lack of efficacy [120]. The major reason behind this failure was the lack of efficient and reproducible animal model with advanced stage of cancer progression (resistance, metastasis and relapse) for the preclinical and clinical evaluation of the drugs under pipeline [6]. Currently, majority of *in vivo* models of cancer are cell line based, more advanced *in vivo* model such as xenograft model and genetically engineered mice model which are considered as a cornerstones of translational cancer research are not cost-effective, required extreme technical expertise and last but not least their availability is always dependent on the tumour type [121,122].

For a comprehensive and cost effective drug screening there is a need of an *in vivo* animal model with high efficiency of metastasis with in short time duration. Transplantation model such as allograft model can fulfil these pitfalls. These allograft cancer models can help the researchers to understand the mechanisms of clinical drug action along with their potential side effects, which is critical before taking a drug candidate to clinical trials. Allograft model generally consist of tumor tissue originated from the same background as a given mouse strain. In this model cancerous cells are normally transplanted into the host mouse. Due to the ancestry similarity between the recipient and host, transplant is effectively accepted by the host immune system for

further tumor development [123]. Subsequently, the tumor growth and metastasis, survival rate and efficacy of given formulation can be assessed by monitoring the animals. One of the advantages of the allograft model is the normal condition of host immune system which can mimic the actual tumor microenvironment [124].

In the present study, we investigated the *in vivo* anticancer efficacy of developed formulations i.e., HTCC 5FU magnetic nanoparticles and gold 5FU magnetic nanoparticles in female Balb/c mice by continuous monitoring of tumor volume, body surface area and body temperature of animals. Further, to access the localization of magnetic nanoparticles into the tumor tissue histopathological studies were also conducted.

### 5.2 Cytotoxicity studies

#### 5.2.1 Materials

Michigan Cancer Foundation-7 (MCF-7) cell lines were procured from National Center for Cell Science (NCCS), Pune, India. N,N-dimethylform- amide (DMF), 3-(4,5-dimethylthiazol -2-yl)-2,5-diphenyl- tetrazolium bromide (MTT), cell culture-grade dimethyl sulfoxide (DMSO), phosphate buffer saline (PBS), Roswell Park Memorial Institute (RPMI) and Dulbecco's modified Eagle (DMEM) medium were procured from Himedia, India. All the solvents and chemicals used in the study were of analytical grade.

#### 5.2.2 Methods

##### 5.2.2.1 *In vitro* cytotoxicity of HTCC 5FU magnetic nanoparticles and gold 5FU magnetic nanoparticles

*In vitro* cytotoxicity of HTCC 5FU magnetic nanoparticles and gold 5FU magnetic nanoparticles was assayed against MCF-7 cancer cell lines (breast cancer cells) using MTT assay [125]. HTCC 5FU magnetic nanoparticles and gold 5FU magnetic nanoparticles of different concentrations (1, 5, 10, 25, and 50 mg/ml) were placed in 24-well microtiter plates individually followed by the addition of MCF-7 cells ($5X10^5$ cells/ml) along with DMEM supplemented with 10% fetal bovine serum (FBS). The plates were then incubated in humidified atmosphere containing 5% $CO_2$ at 37°C for 48 h. MCF-7 cells grown in presence of culture medium only were used as negative control, whereas the MCF-7 cells cultured in presence of sterilized solution of 5FU only were used as a positive control. Subsequently, the MTT solution (60 µl of 5 mg/ml stock) was added to each sample containing well and incubated at 37°C for 4 h. Then, the solution in the wells was removed carefully and 400 µl of DMSO was added to dissolve the MTT formazan

crystals. After that, 100 µl of the dissolved formazan solution of each test sample was transferred to individual wells of 96-well plate to determine the absorbance at 570 nm using micro-plate reader (Fluostar optima, BMG labtech, Germany) [126].

#### 5.2.2.2 Acute toxicity study

The acute toxicity study of developed formulations was evaluated as per the earlier reported method by Barcelona et al.1984, on healthy female Balb/c mice (4-6 weeks old, 15-25 g). Before the experiment, animals were fasted overnight with water *ad libitum*. Three animals administered with a single dose of 200 mg/kg, body weight of developed formulations. Animals were then observed for any sign of toxicity, behavioural changes and mortality after dosing, with special attention given during the first 24 h, and thereafter, for a total time period of seven days [127,128].

#### 5.2.2.3 *In vivo* anticancer activity of HTCC 5FU magnetic nanoparticles and gold 5FU magnetic nanoparticles

##### 5.2.2.3.1 Animal model

The experiment was carried out on healthy, female Balb/c mice (4-6 weeks old, 15-25 g). Animals were procured from the National Institute of Biologicals, Noida, Uttar Pradesh India. The animals were acclimatized at least for seven days before the start of study to the laboratory conditions (25±2°C, relative humidity 44-56%, and light and dark cycles of 12:12 h ) in the cross-ventilated animal house. The study protocol was approved by the Institutional Animal Ethics Committee (IAEC) as per committee for the Purpose of Control and Supervision of Experiments on Animals (CPCSEA) guidelines, India (approval no. 1413/PO/E/S/11/CPCSEA) and experimental proposal number SBRL/IAEC/Dec 2016/12.

##### 5.2.2.3.2 4T1 induced breast cancer

Healthy female Balb/c mice were divided into six groups containing 4 animals in each group as follows, Group: I as control (saline); Group: II as standard (treated with 5FU, 10 mg/kg); Group-III treated with blank HTCC magnetic nanoparticles; Group-IV treated with HTCC 5FU magnetic nanoparticles (equivalent to 10 mg/kg of 5FU); Group-V treated with blank gold magnetic nanoparticles and Group-VI treated with gold 5FU magnetic nanoparticles (equivalent to 10 mg/kg of 5FU). Murine breast cancer 4T1 cells ($2 \times 10^6$ cells in 30 µl of serum-free RPMI media) were subcutaneously injected into the mammary pad of female Balb/c mice. Tumor size (length and width) was recorded using the vernier calliper for the assessment of tumor volume

after every 2 days and body weight was recorded once in a week. Once the tumor volume reached 100 $mm^3$ (about one week after tumor cell inoculation) mice were treated as per their treatment schedule once daily via the tail vein for two weeks.

#### 5.2.2.3.3 Magnetic targeting of HTCC 5FU magnetic nanoparticles and gold 5FU magnetic nanoparticles in mouse model of breast cancer

Magnetic targeting of developed nanoformulations have been achieved by applying external magnetic field to the tumor site using a magnet (250 mT). Immediately after treating the animals (group IV and group VI) with different nanoformulations (HTCC 5FU magnetic nanoparticles and gold 5FU magnetic nanoparticles) a magnet was fixed with its face attached to the tumor of the each mice for 2 h. The other animal groups (group III and group V) treated with blank HTCC magnetic nanoparticles and blank gold magnetic nanoparticles were also observed in the presence of external magnetic field to compare the efficacy of developed nanoformulations under external magnetic field [129]. Daily application of external magnetic field was chosen as a routine practice after the drug treatment for next 14 days. Subsequently, tumor size was measured using a vernier calliper after every 2 days, and the tumor volume (V) was calculated using the following equation [130]:

$$\text{Tumor volume (V)} = \frac{\text{Width}^2}{2} \text{ X length}$$

At the end of study, i.e., on day 21, animals were sacrificed under light anaesthesia; tumor samples were collected, stained with Prussian blue and examined under the light microscope to confirm the accumulation of magnetic nanoparticles in tumors.

#### 5.2.2.3.4 Statistical Analysis

Results were finally tabulated as mean ± SEM (standard error of mean) and examined using One-way Analysis of Variance (ANOVA) by Tukey-Kramer Multiple Comparisons test by GraphPad InStat 3 software (San Diego, CA, USA). A value of $P < 0.05$ was considered to be statistically significant in all the cases.

## 5.3 Results and Discussion

### 5.3.1 Cytotoxicity study

Breast cancer is among the highest ranked cancer found among the Indian females with a rate as high as 25.8 in every 100,000 women and a mortality rate of 12.7 in every 100,000 women [2]. In spite of advances in early detection and treatment, the inherent resistance of breast cancer cells

toward the anticancer agents is the major hurdle for effective chemotherapeutic treatments. Hence, the development of new and effective drug delivery systems is the requisite for treatment of drug-resistant breast cancers.

Efficacy of the developed nanoformulations (HTCC 5FU magnetic nanoparticles and gold 5FU magnetic nanoparticles) were evaluated by analysing their cytotoxic effect against the MCF-7 cells. MCF-7 cells were subjected to different concentration of pure 5FU (1, 5, 10, 25, and 50 mg/ml) and developed nanoformulations (1, 5, 10, 25, and 50 mg/ml).

Growth inhibitions studies revealed a 50% growth inhibition ($GI_{50}$) at 12.1 mg/ml, 10.6 mg/ml, and 4.7 mg/ml exhibited by pure 5FU, HTCC 5FU magnetic nanoparticles and gold 5FU magnetic nanoparticles respectively. A significant decrease in percentage (%) cell viability has been observed for gold 5FU magnetic nanoparticles. Percentage cell viability at a concentration range of 5 mg/ml for different formulations has been observed 61.6 ± 5.3 % (pure 5FU), 52.8 ± 4.5% (HTCC 5FU magnetic nanoparticles) and 50.1 ± 4.6% (gold 5FU magnetic nanoparticles) (Figure 5.1). Observed cytotoxic effect exhibited by nanoformulations is attributed to sustained effect exerted by the formulations through the release of the encapsulated drug. Further studies over a period of 48 h it was observed that gold 5FU magnetic nanoparticles were consistently effective than the pure 5FU in terms of cell viability. Following this light microscopic studies of treated MCF-7 cell lines have also been conducted to evaluate the effect of nanoformulations on cell morphology. The light microscopic analysis showed the significant cell death in the case of nanoformulations which is evident by the changing pattern of normal bilateral symmetric morphology of the MCF-7 cells to non-symmetric spherical disc (Figure 5.2).

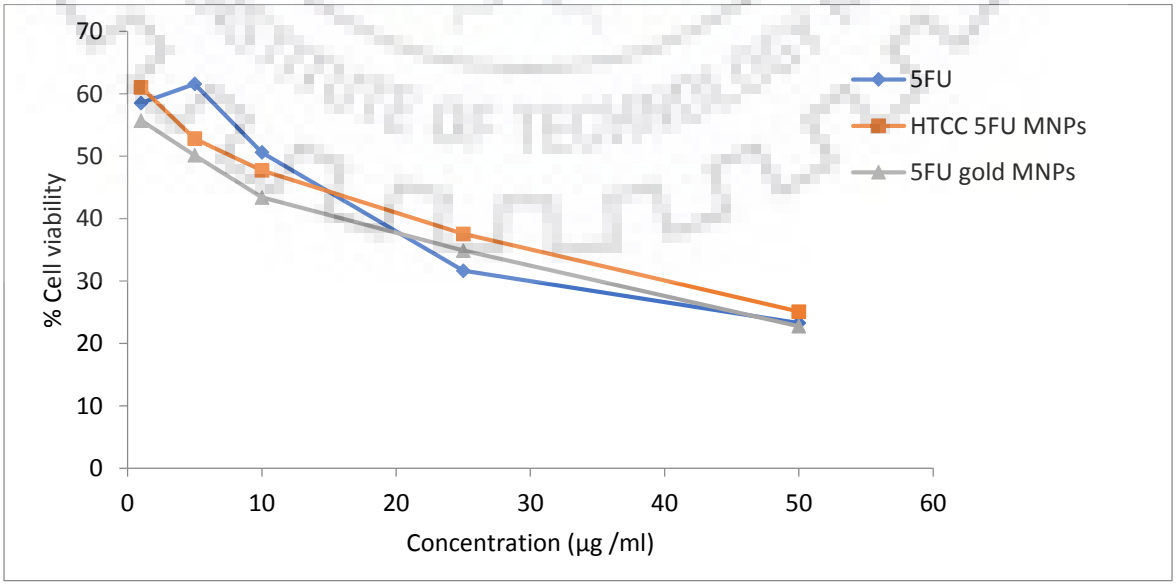


**Figure 5.1 Cytotoxic studies using MCF-7 cell line**

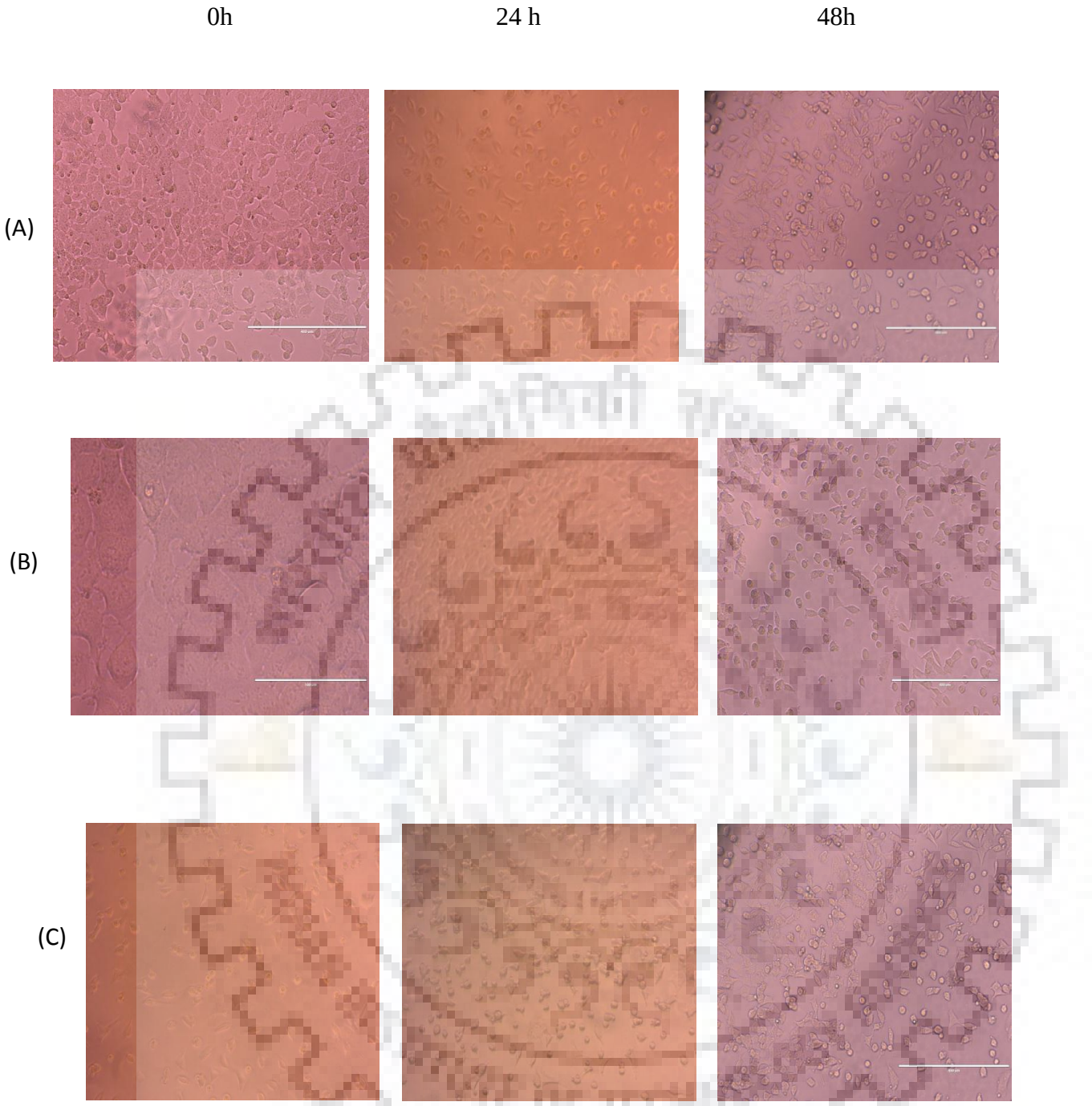


**Figure 5.2 Microscopic images of MCF-7 cells treated with different formulations (A): 5FU, (B): HTCC 5FU magnetic nanoparticles, and (C): Gold 5FU magnetic nanoparticles**

In recent years, nanomedicine extensively utilizes gold nanoparticles as a drug carrier for the treatment of different chronic disorders. Gold nanoparticles posses' several advantages over conventional drug delivery strategies systems such biologically safe for clinical application, diverse optical properties owing to surface plasmon response and ease of synthesis[131,132]. Enhanced permeability and retention effect leads to easily permeation and localisation of gold nanoparticles in the leaky and disordered tumor vasculature. As the tumors are deficient of

lymphatic clearance, prolong circulation time and increased concentration of gold nanoparticles has been observed in the tumor tissue [133]. Gold coated magnetic nanoparticles has a wide biomedical applications due to their low reactivity, biocompatibility and chemical stability. These systems had numerous applications such as drug targeting by virtue of magnetic property of the core and it may also work as a vehicle for many drugs by virtue of an easily modified gold surface. [111]

In the present study body weight, tumor volume and body surface temperature were recorded and compared with control and various treatment groups. Treatment of tumor bearing mice with nanoformulations (HTCC 5FU magnetic nanoparticles and gold 5FU magnetic nanoparticles) significantly decreases the body weight and tumor volume (Figure 5.4 and Figure 5.5). In case of control group (GI) the percentage change in body weight of animals was found to be 18.2% whereas in case of HTCC 5FU magnetic nanoparticles (GIV) and gold 5FU magnetic nanoparticles treated animals (GVI) it was found to be 9.94 % and 9.52 % respectively. The change in body weight of animals treated with the developed magnetic nanoparticles (GIV and GVI) were significantly ($P < 0.001$) comparable with that of the control group animals (GI). For the growth of cancer cells ascitic fluid is essential nutritional requirement and a rapid increase in ascitic fluid with tumor growth would be a means to meet the nutritional requirement of tumor cells. The administered nanoformulations may interfere in production of the cell physiological function and thereby reducing the production of ascitic fluid. The similar results were seen in the earlier reports on *in vivo* studies where the change in body weight of tumor bearing mice was increased due to increase in ascitic fluid volume subsequently the increase in the body weight and ascitic fluid also increased the tumor volume. Similarly the tumor size in terms of relative tumor volume was observed continuously and at the end of study i.e., day 21, it was found to be significantly increased (6.2) in the case of control group animals (GI), whereas it was found to be 3.4 and 2.7 for HTCC 5FU magnetic nanoparticles (GIV) and gold 5FU magnetic nanoparticles (GVI) respectively (Figure 5.6). This effect may be attributed to enhanced permeability and retention effect which leads to easily permeation and localisation of gold 5FU magnetic nanoparticles in the leaky and disordered tumor vasculature. As the tumors are deficient of lymphatic clearance, prolong circulation time and increased concentration of gold nanoparticles has been observed in the tumor tissue [133] . Histopathological studies (Figure 5.7) also inferred the accumulation of magnetic nanoparticles in the tumor tissue of treated animals. Here, the external magnetic field restricted the movement of magnetic nanoparticles which than results in accumulation of these particles in tumor tissue which is evident by blue stained magnetic nanoparticles visible in histopathological images of tumor tissues.[134]

These results conclusively infer that the formulation containing 5FU and gold exerted a synergistic effect for the treatment of tumor which may be a result of multiple factors and moreover, as the release of 5FU from the gold 5FU magnetic nanoparticles was faster as compared to HTCC 5FU magnetic nanoparticles making it more effective.

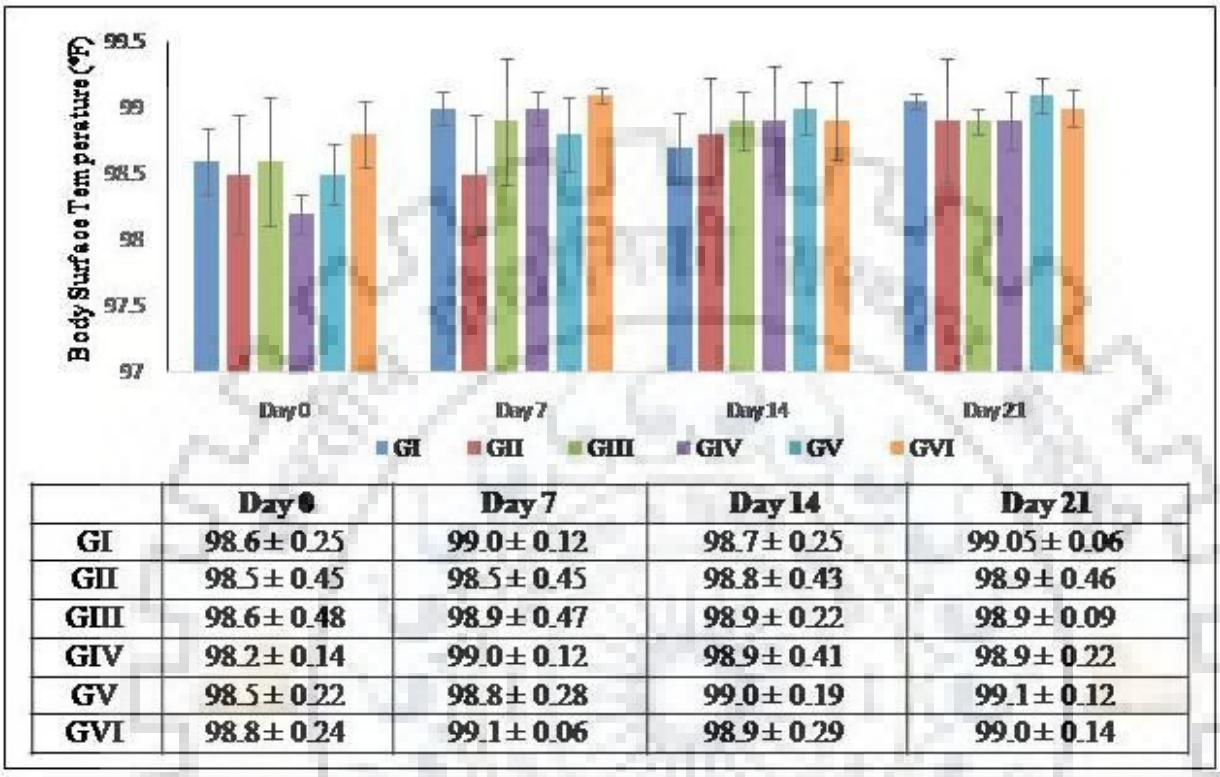


| | Day 0 | Day 7 | Day 14 | Day 21 |
|---|---|---|---|---|
| GI | 98.6 ± 0.25 | 99.0 ± 0.12 | 98.7 ± 0.25 | 99.05 ± 0.06 |
| GII | 98.5 ± 0.45 | 98.5 ± 0.45 | 98.8 ± 0.43 | 98.9 ± 0.46 |
| GIII | 98.6 ± 0.48 | 98.9 ± 0.47 | 98.9 ± 0.22 | 98.9 ± 0.09 |
| GIV | 98.2 ± 0.14 | 99.0 ± 0.12 | 98.9 ± 0.41 | 98.9 ± 0.22 |
| GV | 98.5 ± 0.22 | 98.8 ± 0.28 | 99.0 ± 0.19 | 99.1 ± 0.12 |
| GVI | 98.8 ± 0.24 | 99.1 ± 0.06 | 98.9 ± 0.29 | 99.0 ± 0.14 |

**Figure 5.3 Change in body temperature for Group: I as control (saline); Group: II as standard (treated with 5FU, 10 mg/kg); Group-III treated with blank HTCC magnetic nanoparticles; Group-IV treated with HTCC 5FU magnetic nanoparticles (equivalent to 10 mg/kg of 5FU); Group-V treated with blank gold magnetic nanoparticles and Group-VI treated with gold 5FU magnetic nanoparticles.**

All values are represented as mean±SD, n=4 animals in each group, data were analyzed by one-way ANOVA, followed by Tukey-Kramer Multiple Comparisons Test, a-significant difference as compared to control group (Group I), b-significant difference as compared to standard group (Group II) and $*P < 0.05$, $**P < 0.01$, $***P < 0.001$, ANOVA (Analysis of variance), SD=Standard Deviation.

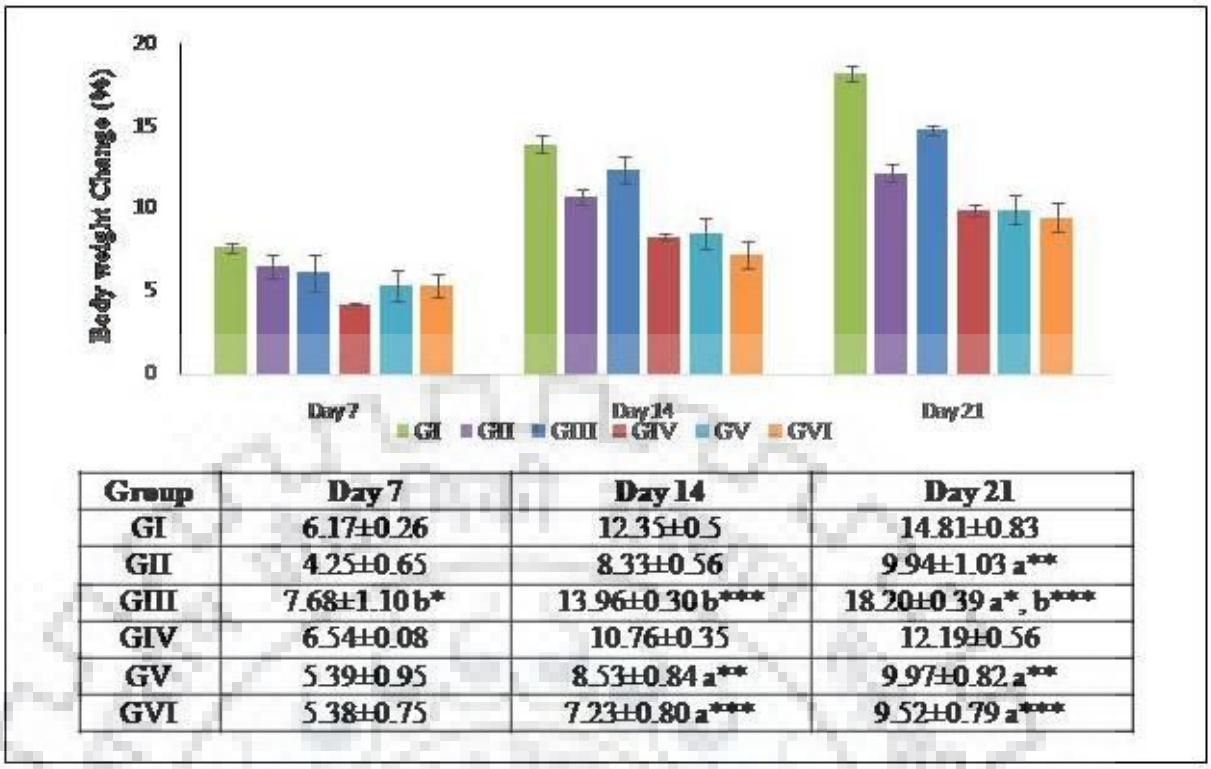


| Group | Day 7 | Day 14 | Day 21 |
|---|---|---|---|
| GI | 6.17±0.26 | 12.35±0.5 | 14.81±0.83 |
| GII | 4.25±0.65 | 8.33±0.56 | 9.94±1.03 a** |
| GIII | 7.68±1.10 b* | 13.96±0.30 b*** | 18.20±0.39 a*, b*** |
| GIV | 6.54±0.08 | 10.76±0.35 | 12.19±0.56 |
| GV | 5.39±0.95 | 8.53±0.84 a** | 9.97±0.82 a** |
| GVI | 5.38±0.75 | 7.23±0.80 a*** | 9.52±0.79 a*** |

**Figure 5.4 Percentage change in body weight for Group: I as control (saline); Group: II as standard (treated with 5FU, 10 mg/kg); Group-III treated with blank HTCC magnetic nanoparticles; Group-IV treated with HTCC 5FU magnetic nanoparticles (equivalent to 10 mg/kg of 5FU); Group-V treated with blank gold magnetic nanoparticles and Group-VI treated with gold 5FU magnetic nanoparticles.**

All values are represented as mean±SD, n=4 animals in each group, data were analyzed by one-way ANOVA, followed by Tukey-Kramer Multiple Comparisons Test, a-significant difference as compared to control group (Group I), b-significant difference as compared to standard group (Group II) and $*P < 0.05$, $**P < 0.01$, $***P < 0.001$, ANOVA (Analysis of variance), SD=Standard Deviation.

**Table 5.1 Tumor volume observed for different nanoformulations**

| Group | Tumor volume ($mm^3$) | | |
|---|---|---|---|
| | Day 7 | Day 14 | Day 21 |
| GI | 103.7±19.8 | 391.1±58.9 | 642.1±42.3 |
| GII | 104.8±6.7 | 201.1±12.1 a*** | 410.9±42.3 a*** |
| GIII | 102.9±13.3 | 347.5±47.9 b*** | 555.5±35.5 a**, b*** |
| GIV | 101.2±9.6 | 192.6±14.8 a*** | 339.3±4.8 a***, b* |
| GV | 102.1±9.7 | 192.9±43.8 a*** | 343.5±42.3 a***, b* |
| GVI | 107.8±9.6 | 169.7±23.2 a*** | 290.4±37.9 a***, b*** |

All values are represented as mean±SD, n=4 animals in each group, data were analyzed by one-way ANOVA, followed by Tukey-Kramer Multiple Comparisons Test, a-significant difference as compared to control group (Group I), b-significant difference as compared to standard group (Group II) and *$P$ < 0.05, **$P$ < 0.01, ***$P$ < 0.001, ANOVA (Analysis of variance), SD=Standard Deviation.

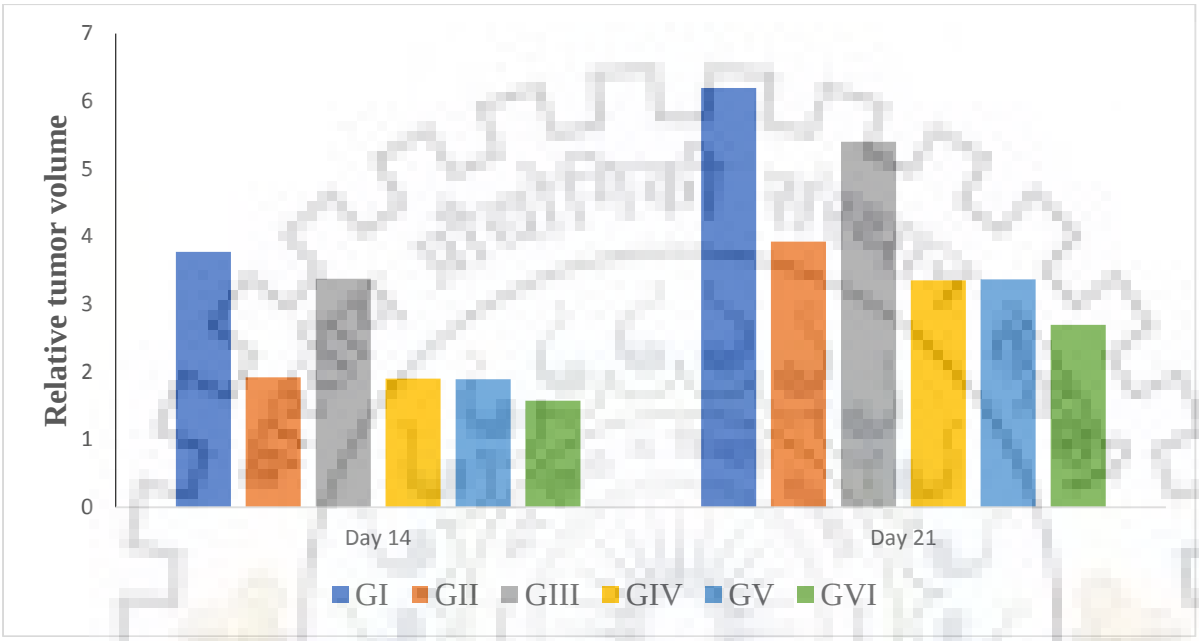


**Figure 5.5 Relative tumor volume observed for Group: I as control (saline); Group: II as standard (treated with 5FU, 10 mg/kg); Group-III treated with blank HTCC magnetic nanoparticles; Group-IV treated with HTCC 5FU magnetic nanoparticles (equivalent to 10 mg/kg of 5FU); Group-V treated with blank gold magnetic nanoparticles and Group-VI treated with gold 5FU magnetic nanoparticles**

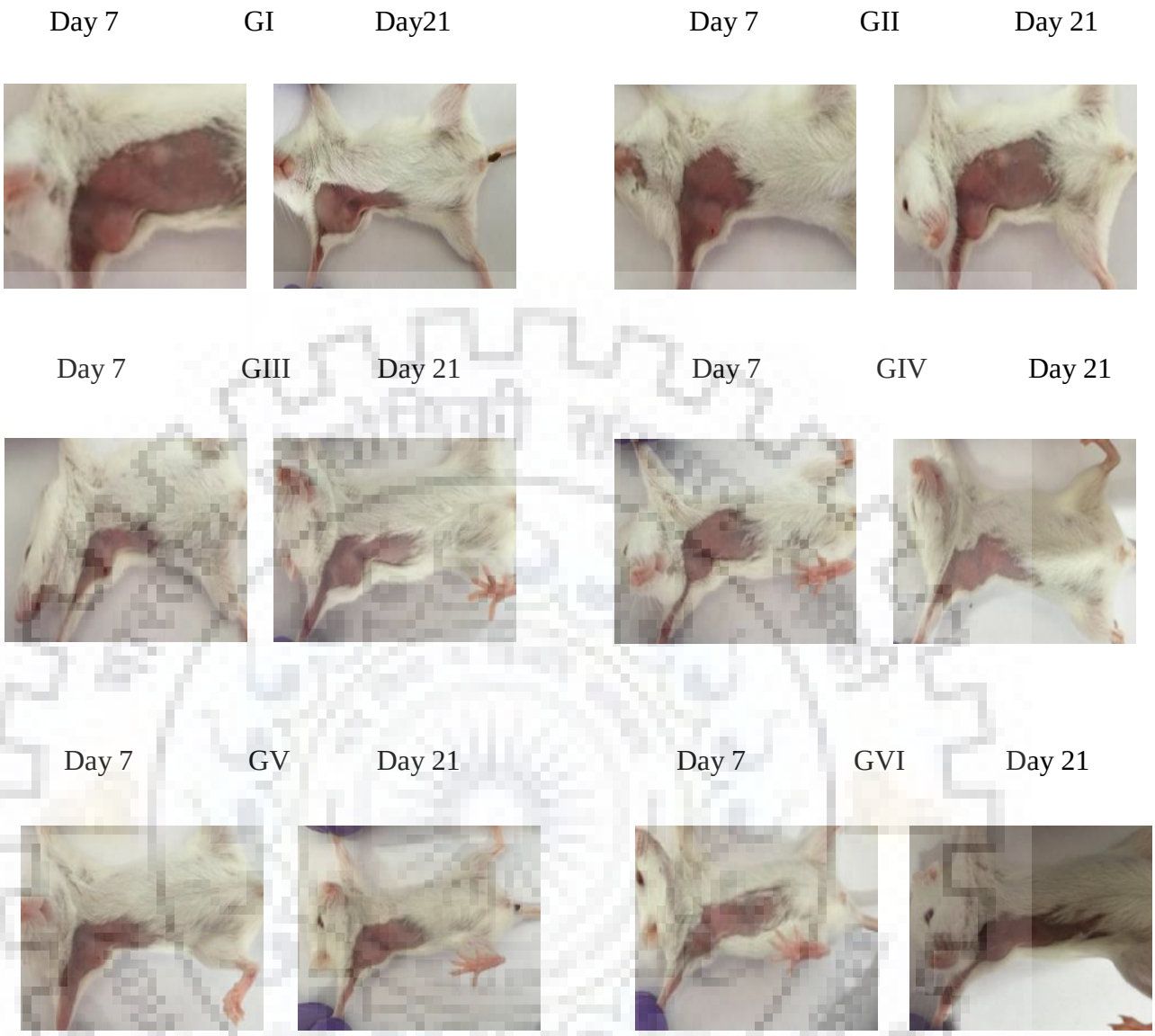


**Figure 5.6 Examination of tumor tissue for Group: I as control (saline); Group: II as standard (treated with 5FU, 10 mg/kg); Group-III treated with blank HTCC magnetic nanoparticles; Group-IV treated with HTCC 5FU magnetic nanoparticles (equivalent to 10 mg/kg of 5FU); Group-V treated with blank gold magnetic nanoparticles and Group-VI treated with gold 5FU magnetic nanoparticles**

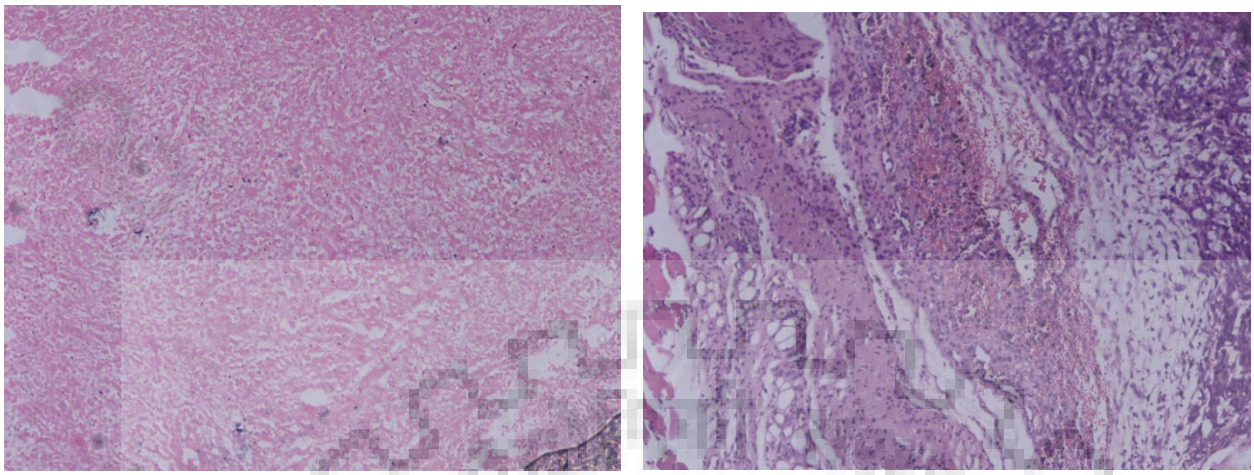

**(A)** **(B)**

**Figure 5.7 Histopathological examination of tumor tissue in the treated Balb/c under light microscope at 10X (A) un-exposed and (B) under external magnetic field**

# CHAPTER 6

## Conclusion and Future Prospects

In the present study, a novel nanoparticulate drug delivery system was used for treatment against breast cancer. The objective behind the work was to limit the distribution of chemotherapy and achieve targeted therapy. Conclusively, the present work elucidates the designing, optimization, and characterization of 5FU based magnetic nanoparticulate drug delivery system. In the present investigation two different formulation of 5FU, HTCC 5FU magnetic nanoparticles and gold 5FU magnetic nanoparticles were designed. Formulation of 5FU nanoparticles was carried out using the bottom up approach for the nanoparticles synthesis and were prepared using separate techniques (i) encapsulation of 5FU with magnetic nanoparticles to form N-(2-hydroxy) propyl-3-trimethyl ammonium chitosan chloride nanoparticles (HTCC 5FU magnetic nanoparicles) and (ii) conjugating 5FU on the gold coated magnetic nanoparticles (gold 5FU magnetic nanoparticles).

The formulations not only demonstrated the targeted effect of drug on to the tumor site but also improved the efficacy of the drug by reducing the toxicity associated with the conventional chemotherapy. The optimization study conducted on the formulation for the selection of a suitable polymer concentration revealed a concentration of 0.5% mg/ml HTCC and 0.8% mg/ml sodium tripolyphosphate (STP) to be optimal for encapsulation of 5FU. The assessed range of particle size, zeta potential, and entrapment efficiency were found to be in the desired range. Further, the morphological studies revealed nanoparticles of spherical shape without any sign of aggregation. Magnetic property of the formulation was also evaluated using vibrating sample magnetometer (VSM) which confirms a superparamagnetic behavior of magnetic nanoparticles with a saturated magnetization of 43 emu/g in bare state which decreased to a value of 30 emu/g and 28 emu/g in HTCC 5FU magnetic nanoparticles and gold 5FU magnetic nanoparticles, respectively. Drug release studies from the formulation suggest the release mechanism to be fickian diffusion in case of HTCC 5FU magnetic nanoparticles (n= 0.239) and non-fickian diffusion in case of gold 5FU magnetic nanoparticles (n=0.534). The results of *in vitro* cytotoxicity conducted using MCF-7 cell line confirmed a significant reduction in the percentage cell viability on administration of nanoformulation when compared with control. Growth inhibition 50% ($GI_{50}$) of 5FU, HTCC 5FU magnetic nanoparticles, and gold 5FU magnetic nanoparticles were found to be 12.1 mg/ml, 10.6 mg/ml and 4.7 mg/ml, respectively. *In vivo* studies conducted on Balb/c mice using an allograft model demonstrated an increased efficacy

and targeting efficiency of nanoformulations as compared to the control with a relative tumor volume of 3.4 and 2.7 for HTCC 5FU magnetic nanoparticles and gold 5FU magnetic nanoparticles whereas the value was much higher 6.7 for the control group. The results of the investigation demonstrate a huge potential of designed formulations in tumor targeting with an improved efficacy.

As, the designed formulations contains gold coated magnetic nanoparticles which were only tested for the therapeutic activity they can further be explored for their potential in diagnosis of tumor in the body and function as a theranostic agent. The present formulation works by regulating the direction and magnitude of external magnetic field which is suitable for surface tumors and can be further investigated for tumor site inside the body.

# REFERENCES


[1] K. D. Miller, R. L. Siegel, C. C. Lin, A. B. Mariotto, J. L. Kramer, J. H. Rowland, K. D. Stein, R. Alteri, and A. Jemal, "Cancer treatment and survivorship statistics, 2016," *CA. Cancer J. Clin.*, vol. 66, no. 4, pp. 271–289, 2016.

[2] S. Malvia, S. A. Bagadi, U. S. Dubey, and S. Saxena, "Epidemiology of breast cancer in Indian women," *Asia. Pac. J. Clin. Oncol.*, vol. 13, no. 4, pp. 289–295, 2017.

[3] R. M. Parks, M. G. M. Derks, E. Bastiaannet, and K. L. Cheung, "Breast Cancer Epidemiology," in *Breast Cancer Management for Surgeons*, Cham: Springer, pp. 19–29, 2018.

[4] K. P. Sunkara, G. Gupta, P. M. Hansbro, K. Dua, and M. Bebawy, "Functional relevance of SATB1 in immune regulation and tumorigenesis," *Biomed. Pharmacother.*, vol. 104. pp. 87–93, 2018.

[5] D. K. Chellappan, K. H. Leng, L. J. Jia, N. A. B. A. Aziz, W. C. Hoong, Y. C. Qian, and K. Dua, "The role of bevacizumab on tumour angiogenesis and in the management of gynaecological cancers: A review," *Biomed. Pharmacother.*, vol. 102. pp. 1127–1144, 2018.

[6] S. A. Mohammed, H. F. K., A. Philip, A. A. Hameeda, and E. Yousifa, "Chemotherapy of breast cancer by heterocyclic compounds," *Int. J. Pharm. Sci. Rev. Res.*, vol. 41, no. 2, pp. 225–231, 2016.

[7] S. Karuppath, P. Pillai, S. V. Nair, and V.-K. Lakshmanan, "Comparison and Existence of Nanotechnology in Traditional Alternative Medicine: An Onset to Future Medicine," *Nanosci. Nanotechnology-Asia*, vol. 8, no. 1, pp. 13–25, 2018.

[8] K. Pathak, S. Pattnaik, and K. Swain, "Chapter 13 – Application of Nanoemulsions in Drug Delivery," in *Nanoemulsions*, pp. 415–433, 2018.

[9] F. Yuan, M. Dellian, D. Fukumura, M. Leunig, D. A. Berk, V. P. Torchilin, and R. K. Jain, "Vascular permeability in a human tumor xenograft: molecular size dependence and cutoff size.," *Cancer Res.*, vol. 55, no. 17, pp. 3752–3756, 1995.

[10] S. K. Hobbs, W. L. Monsky, F. Yuan, W. G. Roberts, L. Griffith, V. P. Torchilin, and R. K. Jain, "Regulation of transport pathways in tumor vessels: Role of tumor type and microenvironment," *Proc. Natl. Acad. Sci.*, vol. 95, no. 8, pp. 4607–4612, 1998.

[11] N. Akhtar and K. Pathak, "Carbon Nanotubes in the Treatment of Skin Cancers: Safety and Toxic ological Aspects," *Pharm. Nanotechnol.*, vol. 5, no. 2, 2017.

[12] B. Haley and E. Frenkel, "Nanoparticles for drug delivery in cancer treatment," *Urol. Oncol.*, vol. 26, no. 1. pp. 57–64, 2008.

[13] P. Kesharwani, K. Jain, and N. K. Jain, "Dendrimer as nanocarrier for drug delivery," *Prog. Polym. Sci.*, vol. 39, no. 2, pp. 268–307, 2014.

[14] S. M. Moghimi, A. Hunter, and J. Murray, "Nanomedicine: current status and future prospects," *FASEB J.*, vol. 19, no. 3, pp. 311–330, 2005.

[15] G. A. Hughes, "Nanostructure-mediated drug delivery," *Nanomedicine.*, vol. 1, no. 1. pp. 22–30, 2005.

[16] M. Yokoyama, "Polymeric micelles as a new drug carrier system and their required considerations for clinical trials," *Expert Opin. Drug Deliv.*, vol. 7, pp. 145–158, 2010.

[17] K. Kato, K. Chin, T. Yoshikawa, K. Yamaguchi, Y. Tsuji, T. Esaki, K. Sakai, M. Kimura, T. Hamaguchi, Y. Shimada, Y. Matsumura, and R. Ikeda, "Phase II study of NK105, a paclitaxel-incorporating micellar nanoparticle, for previously treated advanced or recurrent gastric cancer," *Invest. New Drugs*, vol. 30, no. 4, pp. 1621–1627, 2012.

[18] T. Hamaguchi, K. Kato, H. Yasui, C. Morizane, M. Ikeda, H. Ueno, K. Muro, Y. Yamada, T. Okusaka, K. Shirao, Y. Shimada, H. Nakahama, and Y. Matsumura, "A phase I and pharmacokinetic study of NK105, a paclitaxel-incorporating micellar nanoparticle formulation," *Br. J. Cancer*, vol. 97, no. 2, pp. 170–176, 2007.

[19] A. Takahashi,. Y. Yamamoto, M. Yasunaga, Y. Koga, J. I. Kuroda, M. Takigahira, M. Harada, H. Saito, T. Hayashi, Y. Kato, T. Kinoshita, I. Hyodo, and N. Ohkohchi, "NC-6300, an epirubicin-incorporating micelle, extends the antitumor effect and reduces the cardiotoxicity of epirubicin," *Cancer Sci.*, vol. 104, no. 7, pp. 920–925, 2013.

[20] X. Chen, H. Sun, J. Hu, X. Han, H. Liu, and Y. Hu, "Transferrin gated mesoporous silica nanoparticles for redox-responsive and targeted drug delivery," *Colloids Surf. B Biointerfaces*, vol. 152, pp. 77–84, 2017.

[21] C. Di Ding, Y. Liu, T. Wang, and J. J. Fu, "Triple-stimuli-responsive nanocontainers assembled by water-soluble pillar[5]arene-based pseudorotaxanes for controlled release," *J. Mater. Chem. B*, vol. 4, no. 16, pp. 2819–2827, 2016.

[22] S. K. Das, M. K. Bhunia, D. Chakraborty, A. R. Khuda-Bukhsh, and A. Bhaumik, "Hollow spherical mesoporous phosphosilicate nanoparticles as a delivery vehicle for an antibiotic drug," *Chem. Commun.*, vol. 48, no. 23, pp. 2891–2893, 2012.

[23] M. Sasidharan, H. Zenibana, M. Nandi, A. Bhaumik, and K. Nakashima, "Synthesis of mesoporous hollow silica nanospheres using polymeric micelles as template and their application as a drug-delivery carrier," *Dalt. Trans.*, vol. 42, no. 37, pp. 13381–13389, 2013.

[24] G. Puglisi, M. Fresta, G. Giammona, and C. A. Ventura, "Influence of the preparation conditions on poly(ethylcyanoacrylate) nanocapsule formation," *Int. J. Pharm.*, vol. 125, no. 2, pp. 283–287, 1995.

[25] G. E. Hildebrand and J. W. Tack, "Microencapsulation of peptides and proteins," *Int. J. Pharm.*, vol. 196, no. 2, pp. 173–176, 2000.

[26] C. Bouclier, L. Moine, H. Hillaireau, V. Marsaud, E. Connault, P. Opolon, P. Couvreur, E. Fattal, and J. M. Renoir, "Physicochemical characteristics and preliminary in vivo biological evaluation of nanocapsules loaded with siRNA targeting estrogen receptor alpha," *Biomacromolecules*, vol. 9, no. 10, pp. 2881–2890, 2008.

[27] K. N. J. Burger, R. W. H. M. Staffhorst, H. C. de Vijlder, M. J. Velinova, P. H. Bomans, P. M. Frederik, and B. de Kruijff, "Nanocapsules: lipid-coated aggregates of cisplatin with high cytotoxicity," *Nat. Med.*, vol. 8, no. 1, pp. 81–84, 2002.

[28] Y. Shen, E. Jin, B. Zhang, C. J. Murphy, M. Sui, J. Zhao, J. Wang, J. Tang, M. Fan, E. Van Kirk, and W. J. Murdoch, "Prodrugs Forming High Drug Loading Multifunctional Nanocapsules for Intracellular Cancer Drug Delivery," *J. Am. Chem. Soc.*, vol. 132, no. 12, pp. 4259–4265, 2010.

[29] O. P. Medina, Y. Zhu, and K. Kairemo, “Targeted liposomal drug delivery in cancer.,” *Curr. Pharm. Des.*, vol. 10, no. 24, pp. 2981–2989, 2004.

[30] H. Pandey, R. Rani, and V. Agarwal, “Liposome and their applications in cancer therapy,” *Brazilian Arch. Biol. Technol.*, vol. 59, pp. 1–10, 2016.

[31] K. Pathak, R. Shankar, and M. Joshi, “An Update of Patents, Preclinical and Clinical Outcomes of Lipid Nanoparticulate Systems,” *Curr. Pharm. Des.*, vol. 23, no. 43, pp. 6602–6612, 2018.

[32] Y. (Chezy) Barenholz, “Doxil (R) - The first FDA-approved nano-drug: Lessons learned,” *J. Control. Release*, vol. 160, no. 2, pp. 117–134, 2012.

[33] N. D. James, R. J. Coker, D. Tomlinson, J. R.W. Harris, M. Gompels, A. J. Pinching, and J. S.W. Stewart, “Liposomal doxorubicin (Doxil): An effective new treatment for Kaposi’s sarcoma in AIDS,” *Clin. Oncol.*, vol. 6, no. 5, pp. 294–296, 1994.

[34] T. Cooley, D. Henry, M. Tonda, S. Sun, M. O’Connell, and W. Rackoff, “A Randomized, Double-Blind Study of Pegylated Liposomal Doxorubicin for the Treatment of AIDS-Related Kaposi’s Sarcoma,” *Oncologist*, vol. 12, no. 1, pp. 114–123, 2007.

[35] C. E. Petre and D. P. Dittmer, “Liposomal daunorubicin as treatment for Kaposi’s sarcoma,” *Int. J. Nanomedicine.*, vol. 2, no. 3. pp. 277–288, 2007.

[36] A. H. Sarris, F. Hagemeister, J. Romaguera, M. A. Rodriguez, P. McLaughlin, A. M. Tsimberidou, L. J. Medeiros, B. Samuels, O. Pate, M. Oholendt, H. Kantarjian, C. Burge and F. Cabanillas, “Liposomal vincristine in relapsed non-Hodgkin’s lymphomas: Early results of an ongoing phase II trial,” *Ann. Oncol.*, vol. 11, no. 1, pp. 69–72, 2000.

[37] M. A. Rodriguez, R. Pytlik, Kozak, T. Kozak, M. Chhanabhai, R. Gascoyne, B. Lu, S. R. Deitcher and J. N. Winter, “Vincristine sulfate liposomes injection (Marqibo) in heavily pretreated patients with refractory aggressive non-Hodgkin lymphoma,” *Cancer*, vol. 115, no. 15, pp. 3475–3482, 2009.

[38] B. J. Kennedy, “5-Fluorouracil toxicity: Old or new?,” *Cancer*, vol. 86, no. 7. pp. 1099–1100, 1999.

[39] H. M. Pinedo and G. F. J. Peters, “Flourouracil: Biochemistry and pharmacology,” *J. Clin. Oncol.*, vol. 6, no. 10, pp. 1653–1664, 1988.

[40] M. N. Patel, S. Lakkadwala, M. S. Majrad, E. R. Injeti, S. M. Gollmer, Z. A. Shah, S . H. S. Boddu, and J. Nesamony, “Characterization and Evaluation of 5-Fluorouracil-Loaded Solid Lipid Nanoparticles Prepared via a Temperature-Modulated Solidification Technique,” *AAPS PharmSciTech*, vol. 15, no. 6, pp. 1498–1508, 2014.

[41] S. Tummala, M. N. Satish Kumar, and A. Prakash, “Formulation and characterization of 5-Fluorouracil enteric coated nanoparticles for sustained and localized release in treating colorectal cancer,” *Saudi Pharm. J.*, vol. 23, no. 3, pp. 308–314, 2015.

[42] R. S. Tiğli Aydin and M. Pulat, “5-fluorouracil encapsulated chitosan nanoparticles for pH-stimulated drug delivery: Evaluation of controlled release kinetics,” *J. Nanomater.*, vol. 2012, 2012.

[43] S. PS and J. VG, “Preparation and characterisation of 5-fluorouracil loaded PLGA nanoparticles for colorectal cancer therapy,” *Unique J. Pharm. Biol. Sci.*, vol. 01, no. 02, pp. 52–58, 2013.

[44] Y. Wang, P. Li, L. Chen, W. Gao, F. Zeng, and L. X. Kong, “Targeted delivery of 5-fluorouracil to HT-29 cells using high efficient folic acid-conjugated nanoparticles,” *Drug Deliv.*, vol. 22, no. 2, pp. 191–198, 2015.

[45] R. K. Dutta and S. Sahu, “Development of a novel probe sonication assisted enhanced loading of 5-FU in SPION encapsulated pectin nanocarriers for magnetic targeted drug delivery system,” *Eur. J. Pharm. Biopharm.*, vol. 82, no. 1, pp. 58–65, 2012.

[46] M. S. Karbownik and J. Z. Nowak, “Hyaluronan: Towards novel anti-cancer therapeutics,” *Pharmacol. Rep.*, vol. 65, no. 5. pp. 1056–1074, 2013.

[47] W. B. Liechty, D. R. Kryscio, B. V. Slaughter, and N. A. Peppas, “Polymers for drug delivery systems,” *Annu. Rev. Chem. Biomol. Eng.*, vol. 1, pp. 149–173, 2010.

[48] D. Schmaljohann, “Thermo- and pH-responsive polymers in drug delivery,” *Adv. Drug. Deliv. Rev.*, vol. 58, no. 15. pp. 1655–1670, 2006.

[49] S. H. Lim and S. M. Hudson, “Synthesis and antimicrobial activity of a water-soluble chitosan derivative with a fiber-reactive group,” *Carbohydr. Res.*, vol. 339, no. 2, pp. 313–319, 2004.

[50] A. F. Kotze, M. M. Thanou, H. L. Luessen, A. B. G. De Boer, J. C. Verhoef, and H. E. Junginger, “Effect of the degree of quaternization of N-trimethyl chitosan chloride on the permeability of intestinal epithelial cells (Caco-2),” *Eur. J. Pharm. Biopharm.*, vol. 47, no. 3, pp. 269–274, 1999.

[51] S. hao Zhao, X. ting Wu, W. chun Guo, Y. min Du, L. Yu, and J. Tang, “N-(2-hydroxyl) propyl-3-trimethyl ammonium chitosan chloride nanoparticle as a novel delivery system for Parathyroid Hormone-Related Protein 1-34,” *Int. J. Pharm.*, vol. 393, no. 1–2, pp. 268–272, 2010.

[52] S.D. Li, P.W. Li, Z. M. Yang, Z. Peng, W. Y. Quan, X. H. Yang, L. Yang, and J. J. Dong, “Synthesis and characterization of chitosan quaternary ammonium salt and its application as drug carrier for ribavirin,” *Drug Deliv.*, vol. 21, no. 7, pp. 548–552, 2014.

[53] S. hao Zhao, X. ting Wu, W. chun Guo, Y. min Du, L. Yu, and J. Tang, “N-(2-hydroxyl) propyl-3-trimethyl ammonium chitosan chloride nanoparticle as a novel delivery system for Parathyroid Hormone-Related Protein 1-34,” *Int. J. Pharm.*, vol. 393, no. 1–2, pp. 268–272, 2010.

[54] Y. Xu, Y. Du, R. Huang, and L. Gao, “Preparation and modification of N-(2-hydroxyl) propyl-3-trimethyl ammonium chitosan chloride nanoparticle as a protein carrier,” *Biomaterials*, vol. 24, no. 27, pp. 5015–5022, 2003.

[55] H. Zhang, S. Mardyani, W. C. W. Chan, and E. Kumacheva, “Design of biocompatible chitosan microgels for targeted pH-mediated intracellular release of cancer therapeutics,” *Biomacromolecules*, vol. 7, no. 5, pp. 1568–1572, 2006.

[56] B. Xiao, Y. Wan, X. Wang, Q. Zha, H. Liu, Z. Qiu and S. Zhang, “Synthesis and characterization of N-(2-hydroxy)propyl-3-trimethyl ammonium chitosan chloride for potential application in gene delivery,” *Colloids Surf. B Biointerfaces*, vol. 91, no. 1, pp. 168–174, 2012.

[57] B. Bahrami, M. Hojjat-Farsangi, H. Mohammadi, E. Anvari, G. Ghalamfarsa, M. Yousefi, F. Jadidi-Niaragh, and "Nanoparticles and targeted drug delivery in cancer therapy," *Immunol. Lett.*, vol. 190. pp. 64–83, 2017.

[58] C. L. Ventola, "Progress in Nanomedicine: Approved and Investigational Nanodrugs.," *P T*, vol. 42, no. 12, pp. 742–755, 2017.

[59] J. T. Carstensen, "Preformulation," in *Modern Pharmaceutics*, pp. 174–192, 2002.

[60] A. Gupta and M. Gupta, "Synthesis and surface engineering of iron oxide nanoparticles for biomedical applications," *Biomaterials*, vol. 26, no. 18, pp. 3995–4021, 2005.

[61] A. Akbarzadeh, M. Samiei, and S. Davaran, "Magnetic nanoparticles: Preparation, physical properties, and applications in biomedicine," *Nanoscale Res. Lett.*, vol. 7, 2012.

[62] I. Rosenberger, A. Strauss, S. Dobiasch, C. Weis, S. Szanyi, L. Gil-Iceta, E. Alonso, M. González Esparza, and V. Gómez-Vallejo, "Targeted diagnostic magnetic nanoparticles for medical imaging of pancreatic cancer," *J. Control Release*, vol. 214, pp. 76–84, 2015.

[63] A. H. Lu, X. Q. Zhang, Q. Sun, Y. Zhang, Q. Song, F. Schüth, C. Chen, and F. Cheng, "Precise synthesis of discrete and dispersible carbon-protected magnetic nanoparticles for efficient magnetic resonance imaging and photothermal therapy," *Nano Res.*, vol. 9, no. 5, pp. 1460–1469, 2016.

[64] M. Wu and S. Huang, "Magnetic nanoparticles in cancer diagnosis, drug delivery and treatment (Review)," *Mol. Clin. Oncol.*, 2017.

[65] S. Chattopadhyay, A. Kaur, S. Jain, P. K. Sabharwal, and H. Singh, "Polymer functionalized magnetic nanoconstructs for immunomagnetic separation of analytes," *RSC Adv.*, vol. 6, no. 71, pp. 66505–66515, 2016.

[66] E. Hyperthermia, "Magnetic Properties of Magnetic Nanoparticles for Efficient Hyperthermia," *Nanomaterials*, no. 5, pp. 63–89, 2015.

[67] P. T. Yin, B. P. Shah, and K. B. Lee, "Combined magnetic nanoparticle-based MicroRNA and hyperthermia therapy to enhance apoptosis in brain cancer cells," *Small*, vol. 10, no. 20, pp. 4106–4112, 2014.

[68] N. Raghuwanshi, A. Pathak, A. Patel, P. Vashisth, H. Singh, A. K. Srivastava, and V. Pruthi, "Novel biogenic synthesis of silver nanoparticles and their therapeutic potential," *Front. Biosci.*, vol. 9, pp. 33–43, 2017.

[69] R. Kumar and S. Sahu, "Development of oxaliplatin encapsulated in magnetic nanocarriers of pectin as a potential targeted drug delivery for cancer therapy," *Results Pharma Sci.*, vol. 2, no. 1 1-5, pp. 38–45, 2012.

[70] A. Avdeef, "Physicochemical profiling (solubility, permeability and charge state).," *Curr. Top. Med. Chem.*, vol. 1, no. 4, pp. 277–351, 2001.

[71] M. Mikhaylova, D. K. Kim, N. Bobrysheva, M. Osmolowsky, V. Semenov, T. Tsakalakos, and M. Muhammed, "Superparamagnetism of magnetite nanoparticles: Dependence on surface modification," *Langmuir*, vol. 20, pp. 2472–2477, 2004.

[72] X. N. Pham, T. P. Nguyen, T. N. Pham, T. T. N. Tran, and T. V. T. Tran, "Synthesis and characterization of chitosan-coated magnetite nanoparticles and their application in curcumin drug delivery," *Adv. Nat. Sci. Nanosci. Nanotechnol.*, vol. 7, no. 4, 2016.

[73] A. Pobudkowska and U. Domańska, "Study of pH-dependent drugs solubility in water," *Chem. Ind. Chem. Eng. Q.*, vol. 20, no. 1, pp. 115–126, 2014.

[74] N. Parmar, N. Singla, S. Amin, and K. Kohli, "Study of cosurfactant effect on nanoemulsifying area and development of lercanidipine loaded (SNEDDS) self nanoemulsifying drug delivery system," *Colloids Surf. B Biointerfaces*, vol. 86, no. 2, pp. 327–338, 2011.

[75] P. Singh, D. K. Jangir, R. Mehrotra, and A. K. Bakhshi, "Development and validation of an infrared spectroscopy-based method for the analysis of moisture content in 5-fluorouracil," *Drug Test. Anal.*, vol. 1, no. 6, pp. 275–278, 2009.

[76] D. Dorniani, A. U. Kura, Z. Ahmad, A. Halim Shaari, M. Z. Hussein, and S. Fakurazi, "Preparation of Fe3O4 magnetic nanoparticles coated with gallic acid for drug delivery," *Int. J. Nanomedicine*, p. 5745, 2012.

[77] R. K. Dutta and S. Sahu, "Development of oxaliplatin encapsulated in magnetic nanocarriers of pectin as a potential targeted drug delivery for cancer therapy," *Results Pharma Sci.*, vol. 2, no. 1, pp. 38–45, 2012.

[78] P. Calias and R. J. Miller, "Modification of biopolymers for improved drug delivery," Official Gazette of the United States Patent & Trademark Office Patents, 2001.

[79] W. Friess, "Biopolymers for Parenteral Drug Delivery in Cancer Treatment," In: *Drug Delivery Systems in Cancer Therapy*, pp. 47–95, 2004.

[80] S. K. Nitta and K. Numata, "Biopolymer-based nanoparticles for drug/gene delivery and tissue engineering," *Int. J. Mol. Sci.*, vol. 14, no. 1. pp. 1629–1654, 2013.

[81] W. Paul and C. P. Sharma, "Chitosan, a drug carrier for the 21st century: A review," *S.T.P. Pharma Sci.*, vol. 10, no. 1, pp. 5–22, 2000.

[82] M. Rajan, V. Raj, A. A. Al-Arfaj, and A. M. Murugan, "Hyaluronidase enzyme core-5-fluorouracil-loaded chitosan-PEG-gelatin polymer nanocomposites as targeted and controlled drug delivery vehicles," *Int. J. Pharm.*, vol. 453, no. 2, pp. 514–522, 2013.

[83] P. le Dung, M. Milas, M. Rinaudo, and J. Desbrières, "Water soluble derivatives obtained by controlled chemical modifications of chitosan," *Carbohydr. Polym.*, vol. 24, no. 3, pp. 209–214, 1994.

[84] Y. Xu, Y. Du, R. Huang, and L. Gao, "Preparation and modification of N-(2-hydroxyl) propyl-3-trimethyl ammonium chitosan chloride nanoparticle as a protein carrier," *Biomaterials*, vol. 24, no. 27, pp. 5015–5022, 2003.

[85] J. Kiefer, J. Grabow, H. D. Kurland, and F. A. Müller, "Characterization of Nanoparticles by Solvent Infrared Spectroscopy," *Anal. Chem.*, vol. 87, no. 24, pp. 12313–12317, 2015.

[86] R. Xu, "Progress in nanoparticles characterization: Sizing and zeta potential measurement," *Particuology*, vol. 6, no. 2, pp. 112–115, 2008.

[87] M. Kumar, D. Gupta, G. Singh, S. Sharma, M. Bhat, C. K. Prashant, A. K. Dinda, S. Kharbanda, D. Kufe, and H. Singh, "Novel polymeric nanoparticles for intracellular delivery of peptide cargos: Antitumor efficacy of the BCL-2 conversion peptide

NuBCP-9," *Cancer Res.*, vol. 74, no. 12, pp. 3271–3281, 2014.

[88] N. Kamaraj, P. Y. Rajaguru, P. kumar Issac, and S. Sundaresan, "Fabrication, characterization, in vitro drug release and glucose uptake activity of 14-deoxy, 11, 12-didehydroandrographolide loaded polycaprolactone nanoparticles," *Asian J. Pharm. Sci.*, vol. 12, no. 4, pp. 353–362, 2017.

[89] Z. Rahman, K. Kohli, R. K. Khar, M. Ali, N. A. Charoo, and A. A. A. Shamsher, "Characterization of 5-fluorouracil microspheres for colonic delivery," *AAPS PharmSciTech*, vol. 7, no. 2, pp. E113–E121, 2006.

[90] F. Balestrieri, A. D. Magrì, A. L. Magrì, D. Marini, and A. Sacchini, "Application of differential scanning calorimetry to the study of drug-excipient compatibility," *Thermochim. Acta*, vol. 285, no. 2, pp. 337–345, 1996.

[91] S. K. Motwani, S. Chopra, S. Talegaonkar, K. Kohli, F. J. Ahmad, and R. K. Khar, "Chitosan-sodium alginate nanoparticles as submicroscopic reservoirs for ocular delivery: Formulation, optimisation and in vitro characterisation," *Eur. J. Pharm. Biopharm.*, vol. 68, no. 3, pp. 513–525, 2008.

[92] K. P. Musmade, P. B. Deshpande, P. B. Musmade, M. N. Maliyakkal, A. R. Kumar, M.S. Reddy, and N. Udupa, "Methotrexate-loaded biodegradable nanoparticles: Preparation, characterization and evaluation of its cytotoxic potential against U-343 MGa human neuronal glioblastoma cells," *Bull. Mater. Sci.*, vol. 37, no. 4, 2014.

[93] K. A. Janes, M. P. Fresneau, A. Marazuela, A. Fabra, and M. J. Alonso, "Chitosan nanoparticles as delivery systems for doxorubicin," *J. Control Release*, vol. 73, no. 2–3, pp. 255–267, 2001.

[94] Z. Mohammadi, F. A. Dorkoosh, S. Hosseinkhani, T. Amini, A. A. Rahimi, A. R. Najafabadi, and M. R. Tehrani, "Stability studies of chitosan-DNA-FAP-B nanoparticles for gene delivery to lung epithelial cells," *Acta Pharm.*, vol. 62, no. 1, pp. 83–92, 2012.

[95] B. Galateanu, M. C. Bunea, P. Stanescu, E. Vasile, A. Casarica, H. Iovu, A. Hermenean, C. Zaharia, and M. Costache, "*In Vitro* Studies of Bacterial Cellulose and Magnetic Nanoparticles Smart Nanoomposites for Efficient Chronic Wounds

Healing," *Stem Cells Int.*, vol. 2015, 2015.

[96] H. Vardhan, P. Mittal, S. K. R. Adena, and B. Mishra, "Long Circulating Polyhydroxy butyrate-co-hydroxyvalerate nanoparticles for tumor targeted docetaxel delivery: formulation, optimization, and invitro characterization. Eurpean journal of Pharmaceutical Sciences., 99, pp. 85-94, 2017.

[97] H. vardhan, P. Mittal, S. K. R. Adena, M. Upadhyay, and Brahmeshwar Mishra, "Development of long circulating docetaxel loaded poly(3-hydroxybutyrate-co-3-hydroxyvalerate) nanoparticles: optimization , pharmacokinetic, cytotoxicity and invivo assessments," International Journal of Biological Macromolecules., 103, pp. 791-801, 2017.

[98] S. Wu, X. Yang, Y. Lu, Z. Fan, Y. Li, Y. Jiang, and Z. Hou, "A green approach to dual-drug nanoformulations with targeting and synergistic effects for cancer therapy," *Drug Deliv.*, vol. 24, no. 1, pp. 51–60, 2017.

[99] V. Bansal, M. Kumar, M. Dalela, H. G. Brahmne, and H. Singh, "Evaluation of synergistic effect of biodegradable polymeric nanoparticles and aluminum based adjuvant for improving vaccine efficacy," *Int. J. Pharm.*, vol. 471, no. 1–2, pp. 377–384, 2014.

[100] A. Mohandas, P. T. Sudheesh Kumar, B. Raja, V. K. Lakshmanan, and R. Jayakumar, "Exploration of alginate hydrogel/nano zinc oxide composite bandages for infected wounds," *Int. J. Nanomedicine*, vol. 10, pp. 53–56, 2015.

[101] K. Thanki, V. Kushwah, and S. Jain, "Recent Advances in Tumor Targeting Approaches," In: *Targeted Drug Delivery : Concepts and Design, Advances in Delivery Science and Technology*, pp. 41–112, 2015.

[102] D. J. Jonker, J. A. Maroun, and W. Kocha, "Survival benefit of chemotherapy in metastatic colorectal cancer: A meta-analysis of randomized controlled trials," *Br. J. Cancer*, vol. 82, no. 11, 2000.

[103] P. Pacini, M. Rinaldini, R. Algeri, A. Guarneri, E. Tucci, G. Barsanti, B. Neri, P. Bastiani, S. Marzano, and C. Fallai,"FEC (5-fluorouracil, epidoxorubicin and cyclophosphamide) versus EM (epidoxorubicin and mitomycin-C) with or without

lonidamine as first-line treatment for advanced breast cancer. A multicentric randomised study. Final results," *Eur. J. Cancer*, vol. 36, no. 8, pp. 966–975, 2000.

[104] L. A. Dykman and N. G. Khlebtsov, "Biomedical Applications of Multifunctional Gold-Based Nanocomposites," *Biomaterials*, 81(13), pp. 1771-1789, 2016.

[105] F. Hassan, S. A. A. Mohammed, A. Philip, A. A. Hameed, and E. Yousif, "Gold (III) complexes as breast cancer drug," *Syst. Rev. Pharm.*, vol. 8, no. 1, 2016.

[106] P. Cherukuri, E. S. Glazer, and S. A. Curley, "Targeted hyperthermia using metal nanoparticles," *Adv. Drug Deliv. Rev.*, vol. 62, no. 3, pp. 339–345, 2010.

[107] P.-J. Debouttière, S. Roux, F. Vocanson, C. Billotey, O. Beuf, A. Favre-Réguillon, Y. Lin, S. Pellet-Rostaing, R. Lamartine, P. Perriat, and O. Tillement, "Design of Gold Nanoparticles for Magnetic Resonance Imaging," *Adv. Funct. Mater.*, vol. 16, no. 18, pp. 2330–2339, 2006.

[108] S. F. Chin, K. S. Iyer, and C. L. Raston, "Facile and green approach to fabricate gold and silver coated superparamagnetic nanoparticles," *Cryst. Growth Des.*, vol. 9, no. 6, pp. 2685–2689, 2009.

[109] L. A. Dykman and N. G. Khlebtsov, "Biomedical applications of multifunctional gold-based nanocomposites," *Biochem.*, vol. 81, no. 13, 2016.

[110] C. K. Lo, D. Xiao, and M. M. F. Choi, "Homocysteine-protected gold-coated magnetic nanoparticles: synthesis and characterisation," *J. Mater. Chem.*, vol. 17, no. 23, p. 2418, 2007.

[111] T. Ahmad, H. Bae, I. Rhee, Y. Chang, S.-U. Jin, and S. Hong, "Gold-coated iron oxide nanoparticles as a T2 contrast agent in magnetic resonance imaging.," *J. Nanosci. Nanotechnol.*, vol. 12, no. 7, pp. 5132–7, 2012.

[112] V. Selvaraj and M. Alagar, "Analytical detection and biological assay of antileukemic drug 5-fluorouracil using gold nanoparticles as probe," *Int. J. Pharm.*, vol. 337, no. 1–2, pp. 275–281, 2007.

[113] R. T. Tom, V. Suryanarayanan, P. G. Reddy, S. Baskaran, and T. Pradeep, "Ciprofloxacin-protected gold nanoparticles," *Langmuir*, vol. 20, no. 5, pp. 1909–

1914, 2004.

[114] D. Bhadra, S. Bhadra, S. Jain, and N. K. Jain, "A PEGylated dendritic nanoparticulate carrier of fluorouracil," *Int. J. Pharm.*, vol. 257, no. 1–2, pp. 111–124, 2003.

[115] V. C. Karade, T.D. Dongale, S.C. Sahoo, P. Kollu, A.D. Chougale, P.S. Patil, and P.B. Patil, "Effect of reaction time on structural and magnetic properties of green-synthesized magnetic nanoparticles," *J. Phys. Chem. Solids*, vol. 120, 2018.

[116] U. Kreibig, A. Althoff, and H. Pressmann, "Veiling of optical single particle properties in many particle systems by effective medium and clustering effects," *Surf. Sci.*, vol. 106, no. 1–3, pp. 308–317, 1981.

[117] M. Aslam, L. Fu, M. Su, K. Vijayamohanan, and V. P. Dravid, "Novel one-step synthesis of amine-stabilized aqueous colloidal gold nanoparticles," *J. Mater. Chem.*, vol. 14, no. 12, pp. 1795–1797, 2004.

[118] P. Costa and J. M. Sousa Lobo, "Modeling and comparison of dissolution profiles," *Eur. J. Pharm. Sci.*, vol. 13, no. 2. pp. 123–133, 2001.

[119] G. Shukla, H. Khera, A. Srivastava, P. Khare, R. Patidar, and R. Saxena, "Therapeutic Potential, Challenges and Future Perspective of Cancer Stem Cells in Translational Oncology: A Critical Review," *Curr. Stem Cell Res. Ther.*, vol. 12, no. 3, pp. 207–224, 2017.

[120] C. P. Day, G. Merlino, and T. Van Dyke, "Preclinical Mouse Cancer Models: A Maze of Opportunities and Challenges," *Cell*, vol. 163, no. 1. pp. 39–53, 2015.

[121] N. Gengenbacher, M. Singhal, and H. G. Augustin, "Preclinical mouse solid tumour models: Status quo, challenges and perspectives," *Nat. Rev. Cancer.*, vol. 17, no. 12. pp. 751–765, 2017.

[122] B. W. Simons and C. Brayton, "Chapter 3 – Challenges and Limitations of Mouse Xenograft Models of Cancer," In: *Patient Derived Tumor Xenograft Models*, pp. 25–36, 2017.

[123] D. Nihalani and K. Susztak, "Sirt1–Claudin-1 crosstalk regulates renal function," *Nat. Med.*, vol. 19, no. 11, pp. 1371–1372, 2013.

[124] Y. Yang, H. H. Yang, Y. Hu, P. H. Watson, H. Liu, T. R. Geiger, M. R. Anver, D. C. Haines, P. Martin, J. E. Green, M. P. Lee, K. W. Hunter, and L. M. Wakefield, "Immunocompetent mouse allograft models for development of therapies to target breast cancer metastasis.," *Oncotarget*, vol. 8, no. 19, pp. 30621–30643, 2017.

[125] T. Mosmann, "Rapid colorimetric assay for cellular growth and survival: Application to proliferation and cytotoxicity assays," *J. Immunol. Methods*, vol. 65, no. 1–2, pp. 55–63, 1983.

[126] D. Chumakov, A. Prilepskii, L. Dykman, B. Khlebtsov, N. Khlebtsov, and V. Bogatyrev, "Cytotoxicity evaluation of gold nanoparticles on microalga Dunaliella salina in microplate test system," In: *Progress in Biomedical Optics and Imaging - Proceedings of SPIE*, vol. 10716, 2018.

[127] E. Arif, P. Sharma, A. Solanki, L. Mallik, Y. S. Rathore, W. O. Twal, S. K. Nath, D. Gandhi, L. B. Holzman, E. M. Ostap, Ashish, and D. Nihalani, "Structural Analysis of the Myo1c and Neph1 Complex Provides Insight into the Intracellular Movement of Neph1," *Mol. Cell. Biol.*, vol. 36, no. 11, pp. 1639–1654, 2016.

[128] P. S. Barcellona, A. Campana, V. Rossi, C. Corradino, B. Silvestrini, and F. Angelini, "A Comparative Study of Acute Toxicity of Drugs Used During Anticancer Therapy in Healthy and Tumor-Bearing Mice," In: Disease, Metabolism and Reproduction in the Toxic Response to Drugs and Other Chemicals, pp. 90–93, 1984.

[129] K. T. Al-Jamal, J. Bai, J. T. W. Wang, A. Protti, P. Southern, L. Bogart, H. Heidari, X. Li, A. Cakebread, D. Asker, W. T. Al-Jamal, A. Shah, S. Bals, J. Sosabowski, and Q. A. Pankhurst, "Magnetic Drug Targeting: Preclinical in Vivo Studies, Mathematical Modeling, and Extrapolation to Humans," *Nano Lett.*, vol. 16, no. 9, pp. 5652–5660, 2016.

[130] D. Chumakov, A. Prilepskii, L. Dykman, B. Khlebtsov, N. Khlebtsov, and V. Bogatyrev, "Cytotoxicity evaluation of gold nanoparticles on microalga Dunaliellasalina in microplate test system.Proceedings 2018", vol 10716, pp. 1-7, 2017.

[131] K. K. Jain, "The role of nanobiotechnology in drug discovery," *Adv. Exp. Med. Biol.*, vol. 655, pp. 37–43, 2009.

[132] C. Kim, P. Ghosh, and V. M. Rotello, "Multimodal drug delivery using gold nanoparticles," *Nanoscale*, vol. 1, no. 1, p. 61, 2009.

[133] J. Lee, D. K. Chatterjee, M. H. Lee, and S. Krishnan, "Gold nanoparticles in breast cancer treatment: Promise and potential pitfalls," *Cancer Letters*, vol. 347, no. 1. pp. 46–53, 2014.

[134] P. K. Samudrala, B. B. Augustine, E. R. Kasala, L. N. Bodduluru, C. Barua, and M. Lahkar, "Evaluation of antitumor activity and antioxidant status of Alternanthera brasiliana against Ehrlich ascites carcinoma in Swiss albino mice," *Pharmacognosy Res.*, vol. 7, no. 1, pp. 66–73, 2015.